POTASSIUM CHANNELOPATHIES IN PULMONARY ARTERIAL HYPERTENSION

Michael S. Bohnen

Submitted in partial fulfillment of the
requirements for the degree of
Doctor of Philosophy
under the Executive Committee
of the Graduate School of Arts and Sciences

COLUMBIA UNIVERSITY

2017

ABSTRACT

POTASSIUM CHANNELOPATHIES IN PULMONARY ARTERIAL HYPERTENSION

Michael S. Bohnen

A debilitating illness, pulmonary arterial hypertension (PAH) arises from deleterious remodeling of pulmonary arterioles, leading to increased pulmonary artery pressure, a rise in pulmonary vascular resistance, right sided heart failure and death. The pathogenesis of the disease is incompletely understood; however, certain established pathological features have guided medical treatments to improve mortality rates. For instance, an imbalance of vasoconstrictor molecules, such as endothelin-1, to vasodilator compounds, such as nitric oxide, contributes to excessive pulmonary arterial constriction, and a propensity for pulmonary arterial smooth muscle and endothelial cell proliferation. Therapeutic strategies may aim to restore this imbalance with the use of endothelin receptor antagonists, prostacyclin analogs, and other vasodilating agents.

Mutations in the *BMPR2* gene, the most common genetic cause of PAH, leads to aberrant TGF-ß signaling, which promotes uncontrollable cell proliferation and pathological changes in pulmonary arterioles. Genetic studies have revealed PAH-associated mutations in several other genes within the TGF-ß signaling pathway. More recently, our research group discovered loss-of-function mutations in the *KCNK3* gene encoding the KCNK3 two-pore domain potassium channel in patients with idiopathic and familial PAH.

KCNK3 (also referred to as TASK-1, or $K_{2P}3.1$) represents the first ion channelopathy as a cause of PAH. *KCNK3* is expressed in human pulmonary artery smooth muscle and endothelial cells.

Loss of KCNK3 channel currents leads to membrane depolarization and predisposes to deleterious pulmonary arterial remodeling. Chapter 1 of my thesis explores the impact of *KCNK3* mutations on potassium channel function in cellular models of heterozygous conditions, as all patients with PAH-associated *KCNK3* mutations in our study were heterozygous at the *KCNK3* gene locus.

Furthermore, we explored function of mutant and non-mutant KCNK3 channels in cultured human pulmonary artery smooth muscle cells to better define the electrophysiological consequence of KCNK3 dysfunction, and used a KCNK3-activating pharmacological agent, ONO-RS-082, to gauge the therapeutic potential of KCNK3 as a pharmacological target in PAH. Moreover, the study of KCNK3 channel activity when assembled with the closely related KCNK9 channel provided a platform for exploring the lung-specific phenotype in patients with heterozygous *KCNK3* mutations, despite widespread tissue expression *KCNK3* in the body.

In Chapter 2 of my thesis work, the discovery of a second potassium channelopathy in PAH is characterized. Heterozygous mutations in the *ABCC8* gene, encoding the sulfonylurea receptor 1 (SUR1) protein, were found in pediatric and adult patients with idiopathic and familial PAH. SUR1, a beta subunit of the ATP-sensitive potassium channel (K_{ATP}), assembles with the pore-forming $K_{ir}6.2$ alpha subunit to form K_{ATP}, a channel sensitive to inhibition by intracellular ATP. At the plasma membrane, K_{ATP} inwardly rectifying potassium currents contribute to the resting potential, and may play a pathophysiological role in PAH via dysfunction in pulmonary artery smooth muscle and/or endothelial cells. In this chapter, eight *ABCC8* mutations associated with PAH were functionally characterized, and pharmacological agents were employed to examine the therapeutic potential in targeting SUR1-containing K_{ATP} channels in PAH.

Altogether, the research presented in this dissertation identifies and explores potassium channel dysfunction as a pathogenic mechanism in PAH, due to heterozygous genetic mutations in *KCNK3* and *ABCC8*. Evidence of restoration of mutant KCNK3 and K_{ATP} channel function by pharmacological agents suggests that targeting potassium channels as a therapeutic strategy may alleviate the severe morbidity and mortality burden in patients with PAH.

TABLE OF CONTENTS

LIST OF CHARTS, GRAPHS, ILLUSTRATIONS

(in order of appearance in the text)

LIST OF ABBREVIATIONS

PAH – pulmonary arterial hypertension

PASMC – pulmonary artery smooth muscle cell

PAEC – pulmonary artery endothelial cell

K_{ATP} – ATP-sensitive potassium channel

K_{2P} – two-pore domain potassium channel

K_v – voltage-gated potassium channel

K_{ir} – inwardly-rectifying potassium channel

I_{KN} – non-inactivating potassium current

SUR1 – sulfonylurea receptor 1

ONO – ONO-RS-082

TMD – transmembrane domain

ACKNOWLEDGEMENTS

I would like to thank the many people that have helped me along my educational and personal journey toward becoming a biomedical scientist. The list of people to thank is long, a few highlights are written here.

First and foremost, to Rocky Kass: my most sincere thanks for lending a tremendous amount of your time and expertise to help groom me into a scientist. Working in your lab for a year before med school cultivated my passion for biomedical science, and that opportunity has led me to where I am today. Thanks for your constant support. I have learned important lessons from your leadership; you have cheered me on when things went well, and offered the right dose of constructive feedback when I needed to do better. Thanks for letting me grow and work toward something I could be proud of.

To Wendy Chung, I am extremely grateful for your deep commitment to my learning and investing significant time and energy into supporting our collaborative research projects. Thanks for your numerous extra efforts, and to your research group – including Lijiang Ma and Na Zhu -- for collaborating with me.

A big thanks to my thesis committee members for your time and constructive feedback: Penny Boyden, Wendy Chung, and Steven Marx. Our discussions improved my research, and helped me refine my ability to communicate it. Thanks to Vivek Iyer for serving on my thesis defense committee.

Thanks to all Kass lab members for your friendship and for the many great science discussions. Special thanks to those I have worked closely with: Gary Peng, Seth Robey, Kevin Sampson, Cecile Terrenoire, and Lei Chen. I am lucky to have had a work environment full of such good people. Thank you to the MD/PhD program and the Integrated Program in CMBS at Columbia; a special thanks to Patrice Spitalnik, Jeffrey Brandt, and Zaia Sivo for your support throughout this journey. Thank you to Colin Nichols and Conor McClenaghan at Washington University for collaborating with us and for your expertise on the K_{ATP} studies. Thanks to Regeneron for resources and collaboration, and to the UK group (Dr. Morrell and collaborators) for work on the SUR1 project.

Thank you to the following research contributors for the KCNK3 project: Danilo Roman-Campos, PhD; Cecile Terrenoire, PhD; Jack Jnani; Kevin J. Sampson, PhD; Wendy K. Chung, MD, PhD; Robert S. Kass, PhD. We thank the pulmonary arterial hypertension patients and their families for their generous contribution. We thank Dr. Mark Geraci for data/tissue samples provided through the Pulmonary Hypertension Breakthrough Initiative (PHBI). We thank Dr. Monica Goldklang and the D'armiento laboratory at Columbia University for assisting with gene expression studies. Thank you Jenny Rao for laboratory technical support.

Thank you to the following contributors to the SUR1 project: we thank the patients and their families for their generous contribution. Robyn Barst and Jane Morse were critical members of the team to enroll and clinically characterize patients. Patricia Lanzano provided oversight of the Columbia biorepository. Anthony Marcketta provided bioinformatics support. Jenny Rao assisted with molecular biology and cell culture preparations. Charles Stanley provided helpful discussion.

The following research nurses, study coordinators and data managers provided invaluable support to the NIHR BioResource – Rare Diseases PAH study: Amanda Creaser-Myers, Rosa DaCosta, Margaret Day, Natalie Dormand, Dipa Ghedia, Alan Greenhalgh, Mark Grover, Anna Huis in't Veld, Val Irvine, Fiona Kennedy, Shokri Othman, Alice Parker, Gary Polwarth, Stephen Roney, Gwen Schotte, Debbie Shipley, Della Stokes, Yvonne Tan, Sara Walker, Bath Respiratory Nurse Specialists.

Last, certainly not least, my family. So easy to say, yet surprisingly difficult to write down just how thankful and indebted I am to all of you. The words on the page don't quite convey the feelings behind them. My wife Rachel, Mom, Dad, Rhonda, Jack, Jordy, Becca, Becky, Davit, Noah, Gabe, Sammy, and Bryan – I love you all and thank you for the unconditional love in return. You have all heard the words "ion channel" more times than you probably needed. Rach: thanks for being you, and for putting up with me! You're the best. Mom and Dad: you are the type of people I strive to be one day. Good, kind, and full of integrity. Jord and Becky, thanks for putting up with a younger brother that always wanted (and still wants) to hang out with you. You are amazing role models and friends. To all my in-laws, you treat me like one of your own; it's very special and greatly appreciated.

DEDICATION

To my family.

I love you all very much.

Yay potassium.

INTRODUCTION

Epidemiology of PAH

Pulmonary arterial hypertension (PAH) is defined as a "pre-capillary" cause of pulmonary hypertension, in patients with a mean pulmonary arterial pressure ≥ 25 mmHg, and a PAWP ≤ 15 mmHg.[5] Group 1 pulmonary arterial hypertension according to World Health Organization classification, may be further subdivided into the following four clinical sub-classifications:[5]

1.1) Idiopathic

1.2) Heritable (due to known genetic mutations)

1.3) Drug and toxin induced (eg. Fenfluramine, Aminorex)

1.4) Associated (ie. associated with connective tissue disease, HIV infection, portal hypertension, congenital heart disease, or schistosomiasis infection)

A rare disease, the prevalence of PAH is approximately 5-60 cases per million adults, and the incidence of PAH approximately 2-10 cases per million individuals per year.[6-8] About half of PAH patients carry an Idiopathic (IPAH), Heritable (HPAH), or Drug-induced diagnosis. IPAH patients have no known family history of the disease, and no known genetic cause of the illness. In current patient registries, IPAH patients carry a mean age at diagnosis of 50 to 65 years, however this may be in part attributable to the age characteristics of the patient cohorts under study.[5]

Pulmonary hypertension due to any cause carries an approximate prevalence reported in the UK of 1 case per 10,000, with a 1.8 female to male ratio. Left heart disease is thought to be the most

common cause of pulmonary hypertension in general, although this has not been established through comparative epidemiological studies.[5] On a global scale, high altitude-related and schistosomiasis-associated PAH have major, deleterious impacts in specific regions worldwide.[5]

Genetics of PAH

The first HPAH susceptibility locus, *PPH1*, was mapped to chromosome 2q31-32 by two research groups.[9,10] Following this discovery, bone morphogenetic protein receptor II (*BMPR2*) was identified as the gene within the *PPHI* locus associated with HPAH.[11,12] In PAH, *BMPR2* mutations exist in approximately 70% of cases of familial PAH (FPAH), and in 10-40% of idiopathic PAH cases.[13-16] Additional rare causes of PAH within the TGF-ß signaling pathway include mutations in *BMPR1B*, *SMAD3, SMAD8*, *SMAD9*, endoglin (*ENG*), and activin receptor-like kinase 1 (*ALK-1*).[17] Furthermore, mutations in *CAV1*, which regulates SMAD2/3 phosphorylation, is associated with PAH; and more recently, mutations in *KCNK3*, a two-pore domain potassium channel, were identified in FPAH and IPAH patients.[3] Whole exome sequencing was used to identify mutations in *CAV1* and *KCNK3* as rare causes of PAH in heterozygous patients.[3,17] In addition to inherited and *de novo* mutations in the above-mentioned PAH-associated genes, single-nucleotide polymorphisms, including in transporter and ion channel genes, can predispose to PAH.[18]

Nearly all hereditary cases of PAH arise from autosomal dominant transmission of disease-causing mutations. While accounting for most cases of FPAH, BMPR2 mutations harbor low penetrance, with an estimated risk of developing PAH set at 20 percent.[16,19] Incomplete penetrance and heterogeneous genetics underscore the complex pathogenetic basis for PAH in many patients. For

instance, heterozygous germline *ALK1* and *ENG* mutations cause hereditary hemorrhagic telangiectasia (HHT),[20,21] and rarely cause PAH.

Pathophysiological basis of PAH

At the pulmonary arterial level in PAH patient lungs, an excess of vasoconstriction, proliferation, and thrombosis predominate in the setting of endothelial dysfunction. Patients with IPAH produce reduced amounts of nitric oxide (NO) from pulmonary artery endothelial cells (PAECs). NO is a potent vasodilator of pulmonary arteries, and aids in the suppression of pulmonary artery smooth muscle cell (PASMC) proliferation.[22,23] Moreover, endothelin-1 levels are elevated, promoting pulmonary arterial vasoconstriction and deleterious remodeling.

Treatment options such as endothelin-receptor antagonists, thromboxane inhibitors, nitric oxide, and prostacyclin analogs aim to restore the imbalance of vasoconstrictive versus vasodilatory mediators (Figure I1).[18] Potassium channel dysfunction (as described in detail below) may occur up- or downstream of these pathways to further exacerbate pulmonary vascular cell proliferation and constriction.

In children and adults, intimal hyperplasia may lead to vessel occlusion and plexiform lesions within distal pulmonary arteries.[22] PAEC proliferation predisposes to plexiform lesions. PAECs display increased Tie2 receptor expression in patients with IPAH, leading to serotonin release and excessive PASMC proliferation.[24] Enhanced PASMC proliferation also occurs via increased growth factor signaling, and/or a failure in apoptotic and growth suppressor cell signaling.[25-27] The muscularization of distal pulmonary arterioles in close proximity to the alveolar wall and ducts is

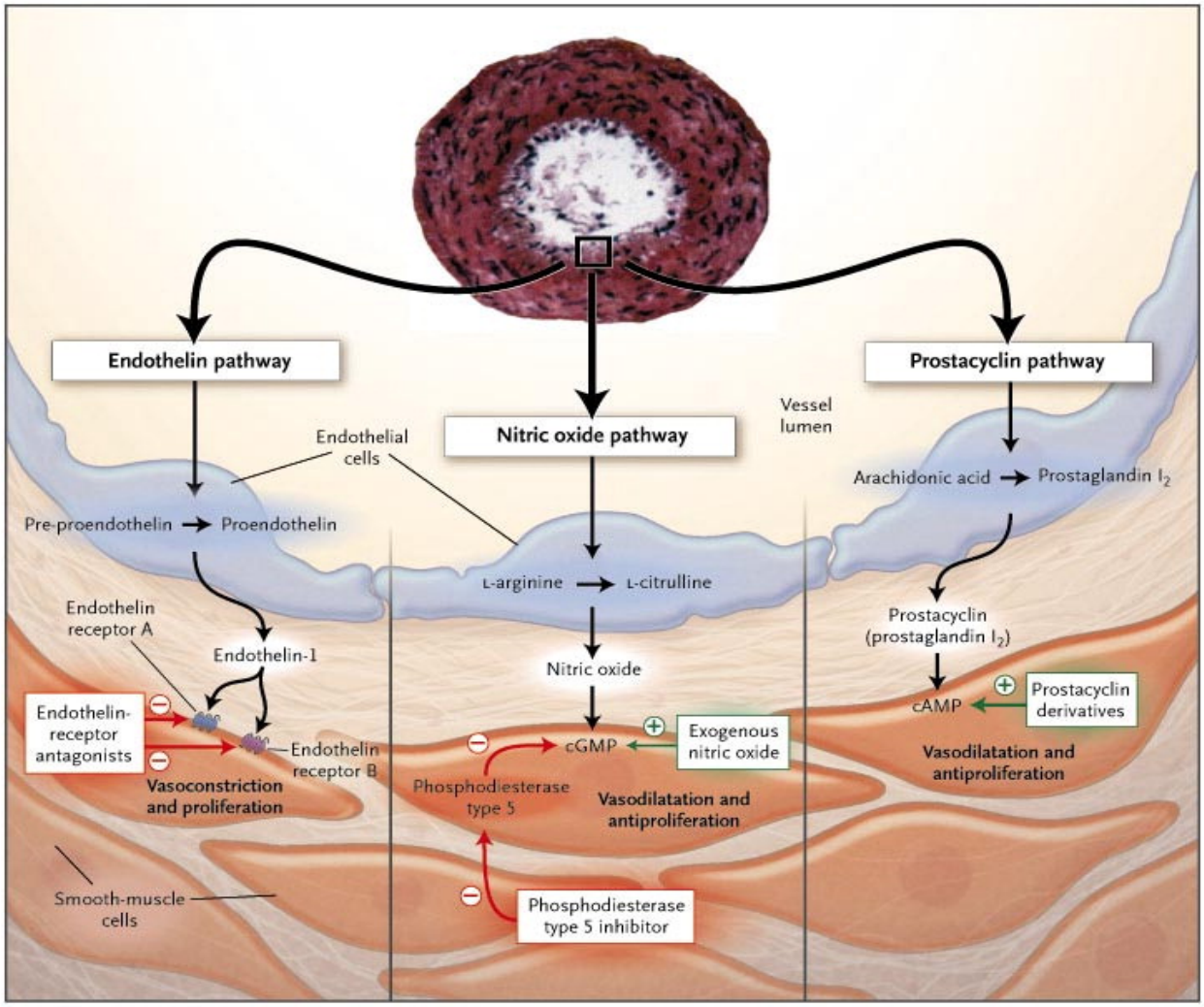

Figure I1. Pathogenic mechanisms guide treatment in pulmonary arterial hypertension. Three signaling pathway molecules involved in PAH pathogenesis -- endothelin-1, nitric oxide, and prostacyclin -- are targeted therapeutically in patients. Reproduced with permission from [2], Copyright Massachusetts Medical Society.

thought to occur in the setting of pericyte differentiation into smooth muscle cells.[22] Ultimately, pathological changes in pulmonary arteries lead to a rise in pulmonary artery pressure, increased pulmonary vascular resistance, and right-sided heart failure.

Smooth muscle cells may be classified based on their predominant phenotype: contractile versus proliferative. Contractile SMCs are considered more highly differentiated, while proliferative

SMCs are less differentiated (or "dedifferentiated" if they were previously in the more differentiated contractile state). In pulmonary hypertension, a relatively high proportion of SMCs exist in the proliferative SMC state,[28] which promotes deleterious pulmonary arterial remodeling. Changes in potassium channel and other channel expression patterns contribute to the transformation from the contractile to proliferative SMC phenotype;[29-31] in cultured PASMCs, downregulation of expressed potassium channels leads to cell depolarization and a predominance of the proliferative SMC phenotype.[32] In a related phenomenon, K^+ efflux from PASMCs aids in the concerted apoptotic intracellular cascades, and PASMCs in PAH patients exhibit resistance to apoptosis, in part due to decreased K^+ channel expression.[33]

At the cellular and molecular level, imbalances in the TGF-ß signaling pathway contribute greatly to altered PASMC and PAEC proliferation, apoptosis, and differentiation, and impacts extracellular matrix secretion and accumulation. Enhanced expression of TGF-ß and glycosaminoglycans occurs, in addition to increased expression of matrix proteins such as tenascin-C and fibronectin.[34] Inflammatory cells (B and T cells, macrophages) may invade pulmonary arteries,[22,35] and increased expression of modulators of inflammation, such as S100A4/Mts1 and fractalkine, has been observed.[36,37] Mutations in *BMPR2* -- or in other TGF-ß pathway genes associated with PAH -- lead to dysregulation of the TGF-ß pathway, increasing the cell proliferation/apoptosis ratio. Furthermore, excessive glycolytic (anaerobic) metabolism and impaired mitochondrial functioning may occur in PASMCs, PAECs, and fibroblasts. The excessive cell growth, impaired apoptosis, and altered cell metabolism in PAH resembles the pathogenesis of cancer.[18]

Certain experimental therapeutic approaches are aimed at alleviating PAH by restoring the proliferation/apoptosis and metabolic balances. Such experimental therapies include pyruvate dehydrogenase kinase inhibitors that would alter metabolic processes; tyrosine kinase inhibitors, rho kinase inhibitors, and inhibitors of transcription factors such as hypoxia-inducible factor [HIF]-1a and nuclear factor of activated T lymphocytes [NFAT], involved in regulating responses to hypoxia and inflammation, respectively.[18] Furthermore, BMPR2 signaling enhancers and potassium channel activators may restore proper cell growth balance.[18] Interestingly, epigenetic changes in superoxide dismutase 2 may predispose to the development of PAH in individuals possessing a known pathogenic PAH mutation, and therefore epigenetic regulation of PAH-associated genes may offer novel therapeutic targets.[38]

Sex hormone balance likely plays a role in PAH development, supported by experimental models of hormone regulation,[39] and by observation that most PAH patients are female, and many female PAH patients are postmenopausal.[40] Insulin resistance may also be more common in female versus male PAH patients, representing another risk factor or disease modifier in PAH.[41] The relationships between insulin regulation, female gender, and mechanisms of PAH development remain unclear to date.

Signs, Symptoms, and Clinical Management

PAH patients present with the clinical signs and symptoms observed in pulmonary hypertension patients in general. Common symptoms include dyspnea, easy fatigability, generalized weakness, angina, and syncope, with symptoms at rest occurring at more advanced stages of the disease. Signs and symptoms of right heart failure, including jugular venous distention, ankle edema,

hepatomegaly, ascites, and abdominal distention worsen as the illness progresses. Other clinical signs include a right ventricular S3 heart sound, accentuation of the pulmonic component of the S2 heart sound, and possible pulmonic and tricuspid regurgitation.[5] Current medical treatment may be divided into three steps,[5,42] summarized here:

1) Treatment with general measures (eg. supervised rehabilitation, birth control and post-menopause hormone therapy, elective surgery, genetic counseling), supportive treatments (eg. digoxin, oxygen supplementation, diuretics), and acute vasodilator testing.
2) Medical therapy initiated with high-dose calcium channel blockers in vasoreactive patients, or other drugs approved for PAH treatment in non-responders (eg. PDE5 inhibitors, endothelin receptor antagonists, prostacyclin analogs).
3) Based on the patient response to steps (1) and (2) above, inadequate responders may be advised to consume drug combinations and/or be referred for lung transplantation.

The genetic basis of PAH may have implications on clinical course and treatment. For instance, adult and pediatric PAH patients with *BMPR2* mutations are not likely to respond to acute vasodilator testing during right heart catheterization, and calcium channel blockers therefore are less likely to provide therapeutic relief in these patients.[43,44] Clinicians do not usually use genetic backgrounds of PAH patients to guide medical management of patients, though as we learn more about potential genotype-phenotype and treatment correlations in patients with disease-causing mutations, clinical management may be further refined.

Genetic testing and counseling may be sought by select PAH patients in order to understand their

own genetic background of the disease (eg. to test for BMPR2 and other PAH-causing genetic mutations in themselves and their family members), and to guide reproductive decision-making. This includes deciding whether to undergo pre-implantation or prenatal genetic testing, to have no prenatal genetic testing, to rely upon gamete donation, or to adopt a child.[5]

Pediatric PAH

The incidence and prevalence of pediatric PAH is seemingly lower than in adult PAH, with a reported 0.7 and 4.4 cases of IPAH per million children, respectively, in the Netherlands.[45] Similarly, incidence and prevalence in the UK is 0.48 and 2.1 cases of IPAH per million children, respectively.[46] IPAH, FPAH, and CHD-PAH are the most common causes of pulmonary hypertension in children, while pulmonary hypertension secondary to respiratory disease may be an important, underreported cause.[47,48]

Pediatric PAH patients carry some genetic and clinical characteristics not found in the adult PAH patient population. The pathogenesis of PAH in infants and neonates is thought to arise from inadequate pulmonary vasculature dilation at birth.[22] Distal resistance arteries experience abnormal muscularization, as well as a significant decrease in number. Intimal hyperplasia, vaso-occlusion, and plexiform lesion may occur in children and adults.[22] Prognosis in general is worse in children; before the advent of modern targeted treatments (eg. prostanoids), pediatric patients had a median survival of approximately 10 months, compared to a median survival of 2.8 years in adults. Prognosis and survival rates have improved in pediatric and adult PAH patient populations alongside newer medical treatments.[49,50]

Fewer studies have been performed in children with PAH compared to adults, and the genetic basis

of PAH in children remains poorly understood overall. Genetic heterogeneity is greater in children than in adults, and PAH in children may occur in the setting of genetic syndromes, including with associated congenital heart disease, hepatic disease, and vascular disease, among other abnormalities.[51-53] The mechanistic basis for the incomplete penetrance and variable expressivity of the underlying PAH-associated mutations also remains unclear.

While similar signs and symptoms of PAH are seen in children and adults, there are key differences. For instance, syncope is more common in children than adults, and right ventricular failure may be a later manifestation of PAH in children. Children may die of sudden death prior to the development of right heart failure.[47,50] A similar treatment algorithm in children to that used in adults has been developed, however this may be due to the relative scarcity of randomized treatment trials in pediatric PAH patients, contributing to difficulty in providing specific pediatric management recommendations.[5,54,55]

Ion Channel Principles

Ion channels are proteins embedded in phospholipid membranes that allow for passage of ions (eg. Na^+, K^+, Ca^{2+}, and Cl^-) between two cellular compartments, or between the intra- and extra-cellular compartments. Ion channels at the plasma membrane govern cellular excitability, and thus control numerous cell processes dependent on the cell type, including metabolism, growth, proliferation, and excitation-contraction coupling.[4] Passage of ions through ion channels occurs by diffusion across the plasma membrane based on the ion's driving force, or electrochemical gradient, and the intrinsic properties of the ion channel (Figure I2).[4]

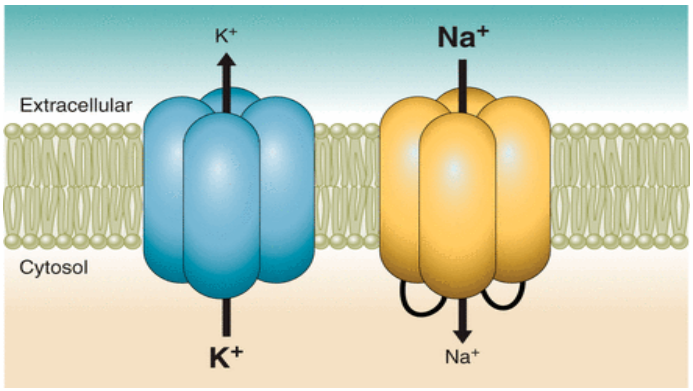

Figure I2. Generic potassium and sodium ion channels at the plasma membrane. K^+ and Na^+ channels allow for selective permeation of ions. Potassium efflux and sodium influx predominate under physiological conditions. Reproduced from Bohnen et al.[4]

The selectivity filter that resides within the conducting pore of the channel is composed of specific amino acid sequences, which allow for selective ion permeation.[56] A variety of ion channels exist that respond to different extracellular and intracellular stimuli (eg. ligands, voltage, temperature, stretch, pH), which may activate or inhibit channel function. Given the focus of my thesis work on potassium channel function (and dysfunction) in pulmonary arterial hypertension, potassium channel structure and function will be exemplified here.

Potassium Channel Structure and Function

There are four classes of potassium channels (Figure I3): voltage-gated (K_v), calcium-activated (K_{Ca}), two-pore domain (K_{2P}), and inwardly rectifying (K_{ir}) potassium channels.[28] K_v and K_{Ca} channels contain four pore-forming alpha subunits; each subunit contains six transmembrane segments (occasionally seven in K_{Ca} channels) and one pore (P-loop) domain. In general, K_v channels play critical roles in cellular repolarization and can contribute to the resting potential; K_{Ca} channels are regulated by intracellular calcium to control excitability.

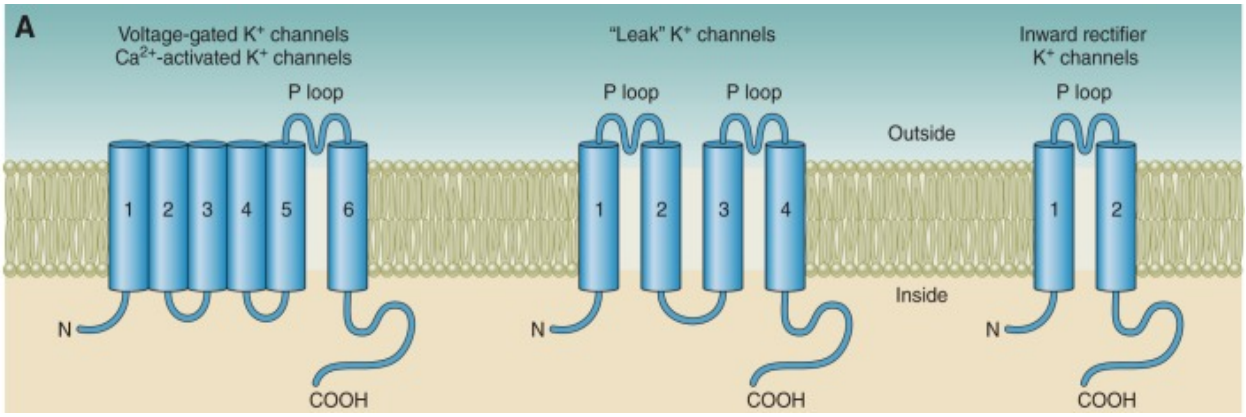

Figure I3. Topology of the four potassium channel classes: K_v, K_{Ca}, K_{2P}, and K_{ir}. Reproduced from Foster and Coetzee,[1] with permission.

K_{2P} channels (eg. KCNK3) contain four transmembrane segments and assemble as dimers; as their name suggests, each subunit within the functional dimer contains two pore (P-loop) domains. K_{ir} channels (eg. K_{ATP}) possess alpha subunits with two transmembrane segments and one pore (P-loop) domain; 4 K_{ir} alpha subunits assemble to form the functional channel pore. Both K_{2P} and K_{ATP} channels contribute background K^+ currents to maintain the cellular resting potential. More details on these channels are provide below under the KCNK3 and K_{ATP} channel sections.

Potassium Channels in Pulmonary Arterial Physiology

A variety of potassium channels from all four K^+ channel classes exist in PASMCs and PAECs. Physiologically, potassium channels play a major role in maintaining pulmonary arterial tone, and balancing vasoconstrictive and vasodilatory responses (Figure I4).

Potassium channel activation leads to vasodilation by preventing activation of voltage dependent calcium channels (VDCCs), and thus keeping intracellular calcium concentrations low (Figure I4,

bottom). Potassium channel inhibition or downregulation leads to depolarization, which activates VDCCs, resulting in an increase in intracellular calcium concentrations (Figure I4, top). Cytosolic calcium initiates excitation-contraction coupling in PASMCs, promoting vasoconstriction, and stimulates cell proliferation. As calcium concentrations rise in the cytosol and nucleus of the cell, a variety of calcium-dependent kinases are activated (eg. calmodulin kinase), in addition to various transcription factors such as NFAT. Activation of kinases and transcription factors promotes cell proliferation by steering the cell into the cell cycle.[28,57]

Native PASMCs possess a resting potential of approximately -50mV.[58,59] Based on physiological intracellular (~150 mmol) and extracellular (~5 mmol) K^+ concentrations, the K^+ equilibrium potential (E_K) is approximately -80mV, derived from the Nernst equation. As such, there is an electrochemical driving force for potassium efflux from cells, which helps maintain the -50mV resting potential of native PASMCs in opposition to the counteracting inward flux of other permeant ions (eg. Na^+, Ca^{2+}) through selective and non-selective channels.[59]

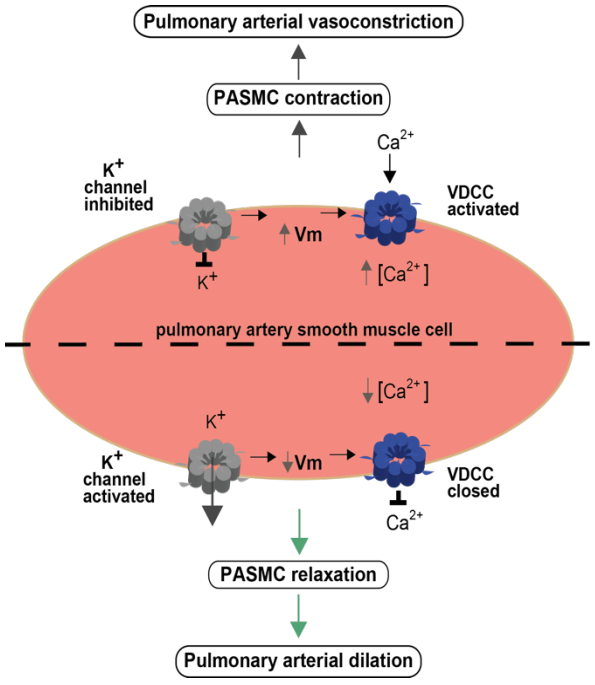

Figure I4. Potassium channels regulate excitability of PASMCs. Inhibition of K^+ channels promotes PASMC membrane (Vm) depolarization, activating VDCCs leading to pulmonary artery constriction (top). Activation of K^+ channels promotes membrane hyperpolarization, inhibiting voltage-dependent calcium channels (VDCC) leading to pulmonary artery dilation (bottom).

Many gene transcripts for various alpha and beta channel subunits of K_v and K_{Ca} channels have been found in PASMCs, including at least 22 alpha-subunit genes of K_v channels, and three K_v channel beta-subunit genes,[60] as well as four K_{Ca} alpha-subunit genes, and four K_{Ca} beta-subunit genes.[61] Not all K^+ channel proteins have been functionally assessed to date.

The $K_v1.2$, $K_v2.1$, and $K_v3.1$ voltage-gated K^+ channels are expressed in PASMCs,[62-64] however these channel subunits activate at membrane potentials depolarized to -40mV,[59,65] making it less plausible that these subunits contribute appreciably to the resting potential at -50mV. However, as voltage-gated potassium channels are comprised of four alpha subunits and heteromeric assembly of alpha subunits is known to occur, heteromeric K_v channel activity could contribute to the resting potential.[59] Indeed, whole-cell and single channel electrophysiological studies have shown that heterotetramers of K_v alpha subunits likely contribute K^+ currents in PASMCs.[61] It was shown that $K_v1.2$/ $K_v1.5$, as well as $K_v2.1$/ $K_v9.3$ heteromers activate at potentials negative to -40mV, and therefore may play a role in setting the resting potential.[62,63] This notion is supported by the fact that these heterodimeric channels demonstrate greater sensitivity to hypoxia than the corresponding homomeric K_v channels and therefore likely contribute to hypoxia-induced membrane potential depolarization.[62,63]

The large-conductance Maxi- K_{Ca} alpha1 subunit is highly expressed in human PASMCs, along with expression of small-conductance SK_{Ca} isoforms.[61] K_{Ca} and K_v channel activity both ultimately contribute to repolarization and to the resting potential to varying degrees, and in doing so control processes such as cell proliferation, vasoconstriction, and regulation of hypoxic pulmonary

vasoconstriction.[66-69]

Other K^+ channels contribute to PASMC excitability as well. For instance, the inwardly rectifying potassium channel subunits $K_{ir}2.1$ and $K_{ir}2.4$ were found to contribute significantly to whole-cell currents in cultured hPASMCs.[70] Furthermore, a distinct K^+ current, described as the non-inactivating K^+ current (I_{KN}) in PASMCs, has been studied. Identified in multiple species,[71-73] I_{KN} is inhibited and/or downregulated by hypoxia, which may lead to PASMC depolarization and sequential activation of K_v currents.[72,73] I_{KN} channel opening was reported to occur at -70mV, with maximal channel current activation at -40mV, as it was speculated that there may be a voltage-dependent component to I_{KN} in PASMCs.[59,71] Further studies suggested that the voltage-independent two-pore domain KCNK3 potassium channel is a main contributor to I_{KN} currents (see further details in the KCNK3 section, below).[73,74]

Potassium channel regulation in PAECs influences pulmonary arterial diameter, including via cross-talk with nearby PASMCs. Enhanced potassium channel activity leads to plasma membrane hyperpolarization, a rise in cytosolic calcium concentrations, promoting nitric oxide release. Nitric Oxide acts on nearby PASMCs to promote vasodilation and prevent excessive proliferation. As such, background potassium conductances, such as those carried by the KCNK3 and KATP channels, can help control PAEC excitability and pulmonary arterial tone.[1] In fact, in pulmonary hypertension, a downregulation of KCNK3 has been observed in PAECs, concomitant with PASMC depolarization and pulmonary vascular cell proliferation.[75] Evidently, the dynamic regulation of pulmonary arterial diameter relies on potassium channel activity in both PAECs and PASMCs.

Hypoxic Pulmonary Vasoconstriction

Resistance pulmonary arterioles respond to hypoxia by constricting.[76] This phenomenon, termed hypoxic pulmonary vasoconstriction, is unique to the pulmonary arterial system. In systemic arteries, hypoxia promotes vasodilation, allowing the tissue in question (eg. skeletal muscle, liver, kidney, etc.) to extract enough oxygen from the blood to meet its metabolic demands. The primary purpose of pulmonary arterioles, however, is to extract oxygen from the alveolar spaces, in order transmit oxygen via the pulmonary veins to the left side of the heart, which pumps oxygenated blood throughout the body. Thus, hypoxia in a region of lung causes pulmonary arteriolar vasoconstriction, intended as a biological "safety mechanism" that shunts blood into pulmonary arterial branches travelling, ideally, to better oxygenated areas of lung. Hypoxia sensing mechanisms in pulmonary arteries in relation to potassium channel function have been studied, however a full understanding of the mechanisms underlying hypoxic pulmonary vasoconstriction remains elusive.

Outside of the pulmonary arterial system, hypoxia may cause enhanced K_v currents and vascular smooth muscle cell hyperpolarization, which promotes vasodilation.[77] In PASMCs, preferential downregulation of K_v channels in the setting of hypoxia contributes to the underlying mechanism of hypoxic pulmonary vasoconstriction and in pathological states leads to excessive pulmonary arterial constriction and proliferation, predisposing to PAH.[77-80] In fact, downregulation of K_v channel functional is more specific to group 1 PAH than to PAH secondary to other diseases,[80] and thus represents a pathogenic disease mechanism.

The K_v1.5 Channel in PAH

In 2007, it was discovered that endothelin-1, a vasoconstrictor molecule, produces an inhibitory

effect on K_v1.5 channels.[81] Given the established role of endothelin-1 in PAH pathogenesis, it was proposed that endothelin-1-mediated inhibition of K_v1.5 leads to excessive pulmonary vasoconstriction and medial hypertrophy of the pulmonary arterial wall in the setting of increased PASMC proliferation.[81] Moreover, novel single nucleotide polymorphisms (SNPs) in the *KCNA5* gene that encodes K_v1.5 were identified in patients with IPAH, and it was suggested that SNPs in the translated and promoter regions of *KCNA5* predispose IPAH patients to decreased expression and function of K_v1.5 channels in PASMCs.[81]

K_v1.5 is preferentially expressed in small, resistance pulmonary artery smooth muscle cells, as opposed to larger pulmonary arteries that do not participate in hypoxic pulmonary vasoconstriction.[76] K_v1.5 channel activity is inhibited by chronic and acute hypoxia (shown in PASMCs), which may lead to resistance pulmonary arterial remodeling via decreased K_v1.5 expression over time.[31,77,82,83] K_v1.5 channel regulation by hypoxia helps explain some of the mechanism underlying hypoxic vasoconstriction in K_v channel-rich resistance pulmonary arterial zones.[82,84] K_v1.5 downregulation has been established in humans and in animal models of PAH as a pathogenic hallmark of PAH, however the overall mechanism of K_v1.5 downregulation by hypoxia remains incompletely understood.[28,31,57,81]

Interestingly, transfection of the *KCNA5* gene, encoding the K_v1.5 channel, into PASMCs, led to plasma membrane hyperpolarization and increased apoptosis.[85] Thus, in theory *KCNA5* gene transfer may represent a potential therapeutic avenue in PAH. In fact, *in vivo KCNA5* adenovirus gene transfer via nebulizer into hypoxia-induced PAH rat lungs decreased pulmonary vascular resistance and caused pulmonary artery medial hypertrophy regression, while restoring hypoxic

pulmonary vasoconstriction.[86]

KCNK3 in Pulmonary Arterial Physiology

The non-inactivating current, I_{KN} (described above), demonstrated robust sensitivity to extracellular pH in PASMCs.[74] I_{KN} was inhibited by extracellular acidosis to pH 6.3, a similar pH-dependence conferred upon the acid-sensitive, two-pore domain KCNK3 channel. The KCNK3-like I_{KN} current was observed in multiple studies, including in human PASMCs.[59,73,87] Given KCNK3's largely voltage-independent, non-inactivating properties, it was suggested that the KCNK3 channel supplies a background current that contributes to the PASMC resting potential.

Early physiological evidence of a role for KCNK3 in regulating pulmonary arterial vascular tone was provided by Gardener et al. in 2004,[88] in a study that demonstrated KCNK3 expression in rat pulmonary arteries, and depolarization upon KCNK3 inhibition. More specifically, extracellular acidosis and anandamide (an endocannabinoid and KCNK3 inhibitor) produced depolarizations, while alkalosis hyperpolarized pulmonary arteries. In wire myograph experiments to measure changes in vessel diameter, application of anandamide caused small but appreciable vasoconstrictive responses.[88]

In 2006, Olschewski and colleagues[73] characterized the impact of KCNK3 channel expression in human PASMCs (hPASMCs). KCNK3 protein was present in primary and cultured hPASMCs in this study. KCNK3 mRNA expression was detected in hPASMCs as well, but the acid-sensitive KCNK5 and KCNK9 channels were not expressed in hPASMCs. mRNA expression of all three acid-sensitive K2P channels was detected in human brain tissue.[73]

On whole-cell patch clamp analysis, I_{KN} in hPASMCs was studied by holding cells at 0 mV for a minimum of 5 minutes in order to isolate I_{KN} by inactivating other voltage-dependent potassium currents,[74] followed by application of a voltage ramp within the physiological voltage range, +60mV to -100mV. An anandamide-sensitive current was measured, and taken as a measurement of the KCNK3 current.[73] The anandamide-sensitive current reversed near the calculated equilibrium potential for potassium (approximately -84mV), and measured I_{KN} currents were pH-sensitive, inhibited by acidosis and activated by alkalosis.

Moreover, it was demonstrated that hypoxia inhibits I_{KN}, and that anandamide has no significant effect on the cellular currents remaining in hypoxic conditions, suggesting that hypoxia and anandamide share a common target, KCNK3. Furthermore, transfection of siRNA targeted against KCNK3 lead to membrane depolarization. Along with the voltage-independent properties of KCNK3, the experimental results suggest that KCNK3 currents play a physiological role in contributing to the resting membrane potential of hPASMCs, and that by extension, KCNK3 inhibition by hypoxia may serve a physiological role in hypoxic pulmonary vasoconstriction.[73] These lines of evidence supported the conclusion that KCNK3 current is a main contributor to I_{KN} in hPASMCs.[73,74]

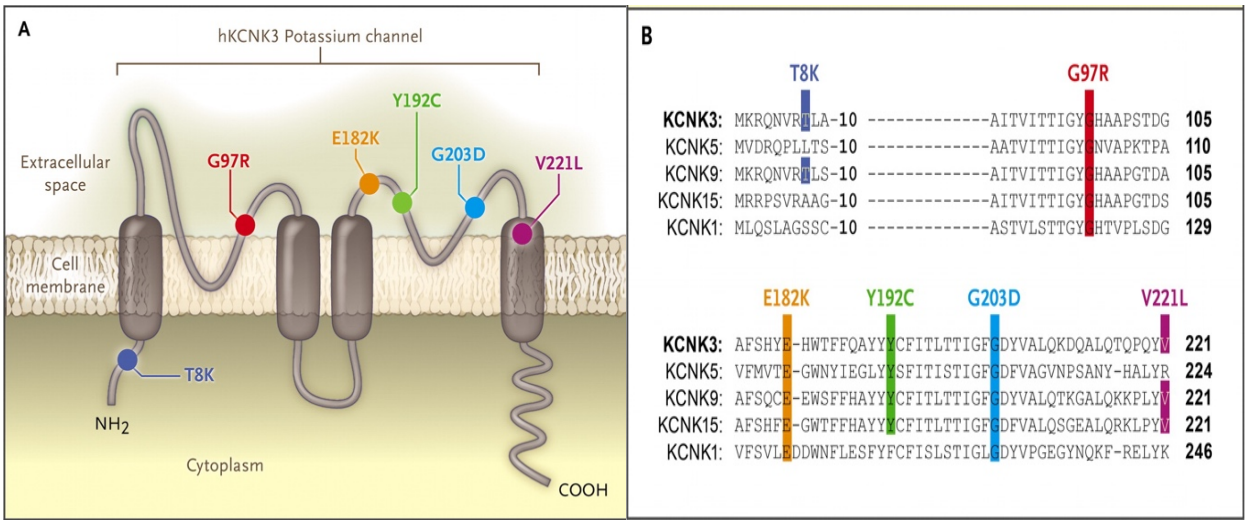

Figure I5. *KCNK3* mutations associated with PAH. Panel A shows the topology of the KCNK3 channel, with the locations of the six mutations associated with PAH. Panel B shows conservation of the mutated residues across two pore domain potassium channels. Reproduced with permission from [3], Copyright Massachusetts Medical Society.

KCNK3 in PAH

In 2013, our research group discovered the first channelopathy in pulmonary arterial hypertension. Using whole-exome sequencing, six novel missense variants (T8K, G97R, E182K, Y192C, G203D, and V221L) were identified in potassium channel subfamily K, member 3 (*KCNK3*), in six unrelated patients with familial and idiopathic PAH (Figure I5). The six patients did not have identifiable mutations in known PAH genes, including *BMPR2*, *ALK1*, *CAV1*, *ENG*, and *SMAD9*.[3] All six patients were heterozygous at the *KCNK3* gene locus, possessing one mutant and one non-mutant *KCNK3* gene. Using *in silico* bioinformatic tools, all mutations were predicted to be damaging. Whole-cell patch clamp electrophysiological studies in COS7 cells expressing mutant versus wildtype KCNK3 channels confirmed loss of function for each mutant KCNK3 channel. Moreover, some mutant KCNK3 channels were pharmacologically rescued by ONO-RS-082, a phospholipase A2 inhibitor and KCNK3 activator. Therefore, we had identified loss of function

KCNK3 mutations as a novel cause of familial and idiopathic PAH and potential therapeutic target.[3]

In 2016, using a monocrotaline-induced pulmonary hypertension rat model, Antigny et al.[75] demonstrated that *KCNK3* expression was reduced in pulmonary hypertension lungs, and that a corresponding reduction in functional KCNK3 channels was observed in freshly isolated PASMCs and PAECs, which was associated with plasma membrane depolarization. Moreover, prolonged application of the KCNK3 activator, ONO-RS-082, alleviated monocrotaline-induced pulmonary hypertension development, as evidenced by a reduction in right ventricular hypertrophy and right ventricular systolic pressure in rats exposed to both monocrotaline and ONO over 28 days, as compared to control rats exposed to monocrotaline alone over the same time span.[75] These results highlight KCNK3 as a viable pharmacologic target in the treatment of pulmonary arterial hypertension.

In addition, Antigny et al.[75] observed reduced *KCNK3* mRNA expression in pulmonary arteries of patients with idiopathic pulmonary arterial hypertension (IPAH), and reduced KCNK3 protein expression in lung tissues of patients with IPAH, signifying that *KCNK3* expression and regulation play a role in the pathogenesis of pulmonary arterial hypertension due to any cause.

The KCNK3 Potassium Channel

The large potassium conductance across the plasma membrane was established decades ago, when the fundamental principles governing ion channel electrophysiology were studied.[89-91] Potassium channels were thus known to contribute to the resting membrane potential, with a proportion of

current designated background (or "leak") potassium current conducted through channel pores and obeying a current-voltage relationship based on the Goldman-Hodgkin-Katz constant field theory.[89,92] By the mid 1990s, the voltage-gated, calcium-dependent, and inwardly rectifying potassium channels were cloned,[89,93-95] and accounted for a large portion of the potassium conductance within cells, but a significant background potassium conductance was still yet to be identified.

In 1996, however, the first TWIK channel (tandem of pore domains in a weak inward rectifying K^+ channel) was cloned, giving rise to a new, emerging family of background potassium channels in mammals.[96] From 1996 to 2003, the two-pore domain family grew to 15 total members, and each two-pore domain channel belonged to one of six subfamilies -- TWIK, TASK, TALK, TREK, THIK, or TRESK -- based on its functional properties and genetic sequence.[89]

Cloning and Characterization of KCNK3

The first TASK (TWIK-related acid-sensitive K^+ channel) channel member, now referred to as TASK-1, was cloned from human kidney in 1996.[97] TASK-1 was the third mammalian two-pore domain K^+ channel discovered overall. By HUGO nomenclature, TASK-1 may be referred to as KCNK3 or $K_{2P}3.1$. In this dissertation, "KCNK3" will be used to describe the gene name as well as the potassium channel.

KCNK3 consists of a 395 amino acid sequence, with four transmembrane segments, and two pore domains, as well as cytoplasmic N- and C-terminal domains that regulate channel trafficking and

expression. Functional KCNK3 channels form dimers from two channel subunits that co-assemble.[97]

Certain structural elements are shared by all members of the two-pore domain family. Each subunit within the functional dimer channel contains two pore-loop ("P-loop") domains, and therefore four P-loops in total are present in the functional two-pore domain dimer channel. In contrast, other potassium channel families have structures containing one P-loop domain per channel subunit, with four P-loops in the functional channel as well, from assembly of four alpha subunits.[89] All K_{2P} mammalian family members possess a four transmembrane domain, two-pore domain structure (see Figure I5, above). Analysis of electrostatic interactions within the pore of two-pore domain channels suggests symmetry of the selectivity filter lining the channel pore, formed from two sets of P1 and P2 loops.[98]

Expression of KCNK3 was found in several tissues, including colon, small intestine, uterus > kidney, heart > lung, prostate > brain > placenta > pancreas.[97] In electrophysiological studies of heterologous *KCNK3* expression in COS cells and *Xenopus* oocytes, KCNK3 was characterized as a non-inactivating and K^+ selective channel with Goldman-Hodgkin-Katz outward rectification, which predicts a curve in the current-voltage plot under asymmetric K^+ concentrations.[97] As such, the outward rectification observed with heterologous expression of KCNK3 currents is a consequence of the physiological asymmetric K^+ concentration gradient inside and outside the cell, leading to varying driving forces for K^+ across the physiological voltage range. Based on these properties, KCNK3 represents a time- and voltage-independent background potassium

conductance, that would contribute to the resting potential of cells in which the channel is expressed.[89]

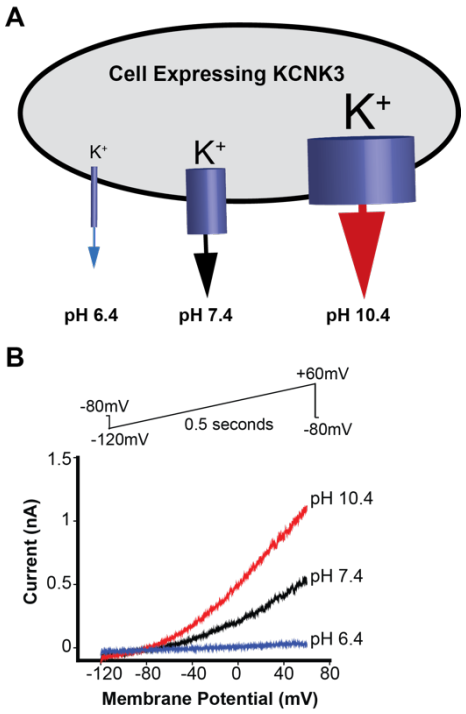

Figure I6. KCNK3 channel regulation by extracellular pH. Panel A shows a generic cell expressing KCNK3. Extracellular acidosis inhibits KCNK3, diminishing potassium efflux, and alkalosis activates KCNK3, enhancing potassium efflux. Panel B shows a whole cell voltage clamp recording of KCNK3 expressed in COS7 cells. A voltage ramp was applied (-120mV to 60mV over 0.5 seconds) every three seconds, from a -80mV holding potential. Physiological pH 7.4 produces intermediate current activity (black curve), pH 6.4 (blue) reduces KCNK3 current, and pH 10.4 (red) maximally activates KCNK3 current.

Regulation of KCNK3 by Extracellular pH

KCNK3 currents are extremely sensitive to extracellular pH within the physiological pH range, with approximately half-maximal activation (p*K*) observed at physiological pH 7.4. KCNK3 currents are inhibited by extracellular acidosis and activated by alkalosis (Figure I6).[97]

It was initially reported that extracellular acidosis inhibits KCNK3 with a p*K* value of 7.4, along with a Hill coefficient of 1.6, implying that both KCNK3 subunits within the functional dimer participate in pH sensing. Furthermore, intracellular pH alterations did not produce changes in KCNK3 currents.[97] Given the voltage-independent properties of KCNK3, it was deduced that the pH sensor must reside in the extracellular portions of the channel, as opposed to within the

transmembrane electric field that bestows voltage-dependence upon, for instance, voltage-gated ion channels.[97] By site-directed mutagenesis and electrophysiological analysis at varying extracellular pH, residue H98 was determined the main pH sensing residue, as mutation of H98 significantly abolished the channel's pH sensitivity. It was determined that the H72 and K210 residues bestowed upon KCNK3 additional, relatively minor pH sensitivity.[99]

KCNK3 Interactions with KCNK9

KCNK9 (also known as TASK-3, or $K_{2P}9.1$) was first cloned from rat cerebellum in 2000,[100] and later in the same year, KCNK9 was cloned from human cerebellum.[101] The *KCNK9* gene encodes the KCNK9 channel, a 374 amino acid protein that shares 62% sequence homology with human KCNK3. Rat and human KCNK9 share 74% amino acid sequence homology,[101] with significant differences in sequence observed 3' to the fourth transmembrane domain. In the initial characterization of human KCNK9, a p*K* value (pH at half-maximal activation) of approximately 6.5 was reported.[101] The Hill coefficient for the pH dependence of KCNK9 was close to 2, suggesting (as for KCNK3 channels) that both KCNK9 subunits participate in pH sensing within the functional dimer channel.[100] The H98 residue in KCNK9 is the major pH sensing residue.[100,102] KCNK9 shares the most structural resemblance to KCNK3, and evidently both channels are inhibited by extracellular acidosis and activated by extracellular alkalosis. However, KCNK9 is more maximally activated at physiological pH 7.4, while KCNK3 is more tightly regulated within the range of physiological pH 7.4.

KCNK3 and KCNK9 channel subunits form functional heterodimers with one another, with heterodimeric channels containing one subunit each of KCNK3 and KCNK9. Heterodimerization of KCNK3 with KCNK9 is the only known heteromeric association within the K_{2P} channel family, and adds to the complexity of the channels' regulation and electrophysiology.[89]

The homodimeric KCNK3 and KCNK9 channels possess distinct electrophysiological and pharmacological properties, while the heterodimeric KCNK9-KCNK3 channels display mixed phenotypes that are not always intermediate in function compared to the homodimeric parent channels.[89,103] For instance, the ruthenium red dye and zinc (Zn^{2+}) have been shown to inhibit KCNK9 homodimeric channels, while KCNK3 homodimers and KCNK9-KCNK3 heterodimers are not inhibited by either agent.[89,103-105] The pH sensitivity of the heterodimeric channels is intermediate, with a p*K* value that lies between the p*K* values of the homodimeric channels. The single-channel conductance of the heterodimer, meanwhile, is equal to that of KCNK9 channels in the presence of extracellular Mg^{2+} ions.[106,107] In the absence of extracellular Mg^{2+}, the single channel conductance of the heterodimer is intermediate between that of KCNK3 and KCNK9 homodimeric channels.[89,107]

To date, KCNK9-KCNK3 heterodimeric channels have been studied in a variety of native tissues, including in cerebellar granule neurons,[106] motoneurons,[108] rat carotid body glomus cells,[107] lateral geniculate thalamocortical relay neurons,[109] hippocampal interneurons,[110] and in cardiac atrial myocytes.[111] Functional diversity depends on the degree of hetero- and homo-dimerization of the two channel subunits and relative proportions of the assembled channels.[89]

Berg et al.[108] determined that hypoglossal motoneurons expressed both KCNK3 and KCNK9 mRNA, and suggested that a significant component of its background potassium channel current consistent is derived from KCNK9-KCNK3 heterodimeric channel currents. This was evidenced by the intermediate pH sensitivity of the heterodimeric channel currents compared to monomer KCNK3 or KCNK9 currents, as well as activation by Isoflurane, a pharmacological feature of KCNK9, but not KCNK3 channels, which are inhibited by isoflurane. The effects of isoflurane could not be attributable to KCNK9 monomeric channel expression as these channels had been blocked by the KCNK9 specific inhibitor, ruthenium red. Heterologous expression of monomeric and heteromeric channel assembly supported these results, as it demonstrated an intermediate pH sensitivity for KCNK9-KCNK3 heterodimers (pK ~ 7.3), compared to monomeric KCNK3 (pK ~ 7.5), and monomeric KCNK9 (pK ~6.8) channel activity in this study.[108]

In cultured cerebellar granule neurons, Kang et al. identified the functional features of KCNK9-KCNK3 heterodimers; the potassium channel currents had an extracellular pH sensitivity that was intermediate between KCNK3 and KCNK9 monomer channel expression, and displayed reduced sensitivity to inhibition by ruthenium red, as compared to KCNK9 monomer channel expression.[106] These two lines of functional evidence demonstrated the presence of KCNK9-KCNK3 heterodimer formation. The electrophysiological evidence for heterodimer formation was replicated by heterologous expression of channel subunits in COS-7 cells. The consistency of the functional assays in native and heterologous expression systems also demonstrated the utility of cell systems in providing a platform to study KCNK9-KCNK3 heterodimer function.[106]

KCNK3 Pharmacology

Anandamide was first reported as a specific KCNK3 inhibitor, within the two-pore domain channel family.[112] As such, anandamide was employed as a pharmacological tool to dissect the contribution of KCNK3 currents in various tissues, including in pulmonary artery smooth muscle cells.[73] While anandamide indeed potently inhibits KCNK3, it is no longer considered a specific KCNK3 blocker, as KCNK9 is blocked by anandamide with similar potency.[89,113] Furthermore, anandamide and/or other endocannabinoids inhibit other ion channels, including TRPV1,[114] Na^+,[115] T-type Ca^{2+} channels,[116] and Shaker-related K_v channels.[117] Ruthenium red, on the other hand, inhibits KCNK9 and has no appreciable effect on KCNK3 channels and thus can be employed as a specific KCNK9 blocker in this context.[89,105,106]

Streit et al.[118] studied the effects of A1899, an experimental compound described as a potent and selective blocker of KCNK3. Through alanine mutagenesis screening of the KCNK3 channel in parallel with electrophysiological studies, the following sites were determined to likely form the binding sites for A1899 intracellularly, leading to KCNK3 inhibition: (a) residues in the M2 and M4 transmembrane segments, including residues that comprise the "halothane response element" (amino acids "VLRFMT" at positions 243-248 in the KCNK3 sequence; both the KCNK3 and KCNK9 channels are targets of anesthetic agents[119,120]); (b) residues in each pore loop including within the potassium selectivity filter (sequence "T**T**IGYG in P1 loop, and T**T**IGFG in P2 loop, with the bolded threonine sites likely serving as binding sites for A1899). Based on the sites of channel block, the authors strongly suggested that A1899 inhibits KCNK3 currents by binding deep within the channel pore to act as a plug to inhibit current.[118] This study provides insights into

the structural basis for pharmacological KCNK3 inhibition, to aid the development of KCNK3 inhibitors and activators for experimental and clinical use. [118]

Of the amino acids in the M2 and M4 segments of KCNK3 identified as components of the A1899 binding site, there is approximately 90% sequence homology with the KCNK9 channel. This would explain shared inhibiting or activating profiles among certain pharmacological compounds on the KCNK3 and KCNK9 channels, and the difficulty in developing fully selective pharmacological agents via binding to the channel's pore.[118] Newer experimental compounds have since been employed as KCNK3 modulators. Please refer to Chapter 1 for experimental results using the recently developed KCNK3 inhibitor, ML365, and the KCNK3 activator, ONO-RS-082.

K_{ATP} in Pulmonary Arterial Physiology

There is relatively less known about the contributions of ATP-sensitive K^+ channels (K_{ATP}) to the resting potential in PASMCs and their contributions to cell excitability in physiological and pathophysiological conditions.[121-123] It has been suggested that a mitochondrial K_{ATP} channel may contribute to regulation of pulmonary arterial remodeling and contraction via mitochondrial metabolic and signaling pathways.[124]

In 1992, it was determined that intracellular levels of ATP regulate the resting membrane potential of PASMCs via inhibition of potassium channels,[125] and it was proposed that K_{ATP} channel currents contribute to maintenance of the resting potential in PASMCs. This conclusion was drawn by lowering intracellular ATP in the patch pipette from 1mM ATP to 0 mM ATP, and observing a change in the resting potential from -55mV to -70mV. At the hyperpolarized potential of -70mV, glibenclamide, a K_{ATP} channel blocker, led to significant membrane depolarization, which

suggested that the hyperpolarization induced by a decrease in intracellular ATP levels was due to activation of the K_{ATP} channels in PASMCs.[125]

Additional studies have attempted to characterize the subunits underlying K_{ATP} function in pulmonary artery smooth muscle and endothelial cells. In the first critical investigation of K_{ATP} channel subunits in human pulmonary arteries, it was reported that $K_{ir}6.1$ and SUR2B were the predominant alpha and beta subunit isoforms, respectively.[126] Importantly, however, the gene expression analysis of channel subunits was derived from RNA from *cultured* hPASMCs, and the authors note that suppression of K_{ATP} channel activity was observed for proliferating cells in culture.[126] Given the downregulation of potassium channels that occurs in PASMCs in culture,[32] it is possible that other isoforms of K_{ATP} channels subunits (eg. $K_{ir}6.2$, SUR1, and SUR2A) are more abundant in native PASMCs. Expression of K_{ATP} subunits in freshly isolated, native human PASMCs was not performed, however expression of K_{ATP} subunits from intact rat pulmonary artery produced differing results, as SUR1 expression was observed in addition to $K_{ir}6.1$ and SUR2B.[126] Thus, it is plausible that certain cellular and/or physiological conditions alter expression of K_{ATP} channel subunits in pulmonary arteries in general, and PASMCs in particular. Both SUR1 and SUR2B expression were reported in guinea-pig bladder SMCs,[127] suggesting that heteromerization of SUR1 with SUR2B may occur in certain smooth muscle tissue types, adding to the complexity of K_{ATP} regulation in smooth muscle cells.

SUR Subunits of the K_{ATP} Channel

Sulfonylurea receptor 1 (SUR1), encoded by the *ABCC8* gene, was first cloned from pancreatic beta cells in 1995.[128] Highest levels of SUR1 mRNA expression were found in the pancreas, heart,

and brain.[1,128] SUR2A and SUR2B, two splice variants of the *ABCC9* gene, were discovered shortly after.[129,130] SUR2B was found to be expressed ubiquitously, while SUR2A expression was found to be high in skeletal muscle, heart, and ovary, with moderate expression found in brain, pancreas (not insulin-secreting cells), and tongue.[1,129,130]

The SUR proteins are all beta subunits of the pore-forming $K_{ir}6.1$ and $K_{ir}6.2$ alpha subunits of the K_{ATP} channel. SUR1 and SUR2A/B are encoded by the *ABCC8* and *ABCC9* genes, respectively, which belong to the superfamily of ATP-binding cassette (ABC) proteins.[1] The SUR proteins harbor intracellular nucleotide-binding folds, which participate in regulation of the K_{ATP} channel via nucleotide binding. The SUR proteins have 17 transmembrane segments that are subdivided into three transmembrane domains: TMD0, TMD1, and TMD2 (Figure I7).[1]

K_{ATP} Channel Structure and Function

The pore-forming alpha subunits of the K_{ATP} channel, $K_{ir}6.1$ and $K_{ir}6.2$, were identified in 1995 in quick succession.[131,132] Belonging to the inwardly-rectifying potassium channel subfamily, a single

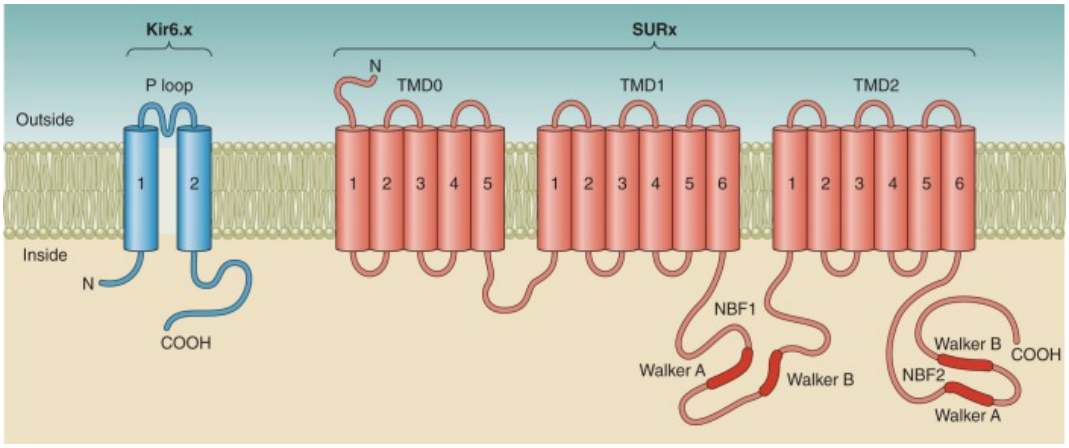

Figure I7. Topology of SURx and $K_{ir}6.x$ subunits. The SURx proteins (eg. SUR1, SUR2A, and SUR2B) have 17 transmembrane segments, divided into transmembrane domains (TMD) TMD0, TMD1, and TMD2. Two cytoplasmic loops contain nucleotide binding folds (NBF1 and NBF2). The $K_{ir}6.x$ alpha subunits (eg. $K_{ir}6.1$, $K_{ir}6.2$) have two transmembrane segments and one P-loop. Four alpha subunits assemble to form the inner pore of the K_{ATP} channel. Reproduced with permission from Foster and Coetzee[1].

$K_{ir}6.1$ and $K_{ir}6.2$ subunit is composed of two transmembrane segments and one pore-forming domain, denoted the "P loop," which resides between transmembrane segments TM1 and TM2,[133] which contains the potassium selectivity filter within it (see Figure I7).[133,134] Potassium selectivity in K_{ir} channel subunits is governed by the signature amino acid sequence T-I-G-[Y or F]-G within the pore domain.[1] Four alpha subunits assemble to form the potassium selective channel pore. Four beta subunits (eg. SUR1, SUR2A, and/or SUR2B) assemble circumferentially around the pore-forming alpha subunits and in doing so regulate channel function and expression (Figure I8A).[1] This mode of assembly was specifically confirmed for SUR1/ $K_{ir}6.2$-containing K_{ATP} channels, in studies that demonstrated a 1:1 stoichiometry of assembly between SUR1 and $K_{ir}6.2$,[135,136] characterized as an octameric or tetradimeric co-assembly of SUR1 with $K_{ir}6.2$, with the four $K_{ir}6.2$ subunits forming the channel pore (Figure I8).[137]

K_{ATP} channels are extremely sensitive to intracellular ATP concentrations, as intracellular ATP decreases the open-probability of K_{ATP} by an inverse relationship.[1,138-140] Nonhydrolyzable ATP analogs block K_{ATP}, demonstrating that ATP itself is a direct substrate for K_{ATP} channel inhibition, and hydrolysis of ATP is not a necessary step involved in ATP's inhibition of the channel.[1,141] Free intracellular ADP also blocks KATP channels, however ADP is approximately 10-20 fold less potent than free ATP channel block.[1,141,142] While free ADP blocks K_{ATP} channels, it is of significant physiological consequence that MgADP activates K_{ATP} by stimulating channel opening. The degree of channel inhibition/activation is thus not solely determined by intracellular ATP concentration, but rather is heavily influenced by the intracellular ATP/ADP ratio.[143]

K_{ATP} channels are open and active across the physiological voltage range, and at the plasma membrane contribute to the negative resting potential via potassium efflux. K_{ATP} channels exhibit relatively weak inward rectification within the K_{ir} family of potassium channels. As such, K_{ATP} channels produce appreciable outward current at more depolarized membrane potentials compared to strong inwardly rectifying potassium channels that produce minimal outward potassium current at depolarized potentials (Figure I8B).[1,144] K_{ATP} channels are not voltage-gated, but rather are voltage-sensitive in the sense that their inwardly-rectifying properties lead to disproportionately less conduction of potassium at more depolarized membrane potentials. Both Na^+ and Mg^+ ions

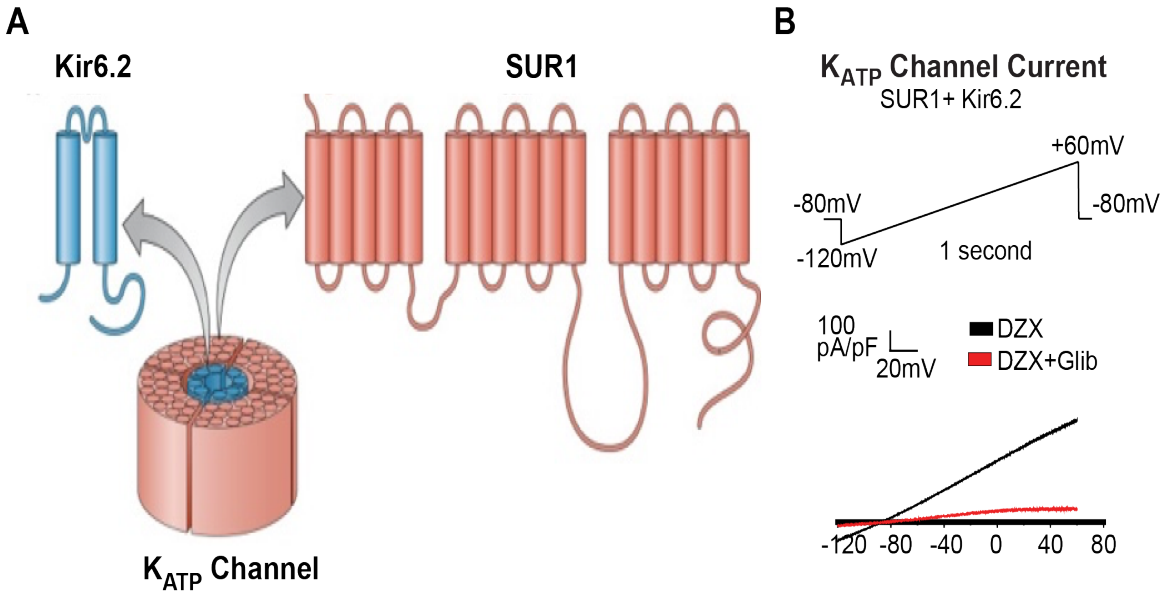

Figure I8. Assembly of functional (SUR1/ K_{ir}6.2) K_{ATP} channels. Panel A demonstrates that K_{ATP} channels form by the assembly of four inner pore-forming K_{ir}6.2 alpha subunits (blue), in association with four SUR1 beta subunits that encircle the pore forming alpha subunits (red). Panel B shows a whole-cell voltage clamp recording in COS7 cell of expressed (SUR1/ K_{ir}6.2) K_{ATP} channel currents. A voltage ramp from -120mV to 60mV over 1 second was applied every 3 seconds from a -80mV holding potential. The K_{ATP} activator, diazoxide 100uM (black), maximally activated the K_{ATP} current, and co-application of the SUR1 inhibitor, glibenclamide 10uM (red), inhibited the current. Weak inward rectification of current is observed. Sample current traces are shown. The vertical scale is 100pA/pF; the horizontal scale is 20mV. Panel A reproduced from Foster and Coetzee,[1] with permission.

have been shown to block outward K_{ATP} -mediated potassium current, thought to contribute to the channel's inward rectification.[1,145,146]

K_{ATP} channels are potently inhibited by intracellular ATP, with an IC50 for channel block of ~ 100 μM originally reported from inside-out patch experiments in ventricular cardiomyocytes.[1,138] Importantly, additional studies have determined that the heterologous co-expression of SUR1 with $K_{ir}6.2$ greatly enhanced sensitivity of K_{ATP} channel inhibition by ATP; heterologous expression of $K_{ir}6.2$ alone had an IC50 of approximately 140 μM,[1,147] while co-expression of SUR1 with $K_{ir}6.2$ enhanced the inhibitory effects of ATP (IC50 of approximately 15 μM).[144] It is believed that ATP's main inhibitory effect on SUR1/ $K_{ir}6.2$ K_{ATP} channels occurs via its binding to the $K_{ir}6.2$ subunits, and that ATP sensitivity of the mature channel is potentiated, via an undetermined mechanism, when SUR1 and $K_{ir}6.2$ subunits co-assemble. It appears, perhaps ironically, that ATP sensitivity conferred upon SUR1/$K_{ir}6.2$ KATP channels is not significantly caused by ATP binding to SUR1's NBF regions, as mutagenesis experiments in NBF1, NBF2, and the linker region between the NBF regions did not prevent channel inhibition by ATP.[1,148] Instead, it appears that the NBF regions of SUR1 confer tremendous sensitivity to K_{ATP} channel activation by MgADP and diazoxide.[148,149]

It has been proposed that SUR1 sensitizes the K_{ATP} channel to ATP inhibition, but at the same time the NBFs within SUR1 hydrolyze nucleotides, blocking the inhibitory effect of ATP on the K_{ATP} channel. MgADP and diazoxide, meanwhile, are thought to contribute to K_{ATP} desensitization of the inhibitory effects of ATP, thereby promoting channel activation.[149] Further evidence that MgADP activates SUR1/ $K_{ir}6.2$ K_{ATP} channels via its binding to SUR1 came from a study in which

$K_{ir}6.2$ expression alone was not activated by MgADP.[150] Adding to the complexity of nucleotide interactions with SUR1/ $K_{ir}6.2$, MgATP, like MgADP, is capable of K_{ATP} activation via binding to SUR1, however the high potency of free ATP inhibition of K_{ATP} generally supersedes, or masks, the activating effects of MgATP.[150] The exact mechanism by which SUR1 assembly with $K_{ir}6.2$ enhances channel sensitivity to ATP inhibition remains unclear.[1]

K_{ATP} (SUR1/ $K_{ir}6.2$) in the Pancreas and Related Pharmacology

SUR1/ $K_{ir}6.2$-containing K_{ATP} channels have been most well characterized in the beta cells of the pancreas. At baseline, K_{ATP} channels are open, leading to potassium efflux. In the fed state, levels of glucose rise in the beta cells, which promote cellular respiration and an increase in the intracellular ATP/ADP ratio. Higher relative ATP concentrations inhibit K_{ATP} currents, leading to cell depolarization, which activates voltage-gated calcium channels. Next, calcium influx promotes exocytosis of vesicle containing insulin, which are released into the blood to regulate blood glucose levels. As such, gain-of-function mutations in *ABCC8* and *KCNJ11* can cause diabetes mellitus due to impaired insulin release from the beta cells, while loss-of-function mutations are associated with congenital hyperinsulinism.

SUR1 is the target of sulfonylurea drugs, such as glibenclamide, which inhibit SUR1/ $K_{ir}6.2$ K_{ATP} channel currents via their binding to SUR1, leading to pancreatic beta cell depolarization and enhanced insulin release. Glibenclamide is clinically employed in patients with diabetes mellitus. Diazoxide is a K_{ATP} channel (and SUR1) activator that requires intracellular ADP for efficacy.[1] Diazoxide causes vasodilation[151] and hyperglycemia,[152] due to activation of K_{ATP} channel isoforms in vascular and pancreatic beta cells, respectively.[1,153,154]

CHAPTER 1:

THE IMPACT OF HETEROZYGOUS *KCNK3* MUTATIONS ASSOCIATED WITH PULMONARY ARTERIAL HYPERTENSION ON CHANNEL FUNCTION AND PHARMACOLOGICAL RECOVERY

SUMMARY

Background- Heterozygous loss of function mutations in the *KCNK3* gene cause idiopathic and familial pulmonary arterial hypertension (PAH). *KCNK3* encodes an acid-sensitive potassium channel, which contributes to maintenance of the resting potential of human pulmonary artery smooth muscle cells. KCNK3 is widely expressed in the body, and dimerizes *in vivo* with other KCNK3 subunits, or the closely related, acid-sensitive KCNK9 channel. We assessed the impact of KCNK3 mutations on channel function in homozygous and heterozygous cellular models of mutant channel expression to determine the pathophysiological and therapeutic implications in PAH.

Methods and Results- We engineered homomeric and heterodimeric mutant and nonmutant KCNK3 channels associated with PAH, and created a platform for the comparison of mutant versus wildtype KCNK3 channel function and pharmacology. Whole-cell patch clamp electrophysiology was performed in human pulmonary artery smooth muscle and COS7 cell lines. We determined that the homomeric and heterodimeric assembled channels in heterozygous KCNK3 conditions leads to mutation-specific severity of channel dysfunction, with a unique pH-dependent mechanism of dysfunction conferred upon the V221L KCNK3 mutant channel. Both wildtype and mutant KCNK3 channels were activated by ONO-RS-082 (10uM) in cultured human pulmonary artery smooth muscle cells causing cell hyperpolarization. We observed robust gene expression of *KCNK3* in healthy and familial PAH patient lungs, but no quantifiable expression of *KCNK9*, and demonstrated in functional studies that KCNK9 minimizes the impact of select KCNK3 loss of function mutations when the two channel subunits co-assemble.

Conclusions- Heterozygous *KCNK3* mutations in PAH leads to variable loss of channel function via distinct mechanisms. Homomeric and heterodimeric mutant KCNK3 channels represent novel therapeutic substrates in PAH. Pharmacological and pH-dependent activation of both wildtype and mutant KCNK3 channels in pulmonary artery smooth muscle cells leads to membrane hyperpolarization. Co-assembly of KCNK3 with KCNK9 subunits can minimize the impact of *KCNK3* loss of function mutations and therefore KCNK9 can provide protection against KCNK3 loss of function in tissues where both *KCNK9* and *KCNK3* are expressed, contributing to the lung specific phenotype observed clinically in patients with PAH due to *KCNK3* mutations.

INTRODUCTION

Pulmonary arterial hypertension (PAH) is a progressive illness characterized by intimal hyperplasia and medial hypertrophy of pulmonary arteries, leading to increased pulmonary vascular resistance, right-sided heart failure, and high mortality rates.[155] A primary disease process of the lung defined by a mean pulmonary arterial pressure ≥ 25 mmHg, pulmonary artery endothelial and smooth muscle cell proliferation and excessive vasoconstriction represent pathogenetic mechanisms in PAH. Mutations in the *BMPR2* gene, a component of the transforming growth factor-β signaling pathway, account for most genetic cases of PAH, while less frequently, mutations in other genes underlie the disease.[5]

We recently identified *KCNK3* as the first ion channelopathy associated with PAH.[3] Using exome sequencing, six distinct mutations in the *KCNK3* potassium channel were identified in patients with familial and idiopathic PAH. All patients were heterozygous at the *KCNK3* gene locus, possessing one mutant and one wildtype (WT) channel. Each of the six *KCNK3* mutations led to loss of channel function, and some mutant channels were functionally rescued by ONO-RS-082 (ONO), a phospholipase A2 inhibitor and KCNK3 activator.[3]

KCNK3 encodes an acid-sensitive two-pore domain potassium channel (also referred to as TASK-1), known for its extreme sensitivity to extracellular pH, especially within the range of physiological pH 7.4.[97] Strongly inhibited by extracellular acidosis and hypoxia, KCNK3 regulates cellular excitability, and is thought to contribute to hypoxic pulmonary vasoconstriction.[73] The voltage-insensitivity of KCNK3 renders the channel open across all voltages, leading to potassium efflux from cells expressing the channel, which contributes to the negative resting potential.

KCNK3 is widely expressed in the human body, including in the central nervous system, heart, adrenal glands, and PASMCs.[74,89]

KCNK3 currents contribute to the resting potential of native human pulmonary arterial smooth muscle cells (hPASMCs) and impact pulmonary arterial tone and smooth muscle cell growth, while KCNK3 downregulation or inhibition leads to PASMC depolarization, proliferation, and pulmonary arterial constriction.[73-75,88] Notably, KCNK3 downregulation was recently identified as a pathogenic hallmark of PAH in humans and in a monocrotaline-induced pulmonary hypertension rat model, and administration of ONO alleviated signs of pulmonary hypertension in the animal model, further implicating KCNK3 as a therapeutic target in PAH.[3,75]

KCNK3 dimerizes *in vivo*, forming functional channels from two subunits linked together.[156] Adding to the complexity of KCNK3 channel interactions, the closely related acid-sensitive KCNK9 channel dimerizes with KCNK3, forming KCNK9-KCNK3 heterodimeric channels in tissues where both channels are expressed.[103,106-108,111] KCNK9 is more maximally activated at physiological pH 7.4 than KCNK3.[100,102] The channels are co-expressed in a variety of tissues, promoting tissue-specific diversity of channel function. Importantly, KCNK3, but not KCNK9, has been shown to be expressed in hPASMCs.[73]

In this study, we investigate: (1) mechanisms of heterozygous *KCNK3* loss of function mutations in PAH by studying channel function over a broad pH range; (2) the capacity of mutant and wildtype KCNK3 channels to serve as therapeutic targets in PAH; (3) the impact of selected *KCNK3* mutations on channel function and pharmacology in physiologically relevant

heterozygous conditions; and (4) the potential role for KCNK9 in underlying the lung-specific disease phenotype conferred upon patients with heterozygous *KCNK3* mutations.

METHODS

Study Patients

Human lung parenchymal samples were obtained from 10 control patients with healthy lungs (failed donor lungs); seven were female, three were male. Samples from patients with familial pulmonary arterial hypertension (FPAH) were obtained; three were female, two were male. Samples from patients with congenital cardiac defect -associated pulmonary arterial hypertension (APAH) were obtained; five patients were female. cDNA samples were provided by the Pulmonary Hypertension Breakthrough Initiative (PHBI).[157] The protocol, "Studying Gene Expression in Pulmonary Arterial and Lung Tissue in Healthy and Diseased Samples," (#AAAQ2454) was approved by the Institutional Review Board at Columbia University Medical Center. *KCNK3* mutations in PAH patients were identified as previously reported.[3]

Quantitative Real-Time Polymerase Chain Reaction (qRT-PCR)

The TaqMan gene expression system was used to quantify mRNA expression (Applied Biosystems). RNA and cDNA from lung samples were prepared for gene expression analysis using a previously described protocol.[157] No-template controls lacking cDNA were included, to verify the specificity of the assay at recognizing cDNA templates of interest. Experiments were performed in duplicate for each sample. Data are expressed as means of the average cycle threshold (Ct) value of duplicates, and as fold changes in expression (2^{ddCt} method). Commercially available assays from Applied Biosystems were used for priming/probing of cDNA samples, including:

1) KCNK3 (Assay ID= Hs00605529_m1)
2) KCNK9 (Assay ID= Hs00363153_m1)
3) GAPDH (Assay ID= Hs02758991_g1)

Expression of KCNK3 and KCNK9 in PAH and control lungs was normalized to GAPDH expression. Average cycle threshold (Ct) values at which signals for each gene appeared were calculated based on 40-cycle assays. For samples in which no amplification signal was produced, a Ct value of "40" was assigned for the purpose of calculating mean Ct values.

Molecular Biology

Mutations were engineered into human *KCNK3* cDNA in a pcDNA3.1+ expression vector by site-directed mutagenesis using QuickChange (Stratagene).[3] Human *KCNK9* cDNA in a pIRES-GFP and pcDNA3.1+ vector was used. Where noted, *KCNK3* constructs were tagged with a C-terminal green fluorescent protein (GFP). Tandem-linked *KCNK3-KCNK3* and *KCNK9-KCNK3* dimer constructs were engineered in pcDNA3.1+ vectors by joining two KCNK subunits with a glycine-rich linker (the vector sequence from the AFLII to BAMHI restriction sites plus 5 glycine residues), and subcloning into a pcDNA3.1+ vector.

Materials

ONO-RS-082 (Enzo Life Sciences), ML365 (MedChem Express), and ruthenium red and DMSO (Life Technologies) were purchased commercially. ONO-RS-082 and ML365 were dissolved in DMSO and ruthenium red in water in 100mM stock solutions and stored at -20°C. Drugs were

diluted to 10μM in drug-containing external solutions, and DMSO 10μM was added where appropriate to control (drug-free) solutions. Lipofectamine, Lipofectamine LTX, and Plus Reagent (Invitrogen) were used for transfection. 0.25% Trypsin/EDTA and Trypsin Neutralizer (Gibco) were used for splitting cell cultures. Human pulmonary artery smooth muscle cells (Gibco) were grown in Smooth Muscle Growth Medium-2 with supplements (SmGM-2 bulletkit, Lonza). COS7 cells (American Type Culture Collection) were cultured in medium containing DMEM 1X + GlutaMAX-1 with 4.5g/L D-Glucose and 110mg/L Sodium Pyruvate (Gibco), and supplemented with 10% Fetal Bovine Serum (Gibco) and 1% Penicillin/Streptomycin (Gibco).

Cell Culture and Heterologous Channel Expression

KCNK3 and *KCNK9* channel constructs were expressed in cultured hPASMC and COS7 cell lines. GFP (in a pcDNA3.1+ vector) was co-expressed or tagged to the C-terminus of the channel as a marker of transfection. A previously established transfection protocol using Lipofectamine reagents was employed in COS7 cells [3], with modifications to optimize efficiency in hPASMCs.

<u>COS7 cells:</u>

On day 0, a T25 flask ~40-50% confluent was transfected with *KCNK3* or *KCNK9* cDNA using the following protocol: 2μg of *KCNK3* or *KCNK9* cDNA (20μl from a stock solution of 0.1μg/μl cDNA) + 1μg GFP if the *KCNK3* construct was not GFP-tagged + 20μl PLUS reagent + OptiMEM medium supplemented with L-glutamine up to 200μl were mixed and incubated at room temperature for 20 minutes. Of note, for co-expression of two *KCNK3* (or *KCNK3* + *KCNK9*) constructs, 1.5μg of each cDNA was transfected.

Next, 20µl Lipofectamine + 180µl OptiMEM medium supplemented with L-glutamine were added to the cocktail and incubated for 20 additional minutes at room temperature. Next, 1.6ml of OptiMEM supplemented with L-glutamine was added to the cocktail and mixed, and the 2ml transfection cocktail was pipetted into the COS7 cell flask after removal of the culture medium. The flask was returned to the 37°C cell culture incubator (conventional growth conditions, 5% CO_2) for approximately 4-6 hours. After incubation, the transfection cocktail was replaced by COS7 culture medium.

On day 1 in the afternoon, cells transfected on day 0 were split into 10cm dishes in the culture hood as follows: culture medium was removed from the T25 flask, and 5ml of 1X PBS was quickly added and removed, before 2ml 0.25% Trypsin/EDTA was added to the flask. The flask was then placed back in the 37°C incubator for approximately 5 minutes. After cells were dislodged from the flask bottom, 5ml of cell medium was added to the flask and pipetted to dislodge more cells. The 7ml cell solution was pipetted out of the flask and transferred into a 15ml conical tube, and centrifuged for 1.5 minutes at 1xg. The conical tube was returned to the culture hood, medium removed, and new cell medium added for cell suspension. Cells were then pipetted into 10cm dishes, and placed back in the 37°C incubator. On day 2 (and day 3 if cells were still healthy), the 10cm dishes were used for patch clamp experiments.

Human Pulmonary Artery Smooth Muscle Cell Line:

In hPASMCs, transfection of *KCNK3* cDNA required the following protocol: On day 0, hPASMCs in a T25 flask were split into 10cm dishes suitable for patch clamp experiments. Cells were split using the manufacturer's protocol (Gibco), which required 0.25% Trypsin/EDTA for cell

detachment from the flask, and Trypsin Neutralizer to resuspend cells before plating in 10cm dishes. Cells were grown in supplemented Smooth Muscle Growth Medium-2 (Lonza).

On day 1, cell were transfected under the culture hood, as follows: per 10cm dish, 0.6µg *KCNK3* cDNA tagged with GFP at the C-terminus (from a cDNA stock solution of 0.1µg/µl) + 0.6µl PLUS reagent + 50µl OptiMEM medium supplemented with L-glutamine, were mixed and incubated at room temperature for 10 minutes. Next, 1.5µl Lipofectamine LTX per dish was added to the cocktail and incubated for an additional 30 minutes at room temperature. Equal proportions (58.1µl) of the cocktail were then pipetted into each 10cm dish, and dishes were returned to the 37°C incubator. On day 2 (and day 3 if cells were still healthy), 10cm dishes were used for patch clamp experiments.

Electrophysiology

KCNK3 channel current and membrane potential changes were recorded by whole-cell patch clamp in hPASMCs and COS7 cells. An Axopatch 200B amplifier (Axon Instruments), Digidata 1440A model, and pClamp 10 software were used for recording and analysis (Molecular Devices, CA). Pipette resistances generally ranged from 1-4 MOhm. For all voltage clamp experiments, cells were held at -80mV and a 500ms voltage ramp was applied once every 3 seconds, with voltage increasing linearly from -120mV to +60mV before returning to holding. Expressed *KCNK3*, *KCNK9*, and tandem dimer constructs were recorded. For current clamp experiments, changes in membrane potential were recorded over time after first applying the voltage ramp to verify stability of the patch and expression of KCNK3 channels.

Perfusion of extracellular solutions containing pharmacological agents or different pH values occurred at recorded intervals during patch clamp experiments, at room temperature under normoxic conditions. All experiments with pharmacological agents were conducted at extracellular pH 7.4.

For experiments in COS7 cells, solutions were prepared as previously reported [3]: pipette (internal) solution (in mmol/L) contained: 150 KCl, 3 MgCl2, 5 EGTA, 10 HEPES, adjusted to pH 7.2 with KOH. Bath (extracellular) solution (in mmol/L) contained: 150 NaCl, 5 KCl, 1 MgCl2, 1.8 CaCl2, 10 HEPES adjusted to pH 6.4, 7.4, or 8.4 with NaOH.

For experiments in hPASMCs, solutions were adapted from a previous study [73]: pipette (internal) solution (in mmol/L) contained: 135 K-methanesulphonate, 20 KCl, 2 Na2ATP, 1 MgCl2, 1 EGTA, 20 HEPES, adjusted to pH 7.2 with KOH. Bath (extracellular) solution (in mmol/L) contained: 140.5 NaCl, 5.5 KCl, 1.5 CaCl2, 1 MgCl2, 10 glucose, 0.5 Na2HPO4, 0.5 KH2PO4, 10 HEPES, adjusted to pH 6.4, 7.4, or 8.4 with NaOH.

In COS7 cells and hPASMCs, solutions at pH 5.0 contained 10 mmol/L 2-(N-morpholino)ethane sulfonic acid instead of HEPES. Solutions at pH 10.4 contained 10 mmol/L Tris-Base instead of HEPES.

Voltage Clamp Analysis

Cell capacitance values were recorded for individual cell recordings, and whole cell currents were normalized to cell capacitance (pA/pF) where indicated. Measurements of current for drug analysis

(ONO-RS-082, ML365, and ruthenium red) were taken at -50mV to minimize contributions from background cellular ionic currents. This was performed by taking the mean current at -50mV over an approximately 5 millisecond range centered around -50mV, from the average of 2 to 6 consecutive traces based on stability of the recording. Measurements of current were taken at +60mV for pH experiments (as previously shown in [3]), by calculating the mean current during the last ~5 milliseconds of the trace, based on the average of 2 to 6 consecutive traces depending on stability of the recording at each pH value.

Leak subtraction was manually performed on all recordings in this study. Based on the Nernst equilibrium potential for potassium (E_K) close to -80mV, negative current values recorded at the holding potential of -80mV were designated as leak current, and a proportional amount of leak current was extrapolated across the voltage ramp range; an assumption applied for analysis given the virtually voltage-independent properties of the KCNK3 and KCNK9 channels. Hence, analysis of mean current in any drug condition at -50mV required adding 5/8 of the value of the leak current at -80mV to the mean current value recorded at -50mV, and analysis of mean current at +60mV required subtracting 6/8 of the value of the leak current at -80mV from the mean current value recorded at +60mV.

Current Clamp Analysis

Measurements of membrane potential were taken as the mean from the last ~10 seconds in any given pH or drug condition. To standardize drug analysis, all ONO membrane potential measurements were taken from the last ~10 seconds of five minutes of ONO application, and all ONO+ML365 membrane potential measurements were taken from the last ~10 seconds of two

minutes of ONO+ML365 application. Using pClamp software, a 50X data reduction of recordings was performed for data transfer compatibility to Origin software for figure purposes. Data analysis was performed on raw data only.

Statistical Analyses

Graphic analysis was performed with Origin 7.0 and 9.0 (Microcal Software, Northampton, MA). pClamp 10 software was used for analysis of raw electrophysiological recordings. Data are reported as means ± SEM, based on *n* observations. Student's *t* tests and one-way ANOVA with post-hoc Tukey tests were applied as indicated, and significant differences were determined based on $p < 0.05$. Statistical tests were performed using Origin and Excel (Microsoft, Bellevue, WA) software.

RESULTS

Functional characterization of *KCNK3* variants identifies a unique acid sensing phenotype

We previously identified six loss of function mutations in *KCNK3* causing PAH.[55] Given the extreme sensitivity of KCNK3 channels to extracellular pH changes within the physiological pH range, here we investigated the mechanistic basis of loss of channel function focusing on possible mutation-induced changes in the pH dependence of the expressed channels. Wildtype (WT) or mutant KCNK3 channels were expressed in COS7 cells, and a whole-cell voltage ramp was applied across a physiological voltage range (Figure 1.1A, top). As expected for WT KCNK3 channels, we observed appreciable K^+ current at physiological extracellular pH 7.4; inhibition of current by acidosis, pH 6.4; and activation of current by alkalosis, pH 10.4 (Figure 1.1A and 1.1B).[97]

Compared to WT KCNK3 channels, all six PAH-associated mutant KCNK3 channels exhibited loss of function at pH 7.4 and pH 10.4 (Figure 1.1B), with one notable exception: V221L KCNK3 conferred loss of function at physiological pH 7.4, with recovery of function observed at alkalotic pH 10.4 (Figure 1.1A and 1.1B). Given its unique alteration in pH dependent regulation of activity, V221L KCNK3 was tested in more physiologic conditions to understand the consequence of dysfunction on channel regulation and pharmacology.

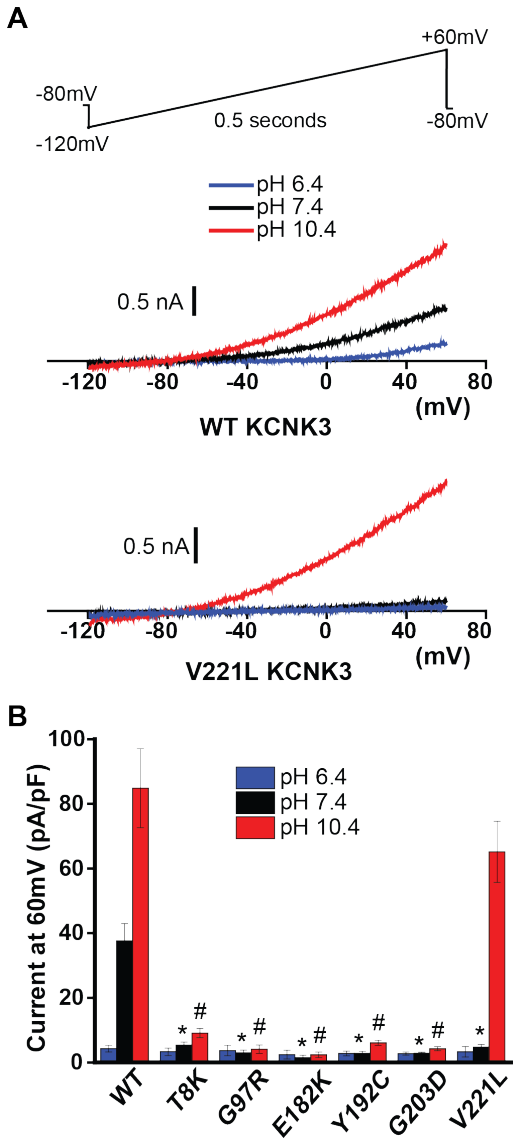

Figure 1.1 PAH-associated mutant KCNK3 channels demonstrate mutation-specific severity of loss of function, across a broad pH range in COS7 cells. **A,** Typical voltage clamp recordings of WT (top) and V221L (bottom) KCNK3. Sample current traces at pH 6.4 (blue), 7.4 (black), and 10.4 (red) are shown. A voltage ramp (top) was applied, -120mV to +60mV over 0.5s, every 3 seconds, from a holding potential of -80mV for all voltage clamp recordings in this study. **B,** Summary of current density (pA/pF at 60mV) of cells expressing WT or one of the PAH-associated mutant KCNK3 channels (n=3 to 9 cells at pH 6.4; n= 6 to 33 cells at pH 7.4; n= 6 to 32 cells at pH 10.4). Bars show mean ± SEM. * indicates $p<0.05$ at pH 7.4; # indicates $p<0.05$ at pH 10.4, for the comparison of WT and each KCNK3 mutant channel by one-way ANOVA and post-hoc Tukey test.

Cultured hPASMCs provide a physiological platform for *KCNK3* expression

KCNK3 currents contribute to the resting potential of native PASMCs, and the downregulation or inhibition of KCNK3 causes PASMC depolarization, excessive proliferation, and pulmonary arterial constriction.[73-75,88] Cultured PASMCs have been employed previously to study overexpressed potassium channel activity, regulation, and pharmacology in the context of PAH.[81,85] We adapted this approach to test the hypothesis that both WT and mutant (eg. V221L) KCNK3 channels represent therapeutic targets in PAH (Figure 1.2).

As loss of function could result from lack of KCNK3 expression, we first engineered a C-terminal GFP-tagged KCNK3 channel (KCNK3-GFP, Figure 1.2A) and screened its function in COS7 cells. We observed a similar pH dependence for KCNK3-GFP versus KCNK3, as well as a significant increase in current density (pA/pF, measured at 60mV) for KCNK3-GFP (Figure 1.2B). In voltage clamp experiments, ONO 10μM activated KCNK3-GFP with similar efficacy to KCNK3 channels (Figure 1.2C; and compare to KCNK3 activation previously reported[55]). The recently developed KCNK3 inhibitor, ML365 10μM,[158,159] produced robust inhibition of KCNK3-GFP currents (Figure 1.2C). Mean current densities (pA/pF) in response to the drugs are summarized in Figure 1.2C, measured at -50mV to minimize interference of background ionic currents.

The use of KCNK3-GFP thus did not appreciably change KCNK3 function or pharmacology, while providing the advantage of increased current density. Next, KCNK3-GFP was expressed in cultured hPASMCs, identified by green fluorescence, and produced similar current density (pA/pF at 60mV) compared to KCNK3-GFP expression in COS7 cells (Figure 1.2D).

Loss of native *KCNK3* expression was previously demonstrated in cultured PASMCs,[32] and confirmed functionally in our system of cultured hPASMCs by applying ML365 10μM in non-transfected hPASMCs, and observing no significant effect on cell currents (Figure 1.2E and 1.2F, and Figure 1.3B). In comparison, KCNK3-GFP expression in hPASMCs produced robust channel activity, inhibited by ML365 10μM (Figure 1.2G and 1.2H, and Figure 1.3B and 1.3C). We thus developed a platform to compare the relative impact of expressed mutant versus WT KCNK3 channels on hPASMC membrane potential, and the effect of KCNK3 pharmacological agents in a more physiological environment (Figure 1.4).

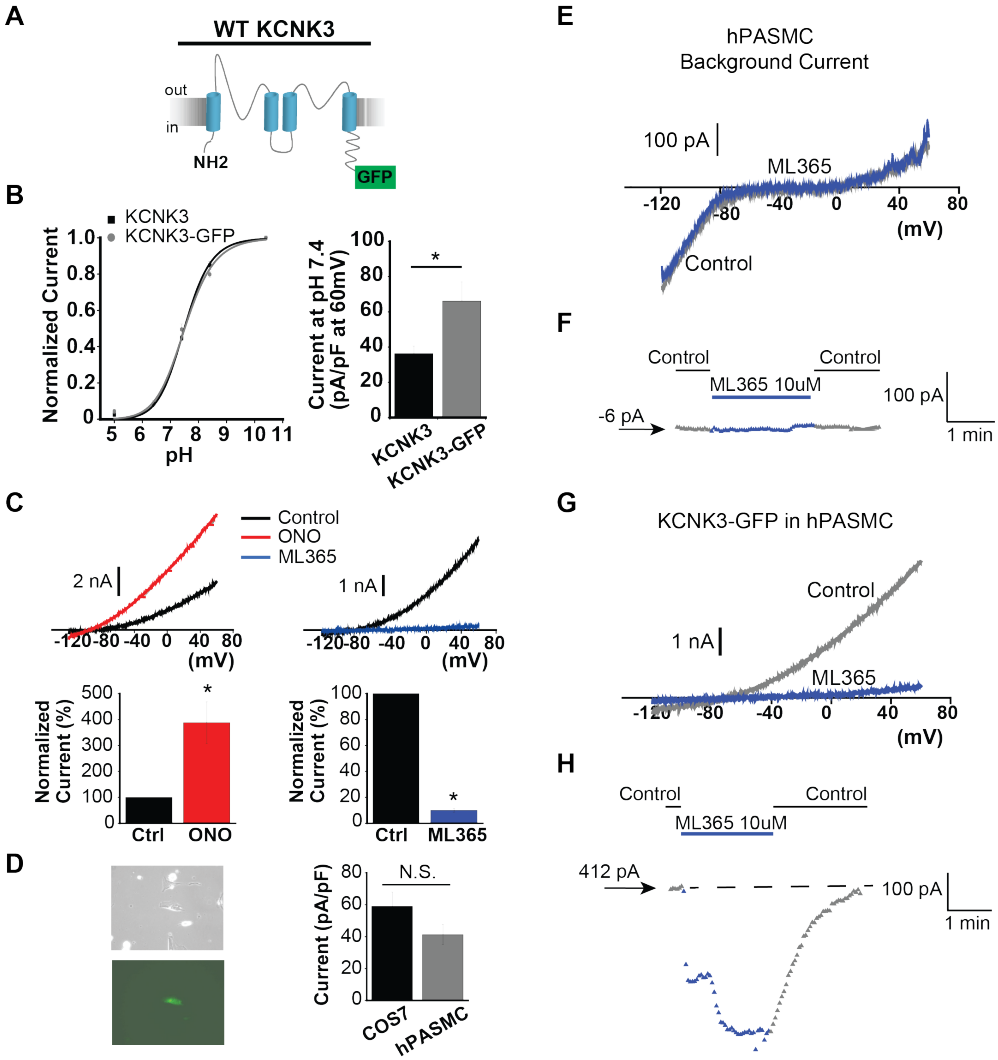

Figure 1.2. KCNK3 expression platform in human pulmonary artery smooth muscle cells (hPASMCs). **A,** KCNK3, tagged with GFP at the C-terminus, was engineered (KCNK3-GFP). **B,** KCNK3-GFP is activated by ONO-RS-082 10uM (red trace, left) and inhibited by ML365 10uM (blue trace, right), under voltage-clamp shown in COS7 cells. Pre-drug (control, black traces) and drug conditions are at pH 7.4. Bar graphs (bottom) show fold change in current at -50mV after ONO (n=8 cells) or ML365 (n=12 cells) application. **C,** Cultured hPASMCs expressing KCNK3-GFP fluoresce green (top, right). Bar graph shows KCNK3-GFP current activity at pH 7.4 (pA/pF at 60mV) in hPASMCs (grey, n=20 cells) versus COS7 cells (black, n=26 cells). **D** Background hPASMC current at pH 7.4 (control, grey trace), and current in ML365 10uM (blue trace) are shown. **E,** Sample ML365 time course of action in control and drug conditions, measured at -50mV, from a starting current amplitude of -6pA indicated by the arrow. **F,** Current from hPASMC expressing KCNK3-GFP is shown at pH 7.4 (control, grey trace), and in ML365 10uM (blue trace). **G,** Sample ML365 time course of action in control and drug conditions, measured at -50mV, from a starting current amplitude of 412 pA indicated by the arrow. Horizontal dashed line is drawn at the starting level of current in control solution. Bar graphs show mean ± SEM. * indicates $p<0.05$ by the paired (panel B) and unpaired (panel C) Student's *t* test.

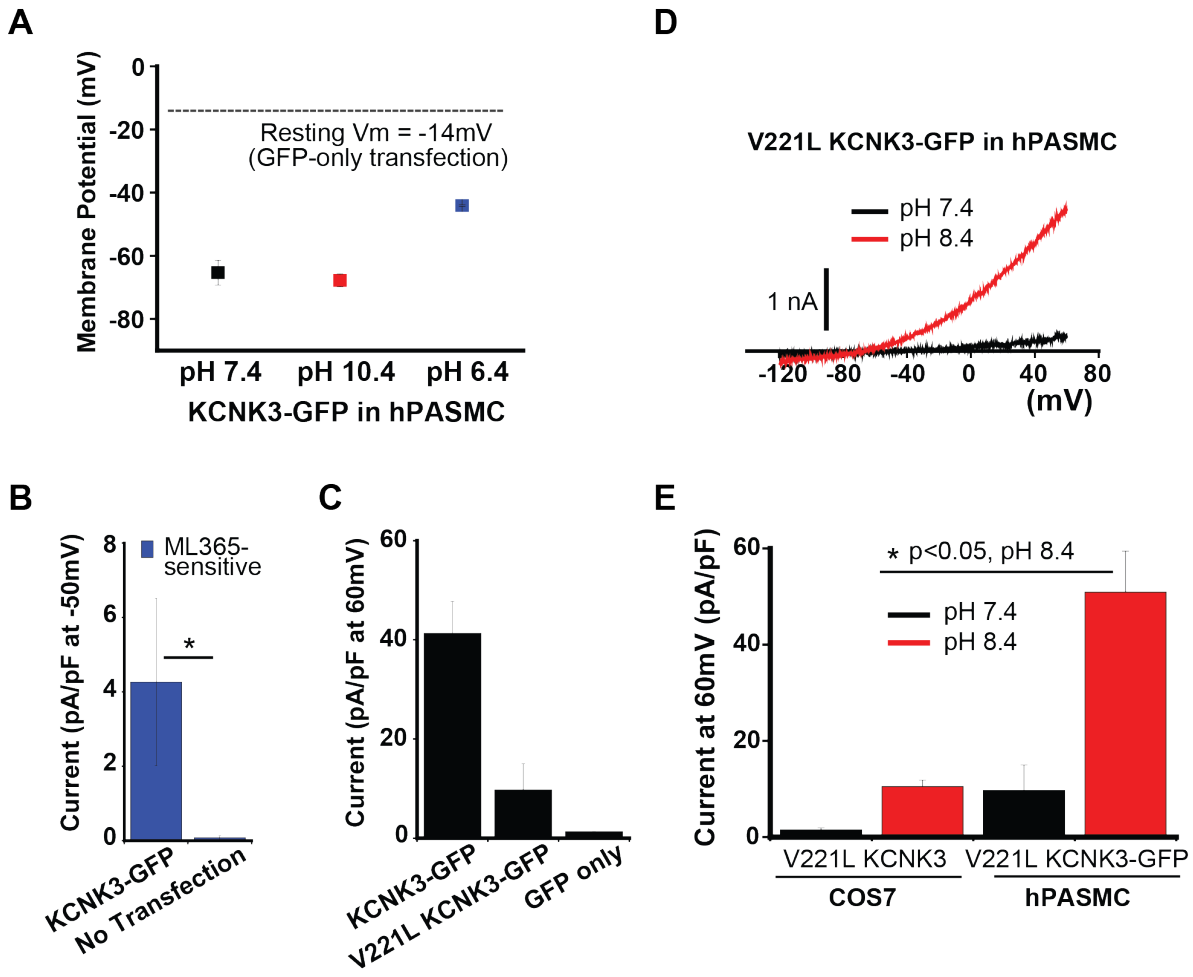

Figure 1.3. KCNK3-GFP expression and activity in hPASMCs. A, Summary of current clamp results of KCNK3-GFP expressed in hPASMCs, with mean membrane potentials (mV) measured at pH 6.4 (blue), pH 7.4 (black), and pH 10.4 (red) shown (n=2 to 4 cells per pH value). **B**, Comparison of the ML365-sensitive current (pA/pF at -50mV, pH 7.4), in hPASMCs expressing KCNK3-GFP (n=3 cells) versus no transfection (n=6 cells). **C**, Gradient of current expression (pA/pF at 60mV, pH 7.4) in hPASMCs expressing KCNK3-GFP (n=20 cells), V221L KCNK3-GFP (n=7 cells), and GFP only (n=3 cells). **D**, Sample current trace of V221L KCNK3-GFP in hPASMC at pH 7.4 (black) and pH 8.4 (red). **E**, Summary of V221L KCNK3 expression in COS7 cells versus V221L KCNK3-GFP expression in hPASMCs (n=4 to 7 cells per lane), showing greater current activity of expressed channels in hPASMCs (pA/pF at 60mV, pH 7.4 in black, pH 8.4 in red). Data are represented as means ± SEM. * indicates $p<0.05$ by the unpaired Student's *t* test.

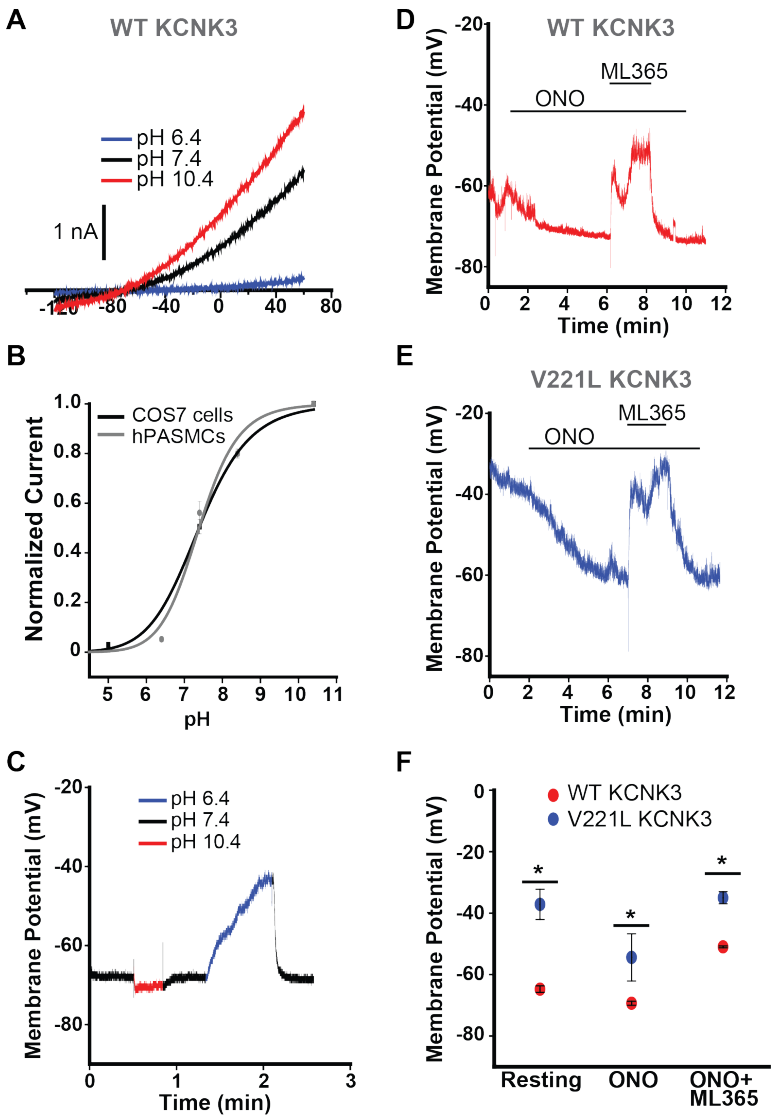

Figure 1.4. Robust response of KCNK3 channels to pH changes and pharmacological modulators in hPASMCs. **A,** Voltage clamp recording of KCNK3-GFP expressed in hPASMCs at pH 6.4 (blue), pH 7.4 (black), and pH 10.4 (red). **B,** KCNK3-GFP expression in hPASMCs (grey curve) versus COS7 cells (black curve) across a broad pH range, with current normalized to max current at pH 10.4 (n =9 to 12 cells per pH data point in COS7; n=2 to 6 cells per pH data point in hPASMCs; fitted by the Hill equation). **C,** Current clamp recording of WT KCNK3-GFP, with changes in membrane potential (mV) measured at pH 6.4 (blue), pH 7.4 (black), and pH 10.4 (red). **D,** Current clamp recording of WT KCNK3-GFP (red trace), showing changes in membrane potential (mV) upon application of ONO, ONO+ML365, or pH 8.4. **E,** Current clamp recording of V221L KCNK3-GFP (blue trace), showing changes in membrane potential (mV) upon application of ONO, or ONO+ML365. **F,** Current clamp summary of WT (red) and V221L (blue) KCNK3-GFP for resting potential, ONO, and ONO+ML365 conditions (n=3 to 11 cells per condition). Data plots represent means ± SEM. * indicates $p<0.05$ by the unpaired Student's *t* test; N.S. indicates no significant difference.

Activation of PAH-associated mutant KCNK3 channels in hPASMCs

KCNK3-GFP expression in hPASMCs produced a consistent pH dependence of expressed channel activity compared to expression in COS7 cells (Figure 1.4A and 1.4B). We recorded membrane potentials in cells expressing KCNK3-GFP at physiological pH 7.4, upon channel activation by pH 10.4, and upon inhibition by pH 6.4. A sample current clamp trace (Figure 1.4C) reveals a resting potential of -68mV at pH 7.4, hyperpolarization to -70mV at pH 10.4, and depolarization to -44mV at pH 6.4 (summarized above in Figure 1.3A).

Next, we determined the relative impact of pharmacological activation and inhibition of KCNK3 in hPASMCs expressing WT or V221L KCNK3-GFP. A recording of a cell expressing WT KCNK3-GFP (Figure 1.4D), demonstrates a resting potential of -62mV at physiological pH 7.4; hyperpolarization by ONO 10μM to -73mV; and depolarization to -51mV upon co-application of ML365 10μM. By comparison, a recording of a cell expressing V221L KCNK3-GFP (Figure 1.4E), reveals a resting potential of -40mV at physiological pH 7.4; hyperpolarization by ONO 10μM to -61mV; and depolarization to -33mV upon co-application of ML365 10μM. A summary of resting potentials, and responses to ONO 10μM, and to ML365 10uM, is shown in Figure 1.4F, for WT and V221L KCNK3-GFP. In each condition, V221L KCNK3-GFP responses are significantly different than WT.

KCNK3 heterodimeric channels are functional reporters of KCNK3 heterozygosity

After demonstrating that PAH-associated mutant KCNK3 channels are potential therapeutic targets in hPASMCs, we investigated the consequence of heterozygosity on channel function more closely. All patients harboring PAH-associated KCNK3 mutations in our study are heterozygous at the KCNK3 locus, possessing one mutant and one WT KCNK3 channel subunit.[55] KCNK3 is known to dimerize, forming functional channels from two subunits joined together.[156] For heterozygous expression, net current is therefore a result of three populations of channels: homodimers of WT or mutant KCNK3, and heterodimers with one of each subunit. To fully characterize the impact of the KCNK3 mutations in clinically relevant heterozygous conditions, we engineered tandem-linked KCNK3 dimers by joining two KCNK3 subunits with a glycine-rich linker. By forcing assembly of mutant and/or WT KCNK3 subunits to one another, we assessed function of discrete proportions of channels that form in a heterozygous patient (Figure 1.5).

We tested function of mutant heterodimeric channels containing the V221L mutation. Figure 1.5A and 1.5B depict the engineered WT KCNK3 homodimer and WT-V221L mutant KCNK3 heterodimer, respectively, with sample current traces shown at extracellular pH 6.4, 7.4, and 10.4 from voltage clamp experiments. Figure 1.5C summarizes current density measurements (pA/pF at 60mV) for each dimer. Significant loss of function was observed at pH 7.4 for WT-V221L heterodimeric channels. We recorded V221L-containing KCNK3 function over a broad pH range, 5.0 through 10.4, and notably, WT-V221L KCNK3 produced an intermediate rightward shift in pH dependence (Figure 1.5D, blue curve), with intermediate channel activity at physiological pH 7.4, compared to WT KCNK3 (Figure 1.5D, black curve), and V221L KCNK3 (Figure 1.5D, red curve), for which we observed an extreme rightward shift in pH dependence.

The dominant-negative impact of KCNK3 heterozygosity on channel function was quantified further, as we observed that the linked heterozygous WT-V221L KCNK3 dimers produce more consistent channel function than co-expression assays of WT+V221L KCNK3 channels. Figure 1.5E shows a scatterplot of individual voltage clamp recordings (n=16 to 33 cells per condition: WT, V221L, WT-V221L heterodimer, and WT+V221L co-expression), with each data point representing the current recorded at physiological pH 7.4, normalized to maximal current at pH 10.4, measured at 60mV. Loss of function was observed for all conditions containing V221L mutant channels (homomeric V221L, WT-V221L heterodimer, and co-expression of WT + V221L). Importantly, we observed greater variation in current when co-expressing WT + V221L channels compared to WT-V221L heterodimer expression, as the co-expression population includes randomly assembled homodimers of WT and V221L KCNK3, in addition to WT-V221L heterodimers.

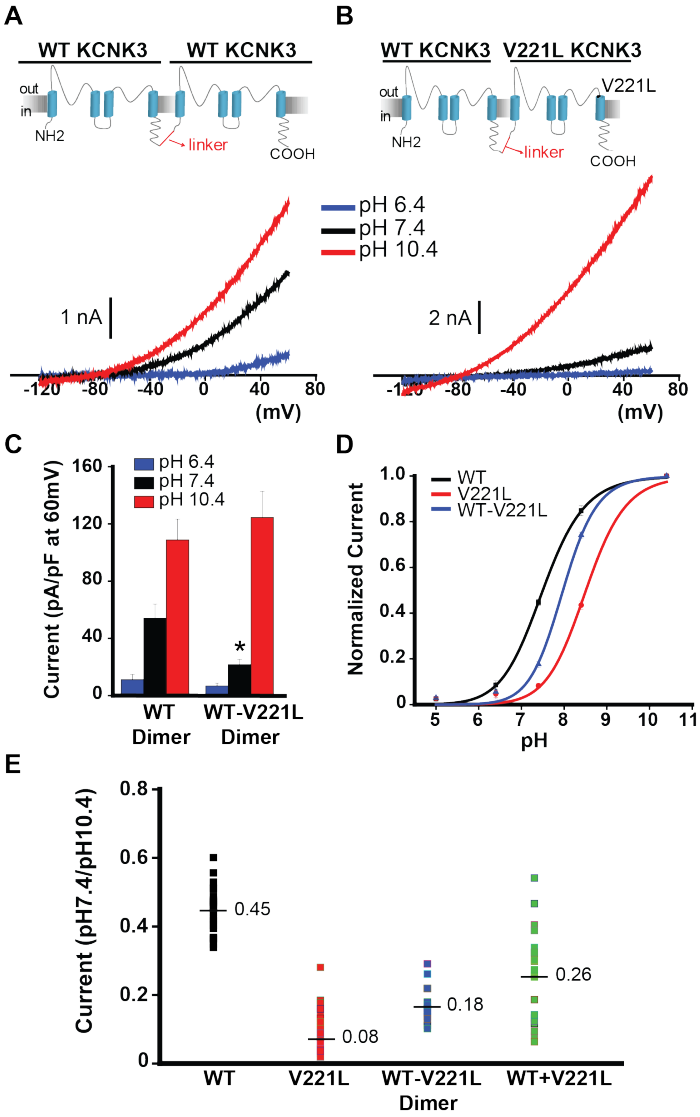

Figure 1.5. Tandem-linked KCNK3 heterodimeric channels are functional reporters of KCNK3 heterozygosity. **A and B,** KCNK3 dimers were engineered by interconnecting two KCNK3 subunits with a glycine-rich linker. The WT KCNK3 homodimer (panel **A**) and the WT-V221L KCNK3 heterodimer (panel **B**) are depicted, with sample voltage clamp recordings for each condition. Current traces at pH 6.4 (blue), 7.4 (black), and 10.4 (red) are shown. **C,** Summary of current densities (pA/pF at 60mV) at pH 6.4, 7.4, and 10.4 (n= 4 to 16 cells per pH bar). **D,** KCNK3 current activity is depicted for WT (black curve), V221L (red curve), and WT-V221L heterodimer (blue curve), at extracellular pH 5.0 through 10.4, with current normalized to max current at pH 10.4 (n= 5 to 33 cells per pH value plotted; fitted by the Hill equation). **E,** Scatterplot of current at pH 7.4 normalized to current at pH 10.4, for WT, V221L, WT-V221L heterodimer, and WT + V221L co-expression. Each dot represents an independent cell recording. Mean current in each condition is displayed at the horizontal line (n=16 to 33 cells per condition, measured at 60mV). Bar graphs and pH curve values show means ± SEM. * indicates $p < 0.05$ for the comparison of WT versus WT-V221L KCNK3 dimer conditions in panel C by the unpaired Student's *t* test; In Panel E, $p < 0.05$ for the comparison of all KCNK3 conditions, calculated by one-way ANOVA and post-hoc Tukey test.

Pharmacological activation of heterodimeric mutant KCNK3 channels

In voltage clamp recordings, WT KCNK3 homodimers (Figure 1.6A) and WT-V221L mutant heterodimers (Figure 1.6B) were activated by ONO 10μM (shown in red), and inhibited by ML365 10μM (shown in blue), in voltage clamp recordings. PAH-associated KCNK3 heterodimeric channels thus represent therapeutic targets in PAH, susceptible to pharmacological recovery. Patients with PAH due to heterozygous *KCNK3* mutation therefore possess a significant proportion of assembled KCNK3 channels (wildtype and mutant) that, dependent on the mutation, represent viable targets for treatment.

As shown previously,[55] cells expressing T8K or E182K KCNK3 channels are modulated by ONO 10μM. Importantly, ONO is not a KCNK3-specific activator and produces variable responses in the presence and absence of KCNK3; as such, it is difficult to quantify the drug's effect, especially in the setting of loss-of-function KCNK3 mutant channels that produce small currents at baseline (Figure 1.7A-C).

In addition to the WT-V221L KCNK3 heterodimer, the WT-E182K KCNK3 heterodimer responds robustly to current activation by ONO 10μM, suggesting that a significant population of channels (wildtype and mutant heterodimeric) in patients with heterozygous KCNK3 mutations respond to pharmacological activation (Figure 1.7D).

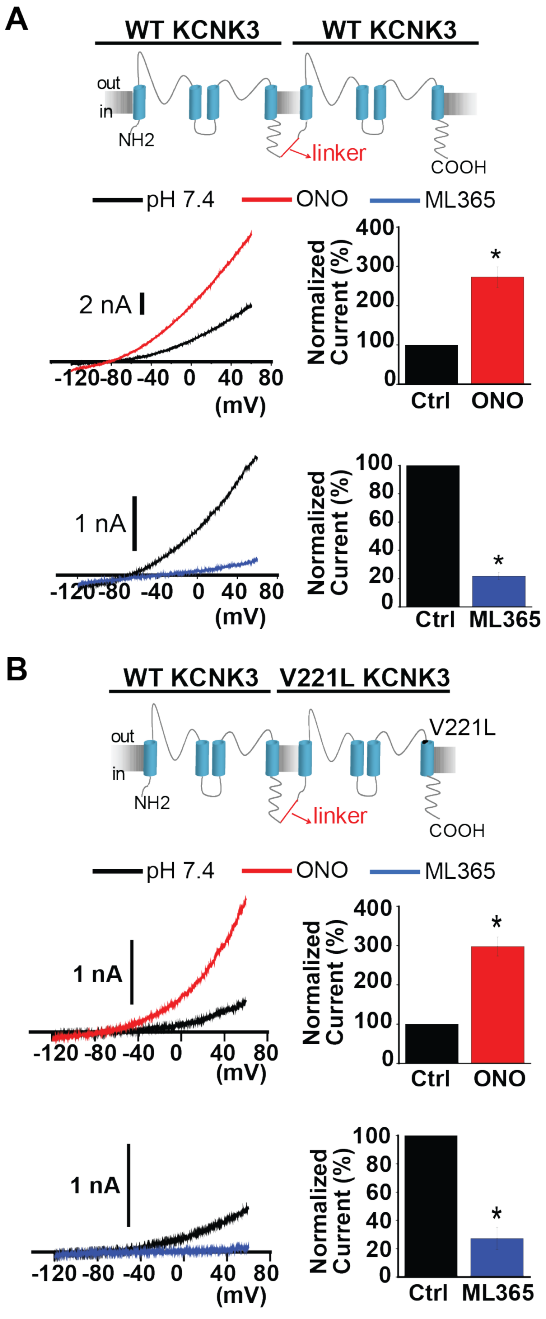

Figure 1.6. Wildtype (WT) and mutant KCNK3 dimers respond to pharmacological modulation. **A,** WT KCNK3 dimer (top) is activated by ONO-RS-082 10uM (red trace) and inhibited by ML365 10uM (blue trace), in current recordings from voltage clamp experiments. Control (pre-drug, pH 7.4) traces are shown in black. Bar graphs show fold change in current at -50mV for the WT KCNK3 dimer, after ONO (red, n=4 cells) or ML365 (blue, n=7 cells) application. **B,** WT-V221L KCNK3 heterodimer (top) is activated by ONO-RS-082 10uM (red trace), and inhibited by ML365 10uM (blue trace), and heterodimer channel activity was confirmed by channel activation at extracellular pH 10.4 (grey dotted traces). Control (pre-drug, pH 7.4) traces are shown in black. Bar graphs show fold change in current at -50mV for the WT-V221L heterodimer, after ONO (red, n=5 cells) or ML365 (blue, n=3 cells) application. Bar graphs display mean ± SEM. * indicates $p<0.05$ by the paired Student's *t* test.

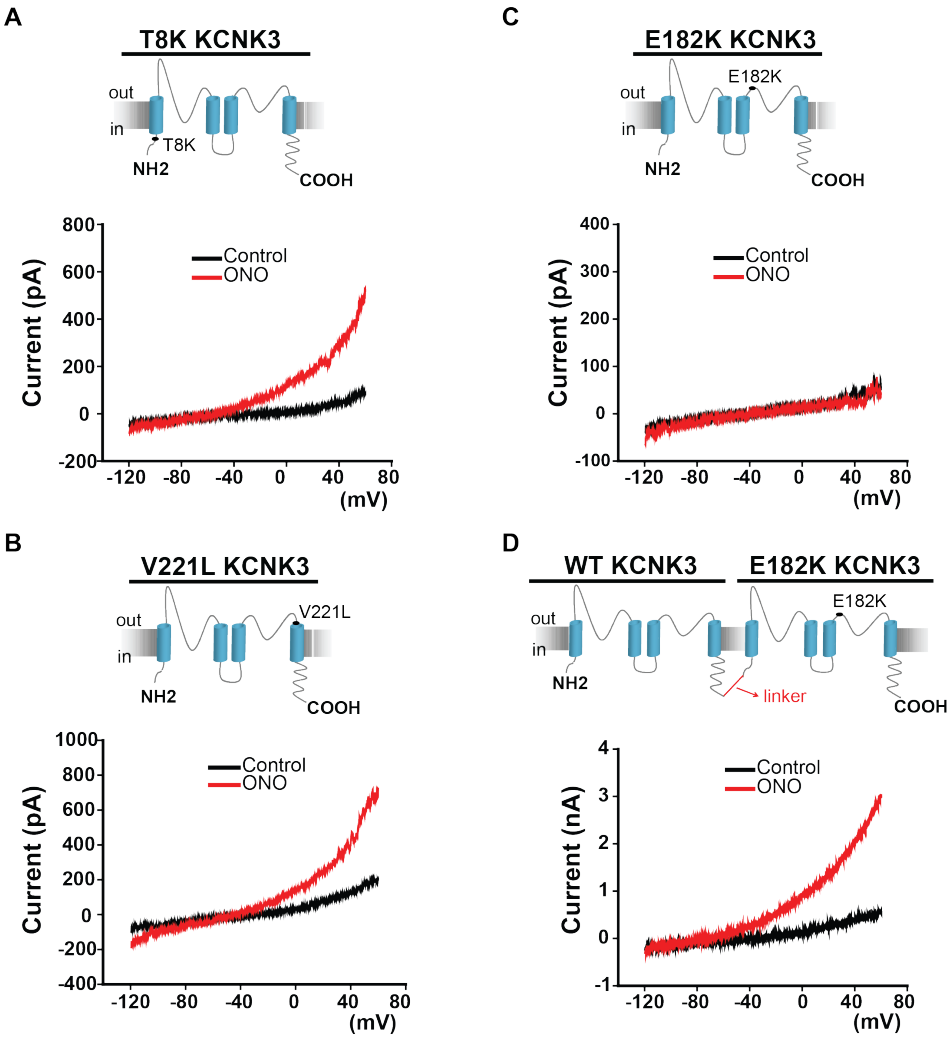

Figure 1.7. ONO-RS-082's effect on homomeric and heterodimeric mutant KCNK3 channels associated with PAH. Voltage clamp recordings in COS7 cells are depicted. **A-D**, The effect of ONO-RS-082 10 μM (red traces) at extracellular pH 7.4 on currents from cells expressing T8K KCNK3 (**A**); V221L KCNK3 (**B**); E182K KCNK3 (**C**); and heterodimeric WT-E182K KCNK3 (**D**). Control (pre-drug) conditions at extracellular pH 7.4 (black traces) are shown for each recording.

KCNK3 and KCNK9 form functional heterodimeric channels

To elucidate the broader impact of KCNK3 heterozygosity on channel function, we investigated the interactions of KCNK3 with a closely related acid-sensitive, two-pore domain potassium channel, KCNK9 (Figure 1.8A, top). Previous reports have shown that KCNK3 heterodimerization with KCNK9 results in functional channels consisting of one KCNK3 subunit and one KCNK9 subunit.[103,106-108,111] We engineered the first known tandem-linked human KCNK9-KCNK3 heterodimer (Figure 1.8B, top).

The true dimeric assembly of KCNK9 with KCNK3 to form KCNK9-KCNK3 heterodimers was confirmed by ruthenium red (RR) sensitivity analysis: KCNK9 was previously shown to be inhibited by RR (10μM), while KCNK9-KCNK3 heterodimers and KCNK3 channels were not inhibited by RR 10μM as KCNK3-containing channels lack a necessary glutamic acid residue (E70) for RR binding and channel pore block.[103] Figure 1.8A (bottom) shows inhibition of KCNK9 currents by RR 10μM at pH 7.4, and Figure 1.8B (bottom) shows no effect by RR 10μM on KCNK9-KCNK3 heterodimer currents. Sample drug time courses are shown in Figures 1.8C and 8D, for KCNK9 and KCNK9-KCNK3, respectively; RR sensitivity data are summarized in Figure 8G, for KCNK9, KCNK3, and KCNK9-KCNK3 (and see Figure 1.9A-C).

After verifying the formation and expression of the KCNK9-KCNK3 tandem dimer, we evaluated the pH dependence of KCNK9-containing channels. KCNK9 has a left-shifted pH dependence profile compared to KCNK3, rendering it more maximally activated at physiological pH 7.4 (Figure 1.8E, and compare with Figure 1.1A). We observed increased K^+ current activity at pH

7.4 for KCNK9-KCNK3 compared to KCNK3 homomeric channels, as expected (Figure 1.8F, and summarized in 1.8H).

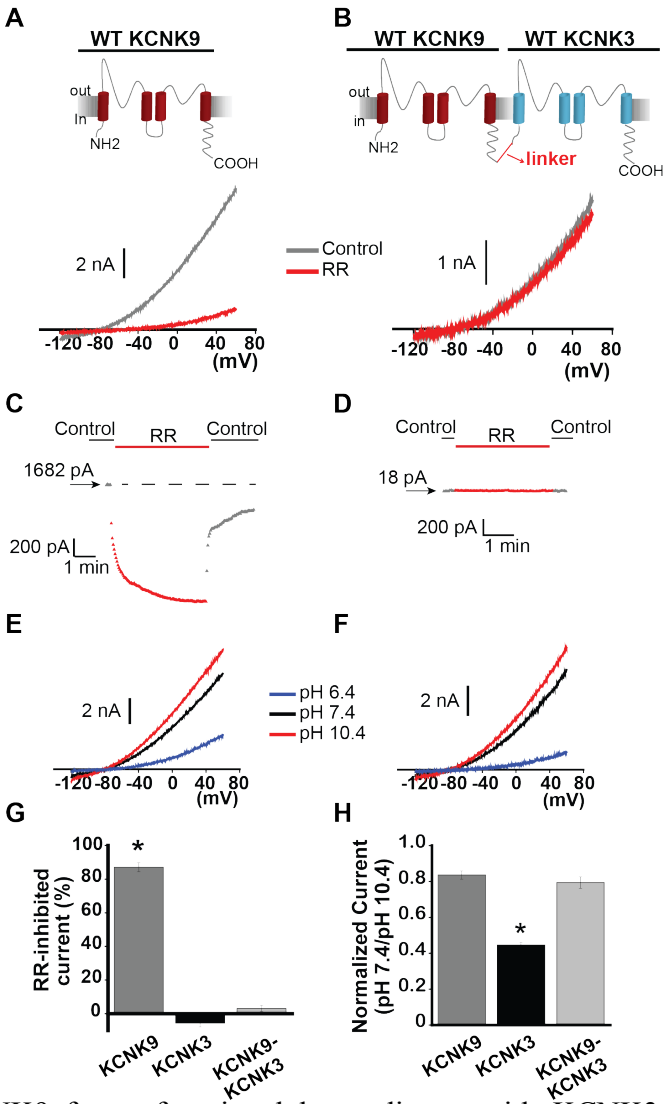

Figure 1.8. KCNK9 forms functional heterodimers with KCNK3. **A,** The effect of ruthenium red (RR) 10uM (red trace) on KCNK9 channels. Control trace (pre-drug, pH 7.4) shown in grey. **B,** The effect of RR 10uM (red trace) on KCNK9-KCNK3 heterodimeric channels. Control trace (pre-drug, pH 7.4) shown in grey. **C,** Sample RR time course of action on KCNK9 in control and drug conditions, measured at -50mV, from a starting current amplitude of 1682 pA indicated by the arrow. Horizontal dashed line is drawn at the starting level of current in control solution. **D,** Sample RR time course of action on KCNK9-KCNK3 heterodimers in control and drug conditions, measured at -50mV, from a starting current amplitude of 18 pA indicated by the arrow. **E,** Voltage clamp recording of KCNK9. **F,** Voltage clamp recording of KCNK9-KCNK3. For **E** and **F,** sample current traces at pH 6.4 (blue), 7.4 (black), and 10.4 (red) are shown. **G,** Summary of RR's effect on KCNK9, KCNK3, and KCNK9-KCNK3, measured by fold change in current at -50mV (n=5 to 8 cells per condition). **H,** Summary of mean current at pH 7.4 normalized to current at pH 10.4, measured at 60mV, for KCNK9, KCNK3, and KCNK9-KCNK3 (n=10 to 25 cells per condition). Bar graphs show mean ± SEM. * indicates $p<0.05$ by the paired Student's *t* test for the comparison of control versus ruthenium red conditions (panel G), and * indicates $p<0.05$ by one-way ANOVA and post-hoc Tukey test for the comparison of KCNK9, KCNK3, and KCNK9-KCNK3 (panel H).

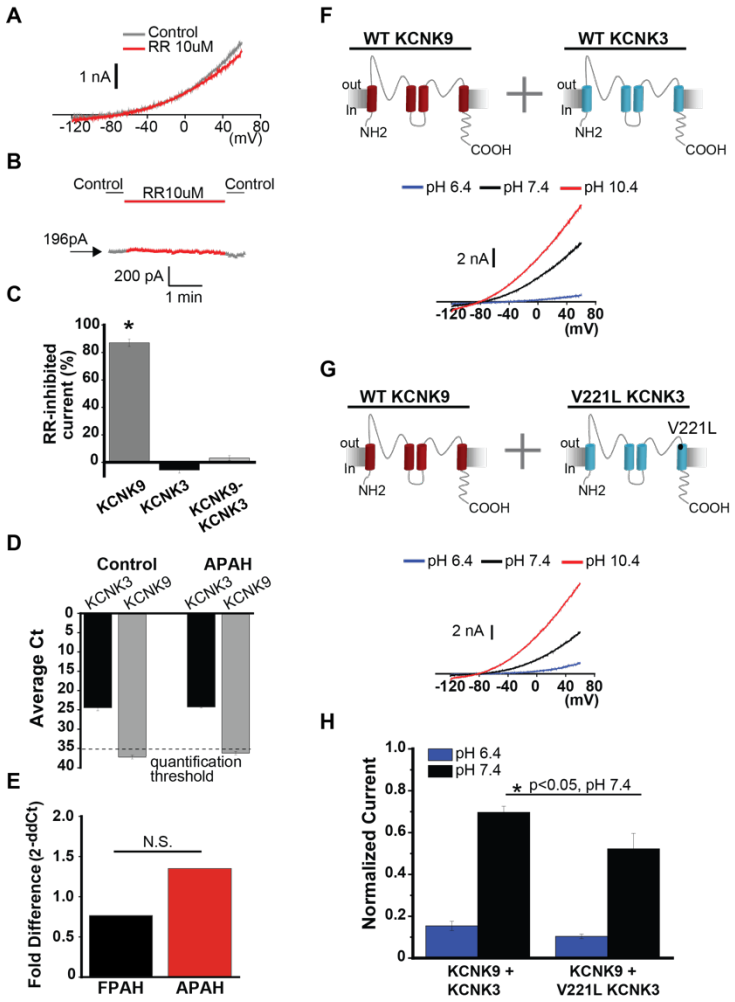

Figure 1.9. A, The effect of ruthenium red (RR) 10 μM (red trace) on KCNK3 channels in COS7 cells is shown. Control trace (pre-drug, pH 7.4) is depicted in grey. **B**, Sample RR time course of action on KCNK3 in control and drug conditions, measured at -50mV, from a starting current amplitude of 196 pA indicated by the arrow. **C**, RR's effect on KCNK9, KCNK3, and KCNK9-KCNK3 channels is summarized, showing fold change in current at -50mV (n=5 to 8 cells per condition). **D**, Quantitative real-time PCR analysis of human lung samples from healthy (Control) and congenital cardiac defect-associated PAH (APAH) patient lungs. Expression of KCNK3 (black bars), and KCNK9 (grey bars) are compared, based on mean cycle threshold (Ct) values observed for each gene; Ct > 35 indicates no quantifiable gene expression (n=5 patient lungs for each lane). Bars shown mean ± SEM. **E**, Fold difference in KCNK3 gene expression, calculated by the 2^{-ddCt} method, in FPAH and APAH versus Control patient lungs. No significant (N.S.) fold changes were observed compared to control. **F-G**, Co-expression of KCNK9 with WT KCNK3 channels (panel F), and KCNK9 with V221L KCNK3 channels (panel G) with sample voltage clamp recordings shown for each condition at pH 6.4 (blue), pH 7.4 (black) and pH 10.4 (red). **H**, Summary of current activity for co-expression of KCNK9 with WT KCNK3 (left) versus V221L KCNK3 (right). Current at pH 6.4 (blue) and pH 7.4 (black) is normalized to max current at pH 10.4 (n=5 to 8 cells per lane). Experiments were performed in COS7 cells. Bar graphs show mean ± SEM. * indicates $p<0.05$ by the paired Student's *t* test for the comparison of control versus ruthenium red conditions in panel C; * indicates $p<0.05$ by the unpaired Student's *t* test in panel H.

KCNK3, but not *KCNK9*, is expressed in healthy and PAH patient lungs

KCNK9 is thought to be co-expressed with *KCNK3* in various tissues outside of the lung, including in the central nervous system, heart, and adrenal glands, and functional heterodimerization of KCNK3 with KCNK9 in multiple tissues has already been studied.[89,100,103,108,111] *KCNK3* is expressed in hPASMCs, while *KCNK9* has been reported absent from hPASMCs.[73] We performed gene expression analysis on whole human lung tissue samples from healthy (control) subjects, and from patients with familial pulmonary arterial hypertension (FPAH). *KCNK3* expression was observed in lungs of control and FPAH patients, while no quantifiable expression of *KCNK9* was observed in control or FPAH patient lungs (Figure 1.10A, top; and see Figure 1.9D and 1.9E). Therefore, of all possible KCNK3/KCNK9 channel combinations, only KCNK3 homomeric channels would be expected to form in human lung tissue (Figure 1.10A, bottom). KCNK9-KCNK3 heterodimerization adds to the complexity of KCNK3 activity, particularly in PAH patients heterozygous at the *KCNK3* gene locus.

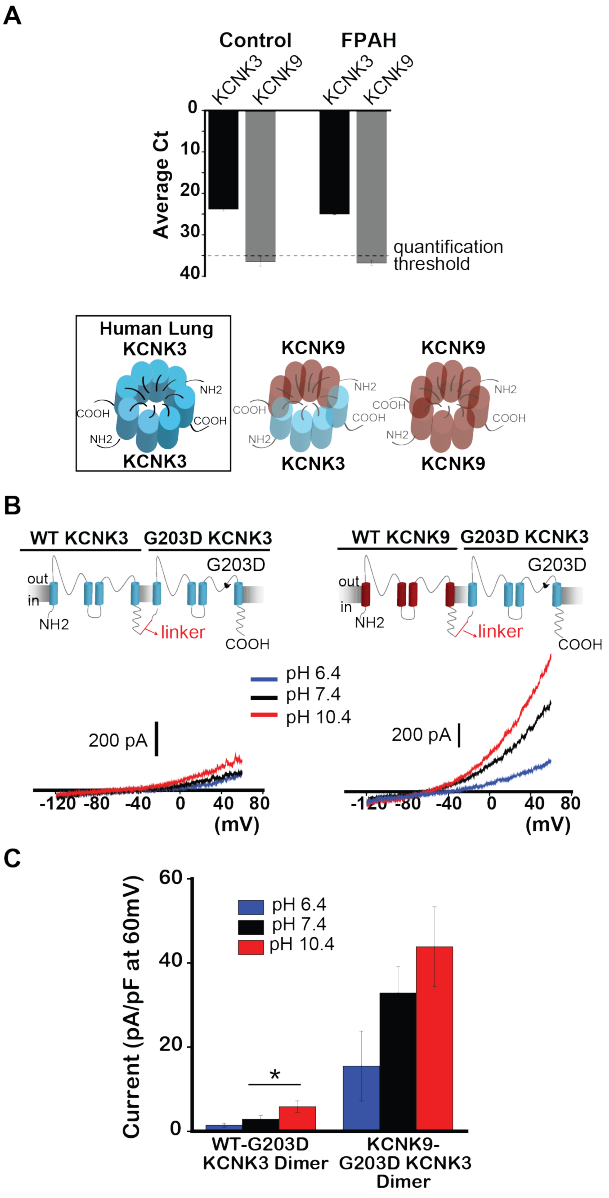

Figure 1.10. KCNK9 protects against KCNK3 dysfunction. **A,** Quantitative real-time PCR analysis of human lung samples from healthy (Control) and familial PAH (FPAH) patient lungs. Expression of *KCNK3* (black bars), and *KCNK9* (grey bars) are compared, based on mean cycle threshold (Ct) values observed for each gene; Ct > 35 indicates no quantifiable gene expression (n=5 patient lungs for each lane). Of the possible KCNK3 + KCNK9 channel combinations, only KCNK3 homomeric channels (boxed, left) are predicted to form in human lungs. **B,** Voltage clamp recordings of the WT-G203D KCNK3 heterodimer (left), and the KCNK9-G203D KCNK3 heterodimer (right), showing current traces at pH 6.4 (blue), 7.4 (black), and 10.4 (red). **C,** Summary of current densities (pA/pF at 60mV) at pH 6.4, 7.4, and 10.4 (n= 4 to 14 cells per pH bar). Bar graphs show mean ± SEM. * indicates $p<0.05$ by the unpaired Student's *t* test.

KCNK9 protects against KCNK3 dysfunction

The lung-specific disease phenotype in patients with heterozygous *KCNK3* mutation, despite widespread tissue expression of *KCNK3*, remains a puzzling phenomenon: are lungs particularly susceptible to *KCNK3* loss of function due, in part, to the absence of KCNK9? We sought to determine whether KCNK9 can recover function of even the severe mutant G203D KCNK3 channel, in order to test the hypothesis that co-assembly of KCNK9 with KCNK3 provides protection against heterozygous *KCNK3* mutation when the channels are co-expressed, while the absence of *KCNK9* in the lungs underlies the lung-specific phenotype in the setting of heterozygous *KCNK3* loss of function.

G203D KCNK3 disrupts the conserved "GxG" potassium selectivity filter amino acid sequence in one of the channel's two pore-loop domains, a region sensitive to dominant-negative mutations.[133,160,161] We first engineered and studied the WT-G203D KCNK3 heterodimer (Figure 10B, left), and indeed observed severe dominant-negative dysfunction, as the mutant channels produced small currents across pH 6.4 through 10.4 (Figure 1.10B and 1.10C; also see Figure 1.11).

Next, we engineered a KCNK9-G203D KCNK3 mutant heterodimer to determine the impact of KCNK9 assembly with G203D KCNK3 (Figure 1.10B, right). We observed appreciable pH-sensitive currents, with significantly increased current density at physiological pH 7.4 and pH 10.4, compared to WT-G203D KCNK3 heterodimeric channels (Figure 1.10B and 1.10C). KCNK9 thus assembles with mutant KCNK3 channels to produce functional recovery and provide protection

against KCNK3 channel dysfunction (see also Figure 1.9F-H for modelling heterozygous co-expression of mutant KCNK3 [eg. V221L] with KCNK9 channels.

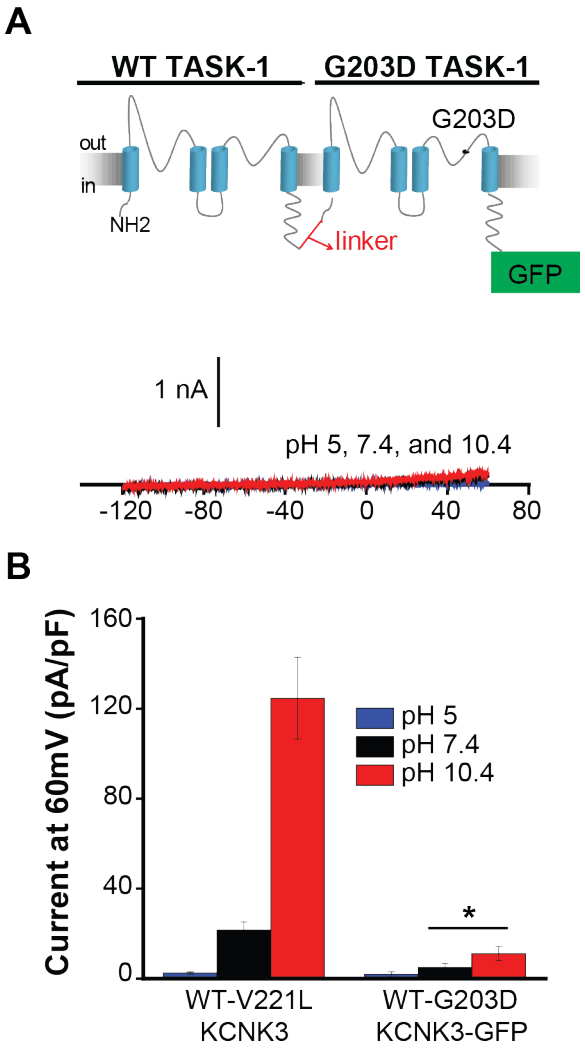

Figure 1.11. KCNK3 heterodimeric GFP fusion dimer confirms the more severe loss of function in G203D versus V221L-containing KCNK3 channels. A, A WT-G203D KCNK3-GFP fusion heterodimer was engineered by interconnecting two KCNK3 subunits with a glycine-rich linker, and inserting a C-terminal GFP tag. Given the relative severity of G203D KCNK3 dysfunction, the GFP fusion construct ensured channel expression in fluorescent cells studied. Sample traces from a voltage clamp recording are shown at extracellular pH 5 (blue), pH 7.4 (black), and pH 10.4 (red), revealing small currents across the pH range. **B**, Summary of current densities (pA/pF at 60mV) at pH 5 (blue), pH 7.4 (black), and pH 10.4 (red) for the WT-V221L KCNK3 heterodimer versus the WT-G203D KCNK3-GFP heterodimer (n= 6 to 16 cells per pH bar). Bars show mean ± SEM. * indicates $p<0.05$ at pH 7.4 and pH 10.4, by the unpaired Student's *t* test.

DISCUSSION

Our initial characterization of *KCNK3* mutations associated with PAH showed loss of function for all disease-associated mutant channels.[55] Here, we have reported five major findings, summarized schematically in Figure 1.12. First, *KCNK3* mutations associated with PAH harbor mutation-specific severity of loss of function that can occur by distinct underlying mechanisms. Second, mutant and WT KCNK3 channels can be pharmacologically activated in hPASMCs to cause membrane hyperpolarization, and thus represent potential targets for PAH treatment. Third, mutant heterodimeric tandem-linked KCNK3 channels provide a valuable tool for evaluating the functional impact of clinically relevant heterozygous KCNK3 conditions, as they report function of a substantial, discrete proportion of formed KCNK3 channels in heterozygous patients. Fourth, mutant heterodimeric KCNK3 channels can be pharmacologically targeted for activation, dependent on the mutation. Fifth, KCNK9 co-expression and assembly with KCNK3 channels protects against KCNK3 dysfunction, which we hypothesize contributes to the lung-specific phenotype observed clinically in patients with PAH-associated heterozygous KCNK3 mutation.

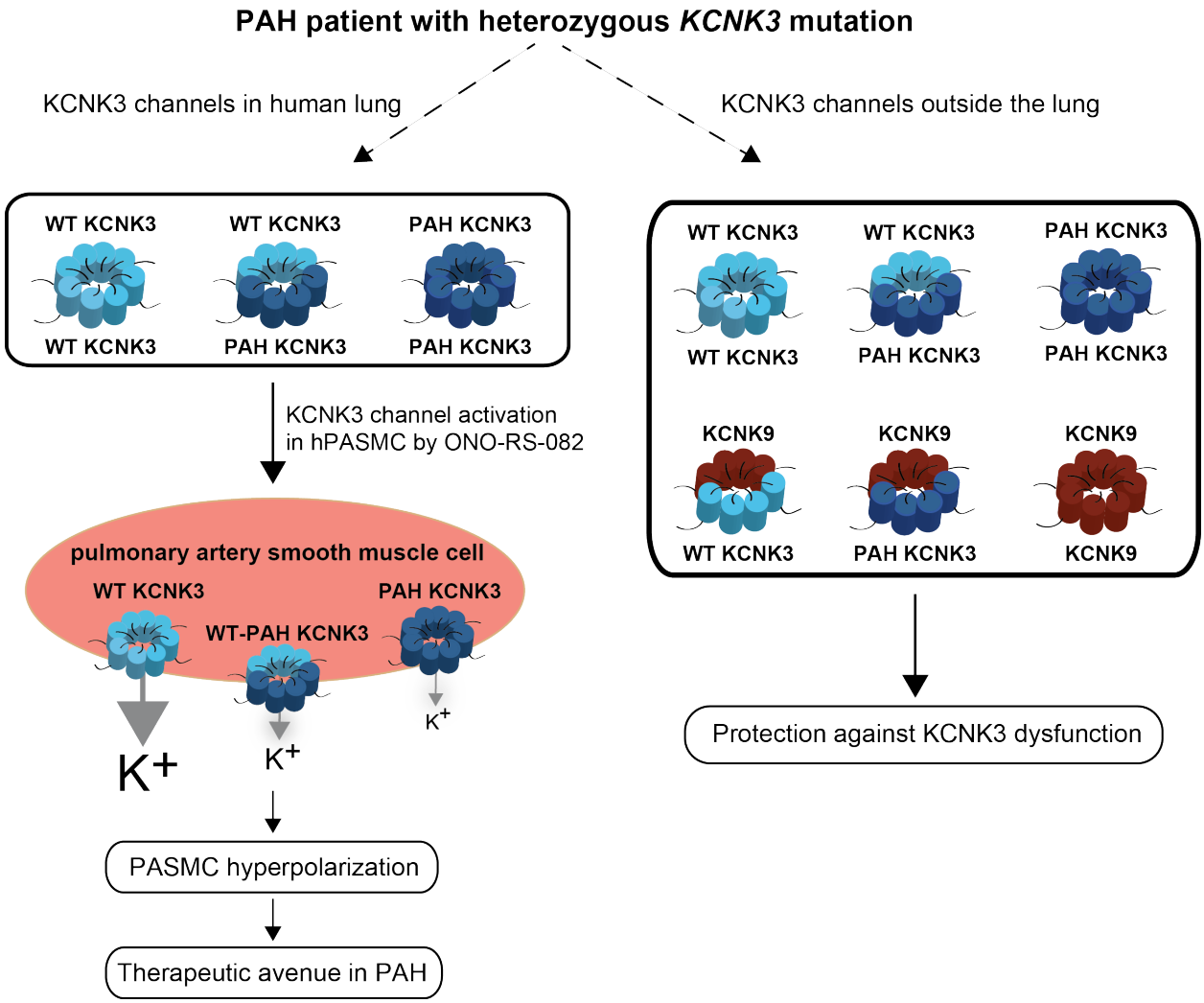

Figure 1.12. Schematic of the proposed impact of heterozygous potassium channel subfamily K member 3 (*KCNK3*) mutation in pulmonary arterial hypertension (PAH). Wildtype KCNK3 (light blue) and mutant ("PAH") KCNK3 (dark blue) homomeric, and heterodimeric channels are expressed in human lung. Additional interactions of KCNK3 with KCNK9 (brown) channel subunits occur outside of the lung, protecting against KCNK3 loss of function. However, in pulmonary artery smooth muscle cells (hPASMCs), only *KCNK3* (and not *KCNK9*) is expressed, and the greater proportion of mutant KCNK3 channels in hPASMCs promotes membrane depolarization. ONO-RS-082, a KCNK3 activator, recovers function of some mutant and wildtype KCNK3 channels leading to PASMC hyperpolarization, which may represent a therapeutic avenue in PAH.

A unique pH-dependent mechanism of mutant KCNK3 channel dysfunction in PAH

Potassium channel mutations confer loss of function by discrete mechanisms of varying severity. In well-studied channelopathies, mechanisms of dysfunction include defects in trafficking, channel assembly, and electrophysiological function, dependent on the location of the mutation.[162,163]

In our study, V221L KCNK3 confers a pH-dependent mechanism of loss of function. Extracellular histidine residues lining the KCNK3 channel pore account for nearly all of the pH sensitivity of KCNK3 directly, as protonation of these residues leads to inhibition of potassium conductance.[156,164] However, other regions, including the extracellular portion of the fourth transmembrane segment of KCNK3 – the location of the V221 residue - may contribute to pH sensing and channel inhibition indirectly by stabilizing the channel pore and the selectivity filter within it.[99,164] The unique properties of V221L KCNK3 can be exploited for KCNK3 structure-function studies in relation to the channel's crucial regulation by pH.

Mutant and wildtype KCNK3 channels are pharmacological targets in hPASMCs

Potassium channels regulate the resting membrane potential of pulmonary artery smooth muscle cells.[60,70,126] Voltage-gated potassium channels are involved in the hypoxic pulmonary vasoconstrictive response,[165] while downregulation of K_v channel expression in PASMCs of PAH patients promotes PASMC excitability and proliferation, and excessive pulmonary arterial vasoconstriction.[80,81,166] Potassium channel openers may provide therapeutic benefit by opposing such deleterious pulmonary arterial remodeling;[167] recently, pharmacological KCNK3 activation by ONO-RS-082 (ONO) attenuated development of pulmonary hypertension in a monocrotaline-induced rat model.[55,75]

We therefore studied mutant and WT KCNK3 activation in human PASMCs. KCNK3 expression is nearly completely lost in cultured PASMCs, as a proliferative versus contractile smooth muscle cell phenotype predominates concomitant with loss of potassium channel expression and cell depolarization.[32] Previous studies have employed anandamide and A293, inhibitors of KCNK3 channel activity, to analyze the functional contributions of KCNK3 on hPASMC excitability.[75,88,112,168] We confirmed loss of native KCNK3 channel activity in cultured hPASMCs using a recently developed, more selective KCNK3 inhibitor, ML365 (Figure 1.2E-H and Figure 1.3B.[158]

We exploited the properties of cultured hPASMCs to compare the relative impact of expressed mutant versus WT KCNK3 channels in a more physiological environment. The current clamp results in Figure 1.4 demonstrate that (1) a gradient exists for the relative contribution of mutant and WT KCNK3 to the resting potential of hPASMCs, with cells expressing mutant KCNK3 more depolarized at rest; and (2) activation of mutant or WT KCNK3 by ONO hyperpolarizes hPASMCs, highlighting PAH-associated mutant and WT KCNK3 channels as viable pharmacological targets. Given the over-expression of *KCNK3* in our system, the results are not meant to suggest that the magnitude of membrane voltage responses is physiological, but rather provide proof of principle for the graded responses of mutant and WT KCNK3 channels to pharmacologic activation in hPASMCs.

Based on the variable time course of activation of KCNK3 by ONO (seconds to minutes, not instantaneous), we hypothesize that ONO does not bind directly to the channel. More likely, ONO

acts on membrane phospholipase pathways to alter KCNK3 phosphorylation. It has been shown that phospholipase C (PLC) activation leads to KCNK3 inhibition,[168] and endothelin-1, a vasoconstrictor and mediator of PAH pathogenesis, inhibits KCNK3 in hPASMCs leading to depolarization, the sensitivity of which requires endothelin-A receptors, PLC, phosphatidylinositol 4,5-bisphosphate (PIP2), diacylglycerol (DAG), and protein kinase C.[169] Activation of endothelin receptors was shown to cause KCNK3 phosphorylation via rho kinase activation,[170] and DAG was recently identified as a direct regulator of KCNK3 downstream of activated G protein-coupled receptors.[171] Ultimately, elucidating the specific pathways involved in KCNK3 activation by ONO will further cultivate KCNK3 activation as a PAH treatment paradigm.[172]

Mutant KCNK3 heterodimeric channel function and recovery

Mature KCNK3 channels dimerize, forming functional channels from two individual KCNK3 subunits that co-assemble.[156] In this study, tandem-linked KCNK3 heterodimers served as a functional reporter of a discrete and substantial population of formed channels in heterozygous patients. The dominant-negative phenotype conferred by the V221L KCNK3 mutation did not prevent pharmacological recovery of function: heterodimeric WT-V221L KCNK3 channels responded to pharmacological activation by ONO. As *KCNK3* downregulation occurs in PAH irrespective of a patient's *KCNK3* genetic status,[75] KCNK3 activation indeed represents a more generalizable therapeutic approach in pulmonary hypertension due to any cause.

While appreciable activation of homomeric mutant channels with marked loss of function at baseline was difficult to discern, we have demonstrated robust current activation of mutant heterodimeric KCNK3 channels by ONO (Figure 1.6; and see Figure 1.7). Thus, in PAH patients

heterozygous at the *KCNK3* gene locus, the majority of formed channels – the combination of WT homodimeric and mutant heterodimeric KCNK3 channels – may respond markedly to pharmacological activation and represent targetable therapeutic substrates.

KCNK9 minimizes the impact of KCNK3 loss of function

Interestingly, none of the PAH patients in our cohort with heterozygous *KCNK3* mutations possessed a primary clinical phenotype outside of the lung, despite widespread *KCNK3* expression in the body.[97] KCNK9, which has been shown to heterodimerize with KCNK3,[103] is absent from human lungs of healthy controls and PAH patients (Figure 1.10A; and see Figure 1.9D and 1.9E), but assembles with KCNK3 in tissues where both *KCNK9* and *KCNK3* are expressed, leading to diversity of channel currents.[106,108,111] It has been shown that KCNK9 protects against cell stress,[173] and the concept of protection by KCNK9 was extended to our study in the context of KCNK3 dysfunction. We observed that KCNK9 heterodimerization with WT and G203D KCNK3 increased current activity at physiological pH 7.4 compared to equivalent KCNK3-only based channels.

We hypothesize that the co-expression of KCNK9 with KCNK3 in tissues outside the lung provides redundancy of channel function and protection against *KCNK3* mutations of varying severity, sparing tissues outside the lung of disease. Perhaps the partial loss of KCNK3 function outside the lung is alleviated by an upregulation of *KCNK9* and/or preferential binding of KCNK9 with mutant KCNK3 to recover function. Meanwhile, the absence of KCNK9 in the lung would leave PASMCs susceptible to excessive depolarization, proliferation, and vasoconstriction in the setting of KCNK3 dysfunction.

Incomplete penetrance was observed in individuals with PAH-associated *KCNK3* mutations.[55] Alongside the mutation-specific severity of KCNK3 dysfunction observed in this study, conceivably, KCNK9 provides greater protection in some individuals than others. Some patients with heterozygous *KCNK3* mutation may develop PAH at a later age of onset, or not develop PAH at all, dependent, in part, on KCNK9 channel activity.

Limitations

The impact of KCNK3 heterozygosity at the pulmonary arterial level remains undetermined. Due to its altered pH dependence easily discerned in electrophysiological studies, the V221L KCNK3 mutation represents a model mutation to incorporate into a rat model (eg. using CRISPR knock-in technology) to recapitulate KCNK3 heterozygosity and evaluate the pathophysiological consequences in the lungs and outside of them.[75,87]

Uncovering the cellular pathways involved in KCNK3 activation by ONO has broader implications than for PAH pathogenesis and treatment alone. For instance, enhanced KCNK3 activity was recently demonstrated in atrial myocytes of patients with chronic atrial fibrillation, leading to shortening of the action potential duration.[174] Mechanistic understanding of ONO's regulation of KCNK3 would aid the development of more selective pharmacological modulators of channel activity.

Conclusions

We have demonstrated, for the first time, that *KCNK3* mutations associated with PAH harbor differing underlying mechanisms of loss of function of varying severity; that mutant KCNK3 channels represent viable therapeutic targets in PAH via activation by ONO-RS-082 in pulmonary artery smooth muscle cells; that engineered mutant heterodimeric KCNK3 channels report function of a substantial proportion of formed KCNK3 channels in heterozygous patients, and that heterodimeric KCNK3 channels can be pharmacologically activated; and lastly, that heterodimerization of KCNK9 with KCNK3 can serve a protective role to minimize the impact of heterozygous KCNK3 loss of function, which may underlie the PAH-specific phenotype observed clinically in patients with heterozygous *KCNK3* mutation.

CHAPTER 2:

LOSS OF FUNCTION MUTATIONS IN *ABCC8* ARE ASSOCIATED WITH PULMONARY ARTERIAL HYPERTENSION

SUMMARY

Background: In pulmonary arterial hypertension, pathological changes in pulmonary arterioles progressively raise pulmonary artery pressure and increase pulmonary vascular resistance, leading to right heart failure and high mortality rates. Recently, the first potassium channelopathy in pulmonary arterial hypertension, due to mutations in *KCNK3*, was identified as a genetic cause and pharmacological target.

Methods: Exome sequencing was performed to identify novel genes in a cohort of 99 pediatric and 134 adult onset group I pulmonary arterial hypertension patients without identifiable mutations in known pulmonary arterial hypertension genes. Novel rare variants in the gene identified were independently identified in a cohort of 680 adult onset patients. Variants were expressed in COS cells and function assessed by patch-clamp and rubidium flux analysis.

Results: We identified a *de novo* novel heterozygous predicted deleterious missense variant c.G2873A (p.R958H) in *ABCC8* (ATP-binding cassette, subfamily C, member 8), in a child with idiopathic pulmonary arterial hypertension. We then examined all individuals for rare or novel variants in *ABCC8* and identified seven additional heterozygous predicted damaging variants. To replicate our findings, we examined a second cohort and identified four additional heterozygous predicted damaging variants in four individuals with adult-onset pulmonary arterial hypertension. *ABCC8* encodes sulfonylurea receptor 1, a regulatory subunit of the ATP-sensitive potassium channel. We observed loss of function for all *ABCC8* variants evaluated, and pharmacological rescue by the SUR1 activator, diazoxide.

Conclusions: Novel and rare missense variants in *ABCC8* are associated with pulmonary arterial hypertension. Identified *ABCC8* mutations decreased potassium channel function, which was pharmacologically recovered.

INTRODUCTION

Pulmonary arterial hypertension is a rare and often fatal disease characterized by distinctive changes in pulmonary arterioles that lead to elevated pulmonary artery pressure and right sided heart failure. Novel treatment options have decreased mortality, but pulmonary arterial hypertension remains a frequently fatal illness. The heterogeneity in disease etiology and nonspecific patient presentation often delays diagnosis, contributing to poor outcomes.

Genetics are recognized to play an important role in the pathogenesis of pulmonary arterial hypertension in patients with and without a family history of disease. Most genetic studies of the disease have been performed in patients with adult-onset disease. Germline mutations in bone morphogenetic protein receptor type 2 (*BMPR2*), a member of the transforming growth factor β (TGFβ) superfamily of receptors, have been identified as the major genetic cause, including in 70% of inherited and 10–40% of idiopathic cases.[13] Mutations in other TGFβ family members comprise additional rare genetic causes. The prevalence of the disease in children is estimated at 2.2 cases per million, an order of magnitude lower than the estimated prevalence of 15-50 cases per million in adults,[7] and there are few genetic studies of individuals with childhood-onset pulmonary arterial hypertension.

We previously used exome sequencing to identify mutations in the KCNK3 potassium channel as a genetic cause of, and novel pharmacological target for pulmonary arterial hypertension.[55] In the current study, we report a novel channelopathy in both pediatric and adult onset pulmonary arterial hypertension, functionally assess mutant channels, and characterize the pharmacological activation of mutant channel function.

METHODS

Genetic studies and analysis presented here were performed by Dr. Wendy Chung and collaborators, the methods and results of which are included in Chapter 2 of this dissertation for completeness. Please see Acknowledgements below for a fuller list of contributors.

The study was approved by the institutional review board at Columbia University Medical Center. Adult cases were also enrolled to the BRIDGE-PAH (UK REC 04/Q0108/44) and to the National Institute for Health Research (NIHR) BioResource—Rare Diseases (UK REC 13/EE/0325)/PAH studies after providing informed written consent.

Columbia Study Participants

We sequenced 99 childhood onset and 134 adult onset pulmonary arterial hypertension patients using exome sequencing. All patients enrolled in the study carried a group I pulmonary arterial hypertension diagnosis, based on World Health Organization classifications; 181 idiopathic and 52 heritable pulmonary arterial hypertension subjects were included. The diagnosis of pulmonary arterial hypertension was confirmed by medical record review, including right heart catheterization. Heritable cases were pre-screened for *BMPR2* and *ACVRL1* mutations by Sanger sequencing and Multiplex Ligation-dependent Probe Amplification. Written informed consent and assent when age appropriate were obtained under a protocol approved by the institutional review board at Columbia University Medical Center.

Exome Sequencing

Sample Preparation and Sequencing: DNA was extracted from peripheral blood leukocytes using Puregene reagents (Gentra Systems Inc., Minnesota, USA). Genomic DNA was prepared for exome capture with a custom reagent kit from Kapa Biosystems and captured with the NimbleGen exome design (SeqCap VCRome 2.1). The samples were sequenced using 75 bp paired-end sequencing on an Illumina v4 HiSeq 2500.

Data processing and analysis: After reads were generated by Illumina's proprietary CASAVA software, sample-specific reads were aligned to the GRCh37/hg19 human genome reference assembly using Burrows-Wheeler Aligner (BWA).[175] Once aligned, duplicate reads were marked with the Picard Mark Duplicates, and GATK[176] was used for insertion/deletion realignment as well as calling SNP and insertion/deletion variants (using Haplotype Caller). Variant Quality Score Recalibration (VQSR) from GATK was applied to evaluate the overall quality score of a sample's variants. After sample-level variant generation, and application of standard quality-control filters for minimum read depth ($\geq$10), genotype quality ($\geq$30), and allelic balance ($\geq$20%); passing variants were classified and annotated based on their potential functional effects (whether synonymous, missense, frameshift, or nonsense variants) and subsequently filtered by their observed frequencies in population control databases such as dbSNP, the 1000 Genomes Project,[177] the NHLBI Exome Sequencing Project, the Exome Aggregation Consortium Database (ExAC),[178] and internal databases in order to filter out common polymorphisms and high frequency, likely benign variants. Algorithms for bioinformatics prediction of functional effects of variants, such as SIFT,[179] Polyphen 2,[180] Meta-SVM,[181] and combined annotation dependent depletion (CADD)[182] along with conservation scores based on multiple species alignments were incorporated as part of the annotation process of variants and used to inform the potential

deleteriousness of identified candidate variants. Family relationships were analyzed using KING http://people.virginia.edu/~wc9c/KING/manual.html).[183]

NIHR BioResource – Rare Diseases (BRIDGE) Study Participants

We sequenced 680 adult onset pulmonary arterial hypertension patients using whole genome sequencing as part of the 10,000 genomes project. All patients enrolled in the PAH cohort had been diagnosed with idiopathic PAH, familial PAH and appetite drug associated PAH and written informed consent was obtained under a protocol approved by the UK Research Ethics Committee. The diagnosis of pulmonary arterial hypertension was confirmed by medical record review, including right heart catheterization.

Whole Genome Sequencing

Sample Preparation and Sequencing: Genomic DNA was isolated from venous blood using standard techniques. Whole-genome sequencing was undertaken using the Illumina TruSeq DNA PCR-Free Sample Preparation kit on the Illumina HiSeq 2500 and HiSeqX platform, generating a minimum coverage of 15x for ~95% of the genome and an average coverage of ~30x.

Data processing and analysis: Reads were aligned to the GRCh37/hg19 reference genome using the Isaac aligner (version 2, Illumina). SNVs, indels and SVs were identified using Illumina's Isaac Variant Caller, Isaac Structural Variant Caller (Manta) and Copy Number Variant Caller (Canvas) [version 2]. Variants are then normalised, merged and annotated with Ensembl Variant Effect Predictor v84 (VEP) [doi:10.1093/bioinformatics/btq330]. Only variants that pass standard

Illumina quality filters in 80% of the whole BRIDGE cohort (n=8066) are taken forward for further analysis.

In order to filter down to likely pathogenic variants the following criteria were applied: a) minor allele frequency is less than 1 in 10,000 in control data sets including unrelated BRIDGE-PAH controls (n=5668), the Exome Aggregation Consortium Database (ExAC)[178] and UK10K WES and WGS [doi:10.1038/nature14962], b) the combined annotation dependent depletion (CADD) score[182] is 15 or higher. Remaining variants were then manually assessed making use of other deleteriousness and conservation scores like SIFT,[179] Polyphen 2,[180] or GERP [doi:10.1371/journal.pcbi.1001025].

Sanger Sequence Confirmation and Segregation Analysis

Candidate predicted pathogenic variants were confirmed by dideoxy sequencing. PCR primers were designed flanking approximately 250 bp of a given variant and sequenced on ABI 3730 capillary sequencing instrument. Capillary sequence reads were analyzed using the Sequencher software package (GeneCodes Inc). Variants identified in heritable pulmonary arterial hypertension were tested in all available family members by dideoxy sequencing for segregation analysis.

Statistical Test of Association of Rare *ABCC8* Variants with PAH

We selected 33,369 European subjects from the Exome Aggregation Consortium (ExAC) and 49,630 Caucasian samples from Geisinger studies independently as controls for testing the genetic association of *ABCC8* and pulmonary arterial hypertension.[178] We focused on rare variants that

have minor allele frequency ≤0.1% estimated by ExAC.[184] We used a binomial test in order to test the null hypothesis that the frequency of rare *ABCC8* alleles in cases is the same as in controls. We tested two groups of rare variants separately: (1) *deleterious* missense variants, defined as variants predicted to be damaging by Meta-SVM[181] and have a CADD[182] score greater than 15; and (2) *benign* variants, including synonymous variants and missense variants predicted to be tolerant by Meta-SVM.

Cohort	N_European Samples	N_Variant Deleterious (Allele_count)	N_Variant Benign (Allele_count)	Enrichment in cases Deleterious (P-value)	Enrichment in cases Benign (P-value)
CU-PAH	150	6 (6)	2 (2)		
GHS50K_EA	49,630	165 (712)	-	2.8 (0.022)	-
ExAC_NFE	33,369	148 (295)	223 (512)	4.5(0.0023)	0.87(1)

Functional Analysis of SUR1 Activity

We performed functional studies of SUR1, encoded by *ABCC8*, in association with its known potassium channel subunit partner, Kir6.2, encoded by *KCNJ11*, to form functional ATP-sensitive potassium (K_{ATP}) channels. Mutations were engineered into *ABCC8* complementary DNA and co-expressed along with *KCNJ11* by transient transfection in COS cells. Using the whole-cell patch-clamp technique, K_{ATP} (SUR1/Kir6.2) currents were directly measured. The application of diazoxide (100μM) activates K_{ATP}, while co-application of glibenclamide (10μM) inhibits K_{ATP}. The glibenclamide-sensitive current served as the primary quantitative measure of wildtype and

mutant SUR1 activity. Rubidium flux assays provided a measure of macroscopic K_{ATP} channel activity in intact cells in the presence and absence of diazoxide or metabolic inhibitors.

Molecular Biology

The pCMV-XL6-ABCC8 vector containing human *ABCC8* cDNA encoding SUR1 protein was used for whole-cell electrophysiology (OriGene). A pECE-mouseKir6.2 cDNA construct was also used, tagged with a C-terminal GFP as a marker of cell transfection. All pulmonary arterial hypertension- associated mutant SUR1s were engineered by site-directed mutagenesis on the human *ABCC8* construct using QuickChange II (Stratagene). In Rubidium flux experiments, pcDNA3.1-mouseKir6.2 and pECE-hamsterABCC8 cDNAs were used to optimize expression, with site-directed mutagenesis performed on the hamster *ABCC8* cDNA construct using QuickChange II (Stratagene) to engineer SUR1 mutants.

Whole-cell Electrophysiology

COS-7 cells (American Type Culture Collection) were transiently transfected using Lipofectamine reagents (Invitrogen) and our laboratory's established protocol.[55] Co-transfection of 1.5µg SUR1 and 0.9µg Kir6.2 cDNA was performed based on an established optimized transfection ratio for SUR/Kir6.2.[185] COS-7 cells were cultured using 5% CO2, DMEM + GlutaMax medium (Gibco), 10% fetal bovine serum (Gibco), and 1% Penicillin/Streptomycin (Gibco).

Whole-cell K_{ATP} currents were recorded under voltage clamp conditions using an Axopatch 200B amplifier (Axon Instruments). A voltage ramp protocol was employed (-120mV to +60mV, 180mV/s), applied every 3 seconds from a holding potential of -80mV, to record K_{ATP} channel

currents. The internal (pipette) solution (in mmol/L) was: 150 KCl, 1.2 MgCl2, 1 CaCl2, 5 EGTA, 10 HEPES, 0.1 MgATP, at pH 7.35 using KOH. The external (bath) solution (in mmol/L) was: 150 NaCl, 5 KCl, 1 MgCl2, 1.8 CaCl2, 10 HEPES, at pH 7.4 using NaOH.

For analysis, whole cell currents were normalized to cell capacitance (pA/pF), and measurements taken at -40mV in each cell, and in each pharmacological condition. Diazoxide (Sigma) was dissolved in DMSO (Life Technologies) to a 100mM stock solution, and diluted to 100μM in diazoxide-containing external solutions. Control external solutions (no drug) contained an equivalent 100μM DMSO. Glibenclamide (Sigma) was dissolved in DMSO (100mM stock solution) and diluted to 10μM when added to diazoxide-containing external solution. The glibenclamide-sensitive current (i.e. the SUR1-dependent current) was taken as the primary measure of SUR1 function in this assay, and these values were obtained by subtracting the current remaining after diazoxide+glibenclamide application (the average current amplitude 8-12 sweeps after the initial application of glibenclamide), from the steady state maximal current achieved by diazoxide. Control conditions before diazoxide application were often not at steady state due to dialysis of intracellular ATP; thus, control current density values were taken as an average of 4-5 sweeps preceding diazoxide application, up to approximately 60 seconds post whole-cell break-in with the patch pipette as an estimate for basal channel function. Graphic analysis was performed using Origin 7.0 and 9.0 (Microcal Software, Northampton, MA). Data are shown as means; T bars indicated standard errors. Asterisks denote $P<0.05$ for the comparison between wildtype SUR1 and each mutant SUR1 or each control condition where indicated, calculated by a one-way ANOVA (post-hoc Tukey test).

Rubidium Flux Assay

Cosm6 cells were cultured in Dulbecco's Modified Eagle's Medium (DMEM) and 48 hours prior to testing were added to 12-well plates such that confluence reached 70-80% on the day of experimenting. Individual wells were transfected 36 hours prior to testing with 0.1µg pcDNA3.1-GFP alone (for control cells) or with 0.6µg pcDNA3.1-mouseKir6.2 and 1µg pECE-hamster ABCC8 using Fugene 6 (Promega). Hamster SUR1 was used for flux assays as this clone provides sufficiently robust expression for the flux assay. On the day of testing cells were incubated in DMEM media containing 1 µCi/ml ^{86}RbCl (PerkinElmer) for > 6 hours at 37°C. After loading cells were washed with Ringer's solution containing (in mM) 118 NaCl, 10 HEPES, 25 $NaHCO_3$, 4.7 KCl, 1.2 KH_2PO_4, 2.5 $CaCl_2$, and 1.2 $MgSO_4$ either alone or supplemented with 2.5 mg/ml oligomycin and 1 mM 2-deoxy-D-glucose to induce metabolic inhibition, or 100µM diazoxide as indicated, and incubated at room temperature for a further 12.5 minutes. Wells were washed with Ringer's solution and incubated with 800µl of Ringer's solution with or without MI supplements or diazoxide (considered time point 0). The incubating solution was collected and replaced at defined time points of 2.5, 5, 12.5 and 27.5 minutes. Cells were then lysed using 2% SDS to yield the remaining intracellular rubidium and the radioactivity of samples was determined by scintillation counting.

The fractional cumulative efflux at each time point was determined from the total content. Apparent rate constants for background, K_{ATP}-independent $^{86}Rb^+$ efflux were obtained from GFP transfected cells using the equation:

$$\text{Efflux} = 1 - e^{-k_1.t}$$

where k_1 represents the rate constant for background efflux. K_{ATP}-dependent efflux was obtained using the equation:

$$\text{Efflux} = 1 - e^{((-k_1.t)+(-k_2.t))}$$

where k_2 is the rate constant for efflux via the K_{ATP}-dependent pathway respectively. The number of active channels is assumed to be proportional to k_2. In metabolic inhibition conditions a time-dependent divergence from a mono-exponential efflux is observed and attributed to inactivation of efflux mechanisms over time, therefore in this condition rate constants were derived from exponential functions fit to early time points only. Data shown represents the mean ± S.E.M. from at least 3 independent experiments, each with multiple replicates ($N \geq 3$, $n \geq 7$). Statistical significance was determined using the one-way ANOVA and post-hoc Tukey test, with a p value < 0.05 deemed statistically significant. The Nichols lab at Washington University executed the rubidium flux assays.

Quantitative Real-Time Polymerase Chain Reaction (qRT-PCR)

Quantitative real-time polymerase chain reaction (qRT-PCR) was performed to derive *ABCC8* expression patterns from healthy human lungs (controls), lungs from patients with familial pulmonary arterial hypertension (FPAH), and lungs from patients with pulmonary arterial hypertension associated with congenital heart defects (APAH). RNA and cDNA for each sample was prepared as previously described.[157] A cDNA sample prepared as a mixture of RNA from 10 different cell lines (Agilent) confirmed expression of *ABCC8*, and samples without cDNA template served as a negative control. The TaqMan gene expression system was used (Applied Biosystems).

Transcript levels were measured by the ABI Prism 7900HT Sequence Detection System (Applera). Applied Biosystems assays were used for priming/probing of cDNA samples, including: ABCC8 (Hs01093774_m1) and GAPDH (Hs02758991_g1).

Fold changes in gene expression, which was normalized to *GAPDH* expression and relative to the control lung samples, was calculated using the 2^{-ddCt} method. qRT-PCR experiments were performed in duplicates for all samples and executed on multiple days. All data/tissue samples were provided by PHBI under the Pulmonary Hypertension Breakthrough Initiative (PHBI).

RESULTS

Inherited and *de novo* variants in *ABCC8*

By exome sequencing, we identified a *de novo* missense variant c.G2873A (p.R958H) in ATP-binding cassette, subfamily C, member 8 (*ABCC8*) (NM_001287174), which was predicted to be deleterious, in a patient diagnosed with idiopathic pulmonary arterial hypertension at the age of 10 (Table 2.1). We then examined all CU-PAH patients for rare or novel variants in *ABCC8* and identified seven additional rare damaging missense variants, predicted by multiple algorithms to be deleterious in seven unrelated patients with idiopathic or familial pulmonary hypertension (Table 2.1). To replicate the findings in the CU-PAH cohort, we evaluated the UK-PAH cohort and identified three additional rare or novel missense and one splice variant in *ABCC8* in three patients with idiopathic and one patient with congenital heart disease associated pulmonary arterial hypertension (Table 2.1). Five variants – c.A214G (p.N72D), c.G558T (p.E186D), c.G718A (p.A240T), c.G2371C (p.E791Q), and c.T2694+2G -- were novel; four rare variants – c.G331A

(p.G111R), c.C403G (p.L135V), c.G2437A (p.D813N), and c.G4414A (p.D1472N) -- have been reported in patients with congenital hyperinsulinism; and two variants – c.C686T (p.T229I) and c.G3941A (p.R1314H) – have been reported in patients with transient neonatal diabetes mellitus.[186-192] Alignment of the *ABCC8* sequence revealed that all missense variants occur at amino acid residues conserved across species and in critical domains (Figure 2.1B).

All individuals were heterozygous for these rare *ABCC8* variants. The L135V, D813N, and R1314H variants were inherited from an unaffected father, while E791Q and D1472N were inherited from an unaffected mother. Seven of the probands were female and five were male. None of the probands had any evidence of hyperinsulinism or transient/permanent neonatal diabetes mellitus although one adult patient had type 2 diabetes. Six of the patients were children at the time of diagnosis. Three patients responded and three patients did not respond to acute vasodilator testing using inhaled nitric oxide during cardiac catheterization. Two patients had evidence of a cardiac arrhythmia (Table 2.1).

To estimate the genetic effect size of *ABCC8* variants, we selected 33,369 European adult subjects from Exome Aggregation Consortium (ExAC) and 49,630 European ancestry subjects from the DiscovEHR study independently as controls,[178] and tested for an excess of rare (minor allele frequency ≤0.1%) predicted deleterious missense variants in cases compared to controls. There were six rare predicted deleterious alleles in 150 pulmonary arterial hypertension cases of European ancestry in the CU-PAH cohort, while 158 unique deleterious variants were observed a total of 295 times in 33,369 controls with exome sequencing in the ExAC dataset and 165 rare unique deleterious variants were observed 721 times in the Regeneron-Geisinger DiscovEHR study. With binomial tests, we observed significant excess of rare predicted deleterious missense

variants in *ABCC8* in CU-PAH cases when comparing to ExAC controls (P-value = 0.0023, Enrichment rate = 4.5) and to DiscovEHR controls (P-value = 0.022, Enrichment rate = 2.8). We tested the association of predicted benign *ABCC8* variants and identified two rare synonymous alleles in cases, 223 unique predicted benign missense variants or synonymous variants observed a total of 512 times in controls, and found no significant difference between the CU-PAH group and ExAC (P-value = 1; relative risk = 0.87).

Table 2.1. Pathogenicity Predictions and Clinical Characteristics of Patients with Pulmonary Arterial Hypertension with *ABCC8* Mutations

Nucleotide and AA variant	c.A214G: p.N72D	c.G331A: p.G111R	c.C403G: p.L135V	c.G558T: p.E186D	c.C686T: p.T229I	c.G718A: p.A240T	c.G2371C: p.E791Q	c.G2437A: p.D813N	c.G2873A: p.R958H	c.G3941A: p.R1314H	c.G4414A: p.D1472N	c.T2694+2 G:p.NA
ExAC_Freq	N/A	0.00002	0.00003	0	0.000008	N/A	0	0.0001	0	0.00003	0	N/A
MetaSVM_pred	D	D	D	D	D	D	D	D	D	D	D	N/A
CADD_phred	22.8	28.4	20.5	19.46	29.4	35	32	35	27.9	23	22.4	25.1
Cohort	UK	UK	CU	CU	UK	CU	CU	CU	CU	CU	CU	UK
PAH type	Congenital heart disease-associated	Idiopathic	Idiopathic	Idiopathic	Idiopathic	Familial, sister and father with PAH	Familial, two affected siblings	Idiopathic	Idiopathic	Idiopathic	Idiopathic	Idiopathic
Inheritance	Unknown	Unknown	Paternal	Unknown	Unknown	Unknown	Maternal	Paternal	De novo	Paternal	Maternal	Unknown
Gender	F	M	M	M	F	F	F	M	F	M	F	F
Age of diagnosis	35	64	5	79	34	Unknown	14	12	10	<1	9	60
RAP M (mmHg)	N/A	11	9	N/A	9	N/A	N/A	25	6	N/A	7	7
PAP M (mmHg)	N/A	44	55	N/A	45	N/A	N/A	54	56	N/A	37	36
AOP M (mmHg)	N/A	Unknown	78	N/A	Unknown	N/A	N/A	48	88	N/A	67	Unknown
PVRi (U*m2)	N/A	19	25	N/A	13	N/A	N/A	29	16	N/A	17	19
Art Sat %	N/A	97	91	N/A	98	N/A	N/A	93	91	N/A	96	97
PCWPm (mmHg)	N/A	15	8	N/A	10	N/A	N/A	N/A	8	N/A	N/A	6
CI (L/min/m2)	N/A	1.5	2.8	N/A	2.7	N/A	N/A	N/A	2.8	N/A	2	1.6
Response to acute vasodilator test	N/A	Unknown	Yes	Unknown	No	Unknown	Unknown	No	Yes	Unknown	Yes	No
Cardiac arrhythmias and other conditions	Large atrial septal defect	Type 2 Diabetes Mellitus	Bigeminy, 1st degree heart block	None	Hearing loss Hypo-thyroidism Lipodermatosclerosis End stage renal failure Raynaud syndrome	None	None	Atrial flutter Nonspecific intra-ventricular block Autism	None	None	None	None

Abbreviations: AA= amino acid, M=male, F=female, N/A=not available, RAP M=mean right atrial pressure, PAP M=mean pulmonary arterial pressure, AOP M=mean aortic pressure, PVRi=pulmonary vascular resistance index, Art Sat=arterial oxygen saturation, PCWPm=mean pulmonary capillary wedge pressure, CI=cardiac index. UK=United Kingdom cohort, CU=Columbia University cohort.

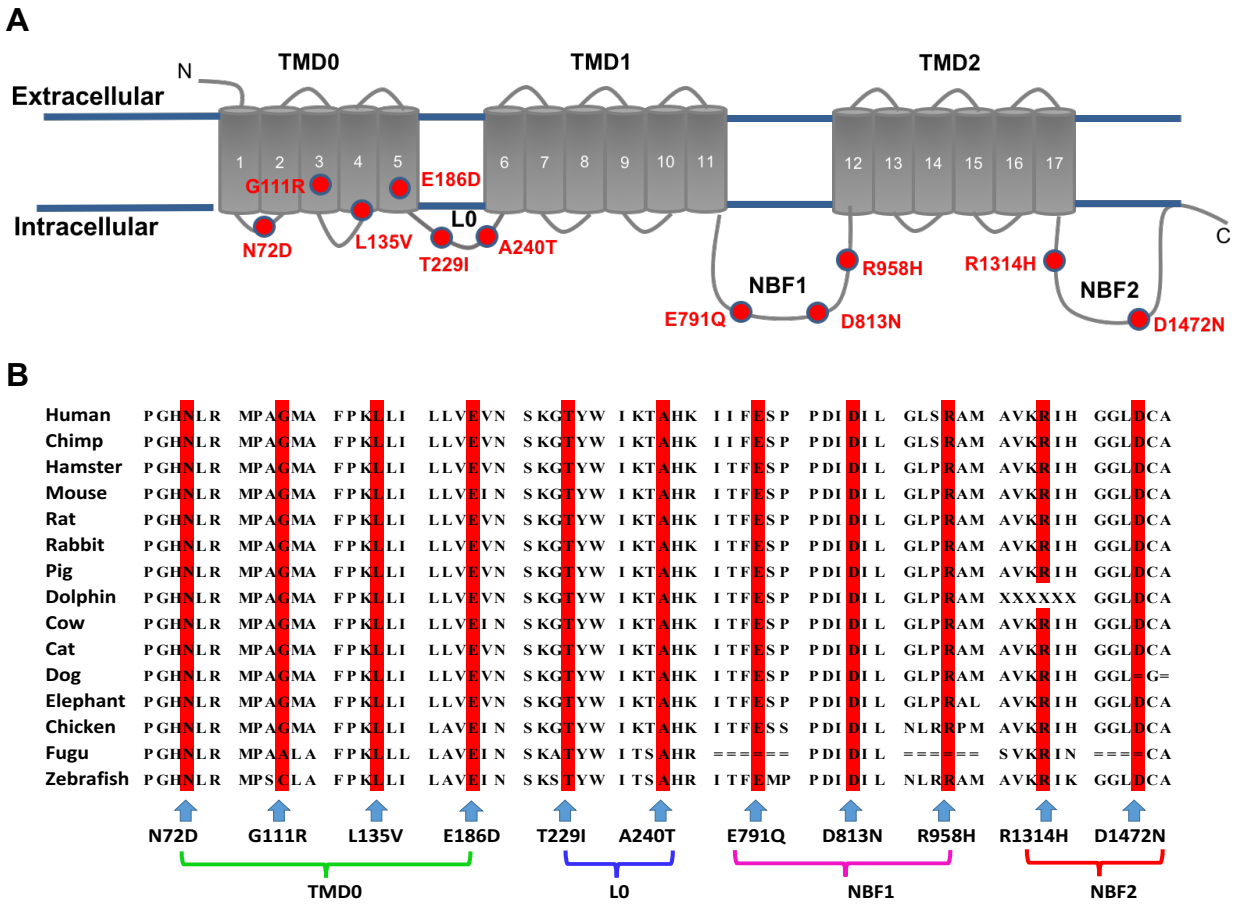

Figure 2.1. Topologic analysis of the SUR1 protein encoded by *ABCC8*, and sequence alignment of *ABCC8* across species. Panel A shows the topology of the SUR1 protein. The 17 transmembrane segments are grouped into transmembrane domains (TMD): TMD0, TMD1, and TMD2. The two nucleotide-binding fold domains (NBF1 & 2) are indicated. Variants N72D, G111R, L135V, and E186D are located in TMD0; T229I and A240T are located in the cytoplasmic loop, L0; E791Q, D813N, and R958H are located in NBF1; R1314H and D1472N are located in NBF2. The position of each mutation is indicated by a red circle. Panel B shows the alignment of human *ABCC8*-encoding SUR1 protein with 14 different species, demonstrating conservation across species of each amino acid found mutated in this study.

Functional characterization of *ABCC8* mutations

ABCC8 encodes the sulfonylurea receptor 1 (SUR1) protein, a regulatory subunit of the K_{ATP} channel, which associates with the pore-forming Kir6.2 subunit.[144] SUR1 controls cell excitability by regulating trafficking and expression of the K_{ATP} channel, and confers sensitivity of K_{ATP} channels to magnesium-nucleotides and pharmacological modulators. SUR1-dependent K_{ATP} channels are prominent in neuronal and pancreatic tissues, but present in many other tissues, including cardiac atria.[144,193,194] We also demonstrate that *ABCC8* is expressed in lungs of patients with pulmonary arterial hypertension and in healthy individuals (Figure 2.2), providing a potential target for influencing and modulating pulmonary arterial hypertension.

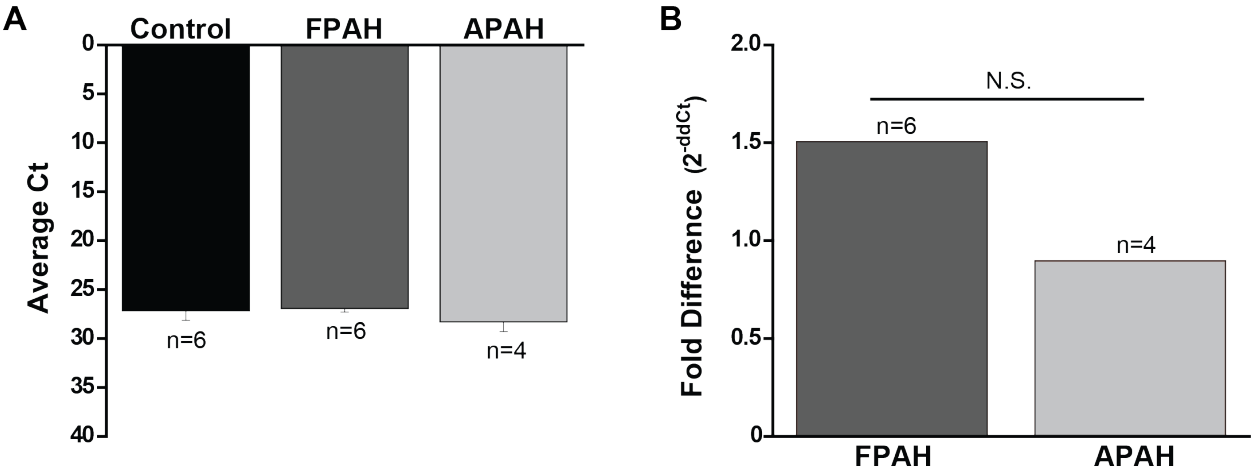

Figure 2.2. Quantitative Real-Time Polymerase Chain Reaction (qRT-PCR) results of human lung samples from patients with familial pulmonary arterial hypertension (FPAH), pulmonary arterial hypertension associated with congenital heart defects (APAH), and from healthy (Control) lungs. ABCC8 lung expression was quantified against an endogenous housekeeping gene, GAPDH. Panel A shows average cycle threshold (Ct) values at which ABCC8 appears in each condition. Panel B displays relative expression (2^{-ddCt}) of ABCC8 in FPAH and APAH samples compared to Control samples. No significant differences in expression of ABCC8 in Control, FPAH, and APAH were observed.

We examined the consequence of eight of the twelve identified *ABCC8* variants putatively associated with pulmonary arterial hypertension on SUR1 function using two complementary measures of K_{ATP} activity: (1) patch-clamp electrophysiology provided a direct measurement of whole cell K_{ATP} conductance in individual cells across different membrane potentials; and (2) rubidium ($^{86}Rb^{+}$) flux assays provided quantification of channel activity using $^{86}Rb^{+}$ efflux as a measure of macroscopic K_{ATP} conductance from a population of intact cells. By co-expressing Kir6.2 with SUR1 in COS cells, functional K_{ATP} channels were formed in each assay. All SUR1 variants tested demonstrated loss of function in at least one functional assay.

First, we used patch-clamp experiments to directly measure SUR1-dependent K_{ATP} channel activity by applying a voltage ramp in whole-cell conditions (Figure 2.3A), using an established assay.[195] We maximally activated K_{ATP} channel currents with diazoxide (100μM), a selective SUR1 activator. Once steady-state diazoxide current activation was achieved, glibenclamide (10μM) – which inhibits K_{ATP} channels by binding to the SUR subunit – was co-applied. The glibenclamide-sensitive current was taken as the SUR1-dependent K_{ATP} current[195] (Figure 2.3 and Figure 2.4).

Robust SUR1-dependent K_{ATP} currents were measured in cells expressing Kir6.2 and wildtype SUR1 (Figure 2.5A). By contrast, currents were much smaller in cells expressing A240T SUR1, one of the novel SUR1 variants identified, similar to currents in cells expressing D813N or D1472N SUR1, previously reported mutations in congenital hyperinsulinism patients (Figure 2.5B). Further analysis demonstrated significantly reduced SUR1-dependent currents in six of eight SUR1 mutants evaluated, and non-significant reductions in L135V and R958H (Figure 2.5C).

Figure 2.3. Whole-cell patch-clamp was used to measure expressed K_{ATP} currents in response to pharmacological agents. Panel A shows sample K_{ATP} channel current traces from wildtype SUR1+Kir6.2, activated by diazoxide 100µM (black curve) and inhibited by co-application of glibenclamide 10µM (red curve). A voltage ramp from -120mV to +60mV over 1 second was applied every 3 seconds, from a -80mV holding potential. The vertical scale is 100 pA/pF, and the horizontal scale is 20 mV. Panel B shows equivalent sample traces for all mutant SUR1-containing K_{ATP} channels. Panel C shows equivalent traces for wildtype and control conditions: (1) Kir6.2 only; (2) SUR1 only; (3) no K_{ATP}; (4) L1016M SUR1 (identified benign variant) + Kir6.2. Panels D and E summarize current densities from Panels A-C, measured at -40mV (n=4 to 30 cells per condition). Panel F summarizes the diazoxide-activated current for wildtype and all mutant SUR1-containing K_{ATP} channels. Data are shown as means; T bars indicate standard errors. In panel F, $P<0.05$ for the comparison of diazoxide-activated current of each K_{ATP} channel (mutant and wildtype) versus no K_{ATP} expression, calculated by the paired Student's *t*-test.

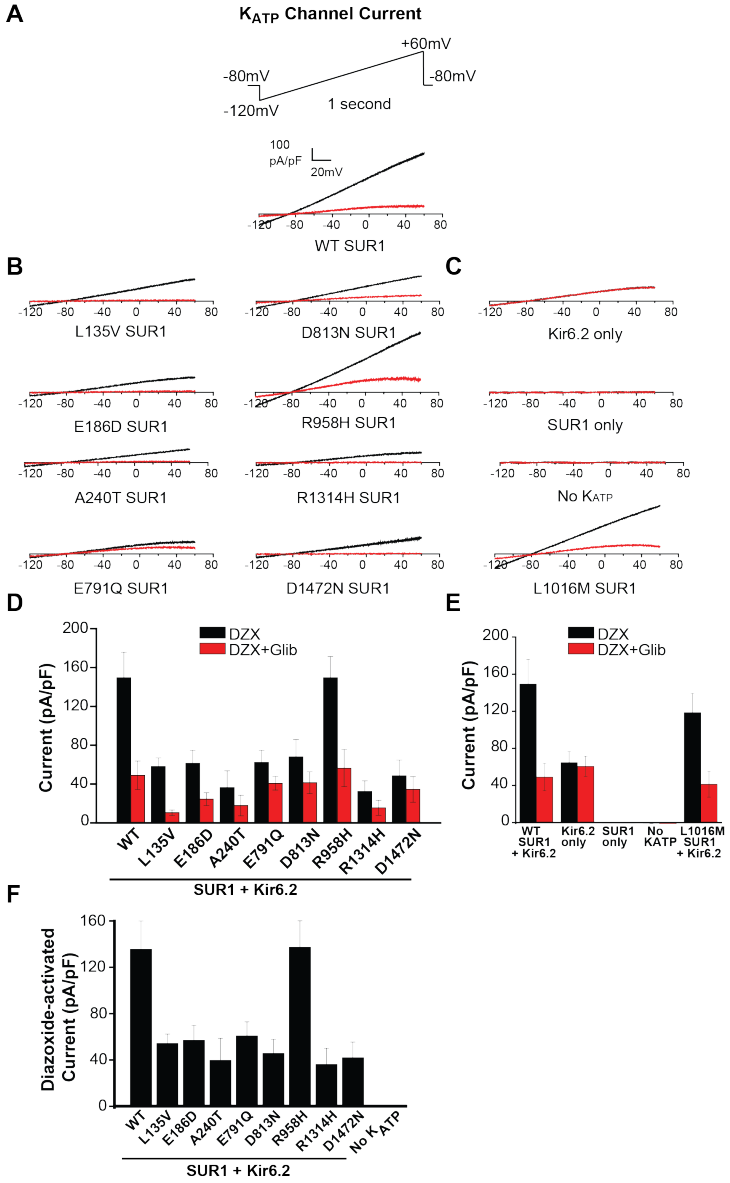

Figure 2.4. Whole-cell voltage clamp was used to measure the SUR1-dependent current of wildtype versus mutant K_{ATP} (SUR1/Kir6.2) channels. Panel A shows a sample glibenclamide-sensitive current trace (SUR1-dependent current) from wildtype K_{ATP}. A voltage ramp from -120mV to +60mV over 1 second was applied every 3 seconds, from a -80mV holding potential. The vertical scale is 100 pA/pF, and the horizontal scale is 20 mV. Panel B shows equivalent sample traces for all mutant SUR1-containing K_{ATP} channels. Panel C shows equivalent sample traces for wildtype and control conditions: (1) Kir6.2 only; (2) SUR1 only; (3) no K_{ATP}; (4) L1016M SUR1 (identified benign variant) + Kir6.2. Panels D and E summarize current densities from Panels A-C, measured at -40mV (n=4 to 30 cells per condition). Data are shown as means; T bars indicate standard errors. Asterisks denote $P<0.05$ for the comparison between wildtype SUR1 and each mutant or control condition, calculated by one-way ANOVA (post-hoc Tukey test).

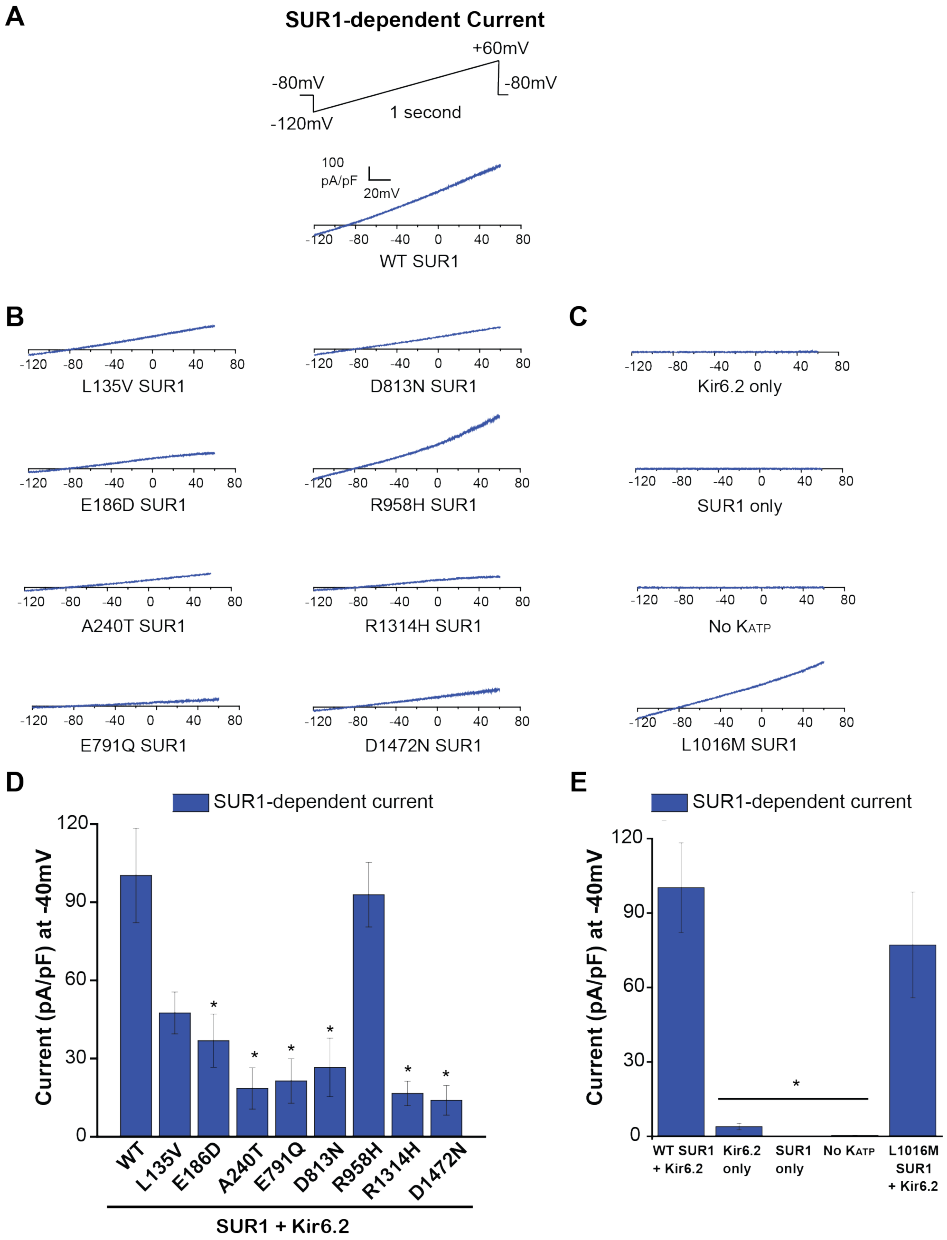

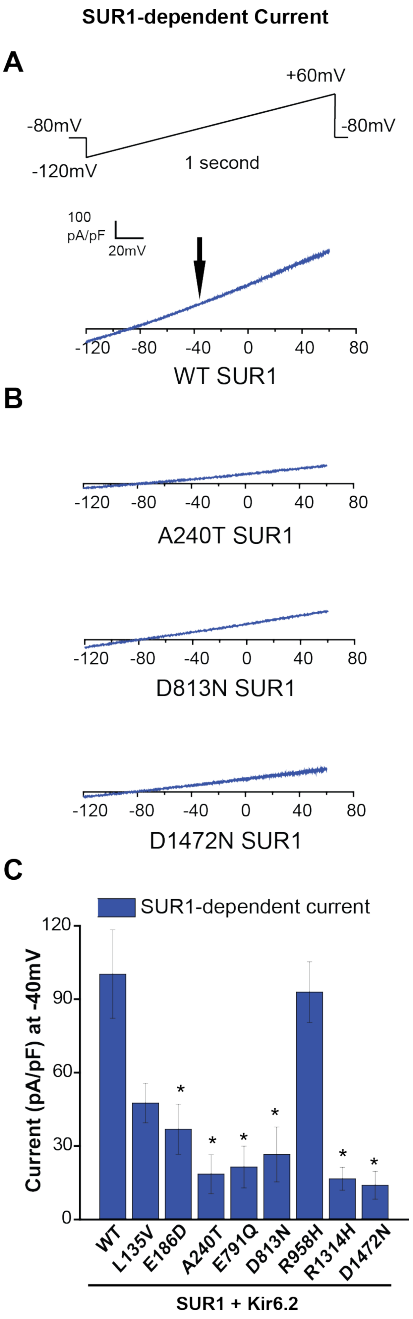

Figure 2.5. Electrophysiological consequence of SUR1 mutations on K_{ATP} channel function. Whole-cell voltage clamp was used to measure expressed wildtype (WT) versus mutant K_{ATP} channel currents containing SUR1+Kir6.2 in COS7 cells. Panel A shows a wildtype SUR1-dependent K_{ATP} current trace. A voltage ramp from -120mV to +60mV over 1 second was applied every 3 seconds, from a -80mV holding potential. For all sample current traces, the vertical scale is 100 pA/pF, and the horizontal scale is 20mV. Panel B shows SUR1-dependent current traces of mutant K_{ATP} channels containing A240T, D813N, or D1472N SUR1 as indicated. Panel C summarizes SUR1-dependent K_{ATP} current densities (pA/pF) for the eight SUR1 mutants evaluated and wildtype, measured at -40mV (indicated by the black arrow in Panel A); 8 to 30 cells were studied per condition. Data are shown as means; T bars indicate standard errors. Asterisks indicate $P<0.05$ for the comparison between wildtype SUR1 and each mutant, as calculated by a one-way ANOVA and post-hoc Tukey test.

Next, $^{86}Rb^{+}$ efflux rate was recorded as a measure of K_{ATP} channel activity in cells expressing wildtype or mutant SUR1 along with Kir6.2 (Figure 2.6), in basal metabolic conditions and in metabolic inhibition. Compared to wildtype SUR1, basal conditions yielded marked decreases in efflux rate for the A240T, D813N, and D1472N variants, and smaller decreases for L135V, E791Q, R958H, and R1314H [Figure 2.6A and 2.6B; and Table 2.2-S1]. In metabolic inhibition (extracellular solution supplemented with 2-deoxy-D-glucose and oligomycin to impair ATP synthesis and relieve K_{ATP} channels from inhibition by intracellular nucleotides), the flux rates for the L135V, A240T, D813N, R958H and D1472N mutants were markedly lower than wildtype (Figure 2.6C and 2.6D; and Table 2.2-S2). The E791Q and R1314H mutant fluxes were slightly reduced, while no decrease in flux under basal or metabolic inhibition conditions was observed for E186D.

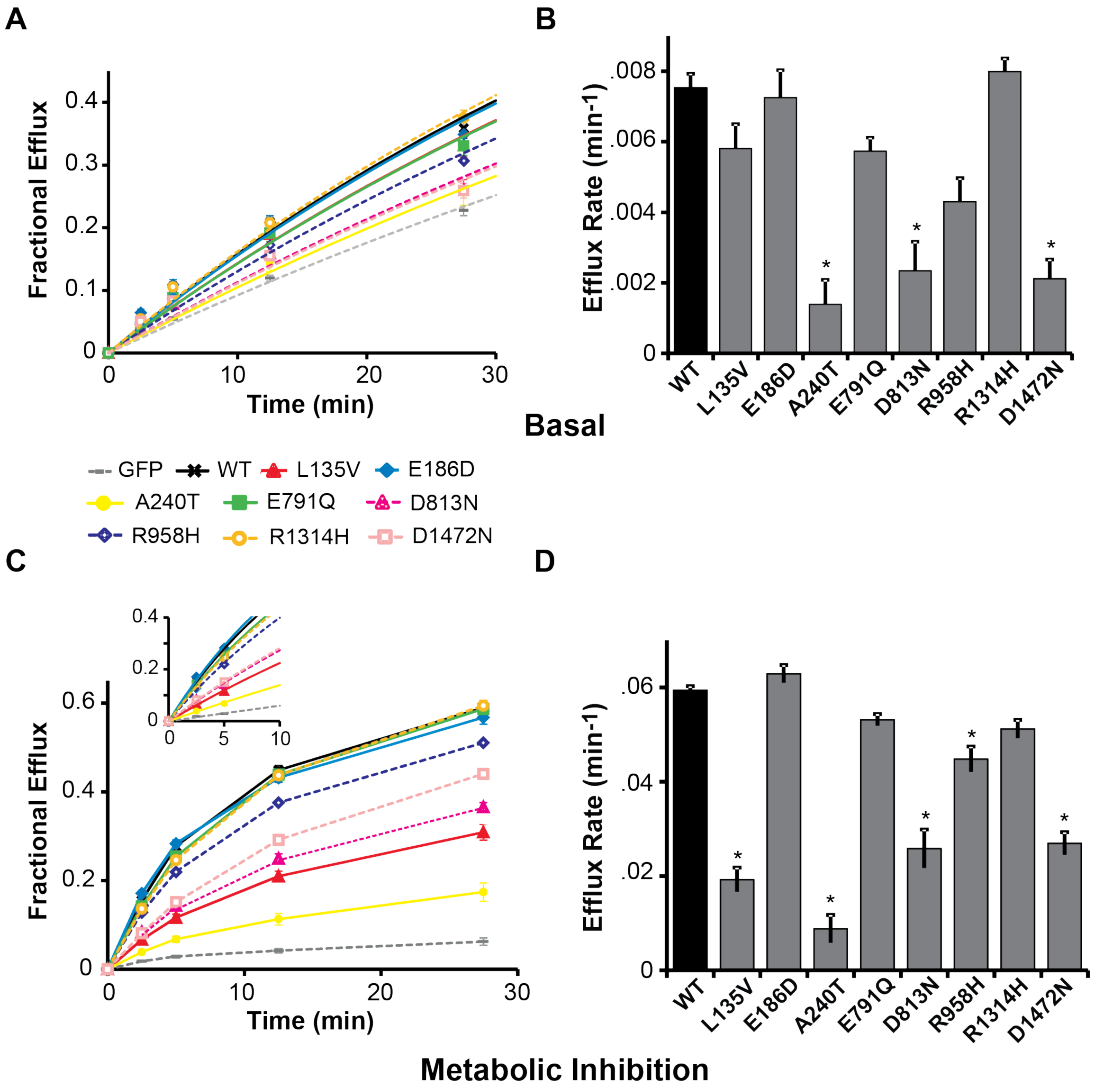

Figure 2.6. Functional impact of SUR1 mutations on macroscopic K_{ATP} channel activity. $^{86}Rb^{+}$ efflux was measured over time from COSm6 cells expressing K_{ATP} channels containing SUR1+Kir6.2. Panel A shows basal efflux for wildtype (WT, black curve) versus mutant (colored curves) SUR1-containing K_{ATP} channels, and GFP-alone (gray curve). Panel B displays the mean rate constants for K_{ATP}-dependent $^{86}Rb^{+}$ efflux under basal conditions. Panel C shows efflux from cells exposed to solution containing oligomycin and 2-deoxy-D-glucose to induce metabolic inhibition of cells, thereby relieving K_{ATP} channels from intracellular inhibition by ATP. Wildtype versus mutant SUR1-containing K_{ATP} channels, and GFP-alone, are compared. The inset shows exponential fits to early time points which were used to derive the efflux rate constants (see Supplementary Appendix). Panel D shows the mean rate constants for K_{ATP}-dependent $^{86}Rb^{+}$ efflux under metabolic inhibition conditions. For each condition, 7 to 10 cell populations were studied. Data are shown as means; T bars indicate standard errors. Asterisks indicate $P<0.05$ for the comparison between wildtype SUR1 and each mutant, as calculated by a one-way ANOVA and post-hoc Tukey test.

Table 2.2. Sub-tables S1-S3 show rate constants derived from rubidium flux experiments measuring K_{ATP} channel (SUR1/Kir6.2) activity.

	K (min^{-1})	
GFP (K_1)	$9.7x10^3 \pm 4.0x10^4$	
WT	$7.5x10^3 \pm 7.0x10^4$	
L135V	$5.8x10^3 \pm 7.8x10^4$	
E186D	$7.3x10^3 \pm 6.9x10^4$	
A240T	$1.4x10^3 \pm 4.0x10^4$	*
E791Q	$5.7x10^3 \pm 6.6x10^4$	
D813N	$2.3x10^3 \pm 3.7x10^4$	*
R958H	$4.3x10^3 \pm 5.5x10^4$	*
R1314H	$8.0x10^3 \pm 1.2x10^3$	
D1472N	$2.1x10^3 \pm 4.4x10^4$	*

Table S1: Rate constants for $^{86}Rb^+$ efflux in basal conditions.

	K (min^{-1})	
GFP (K_1)	$6.2x10^3 \pm 8.2x10^4$	
WT	$5.9x10^2 \pm 2.6x10^3$	
L135V	$1.9x10^2 \pm 1.9x10^3$	*
E186D	$6.3x10^2 \pm 2.9x10^3$	
A240T	$8.8x10^3 \pm 1.2x10^3$	*
E791Q	$5.3x10^2 \pm 2.7x10^3$	
D813N	$2.6x10^2 \pm 1.9x10^3$	*
R958H	$4.5x10^2 \pm 2.4x10^3$	*
R1314H	$5.1x10^2 \pm 4.1x10^3$	
D1472N	$2.7x10^2 \pm 2.2x10^3$	*

Table S2: Rate constants for $^{86}Rb^+$ efflux in MI conditions.

	K (min^{-1})	
GFP (K_1)	$1.4x10^2 \pm 6.1x10^4$	
WT	$4.5x10^2 \pm 5.6x10^3$	
L135V	$3.7x10^2 \pm 3.9x10^3$	
E186D	$3.5x10^2 \pm 3.2x10^3$	
A240T	$5.8x10^3 \pm 9.3x10^4$	*
E791Q	$3.8x10^2 \pm 4.8x10^3$	
D813N	$1.8x10^2 \pm 2.3x10^3$	*
R958H	$3.2x10^2 \pm 3.3x10^3$	*
R1314H	$2.9x10^2 \pm 2.6x10^3$	
D1472N	$2.0x10^2 \pm 2.9x10^3$	*

Table S3 : Rate constants for $^{86}Rb^+$ efflux in 100μM diazoxide.

Thus, there was a decrease in basal and/or maximal channel activity for all SUR1 mutants associated with pulmonary arterial hypertension tested in our study. As discussed below, such loss of function could result from various mechanisms, but any channel activity present might be augmented by selective potassium channel opening drugs, such as diazoxide. Consistent with this suggestion, all mutants tested were pharmacologically activated by diazoxide (100μM) in rubidium efflux (Figure 2.7A and 2.7B; and Table 2.2-S3), and electrophysiological assays (Figure 2.7C and 2.7D; and see Figure 2.3F).

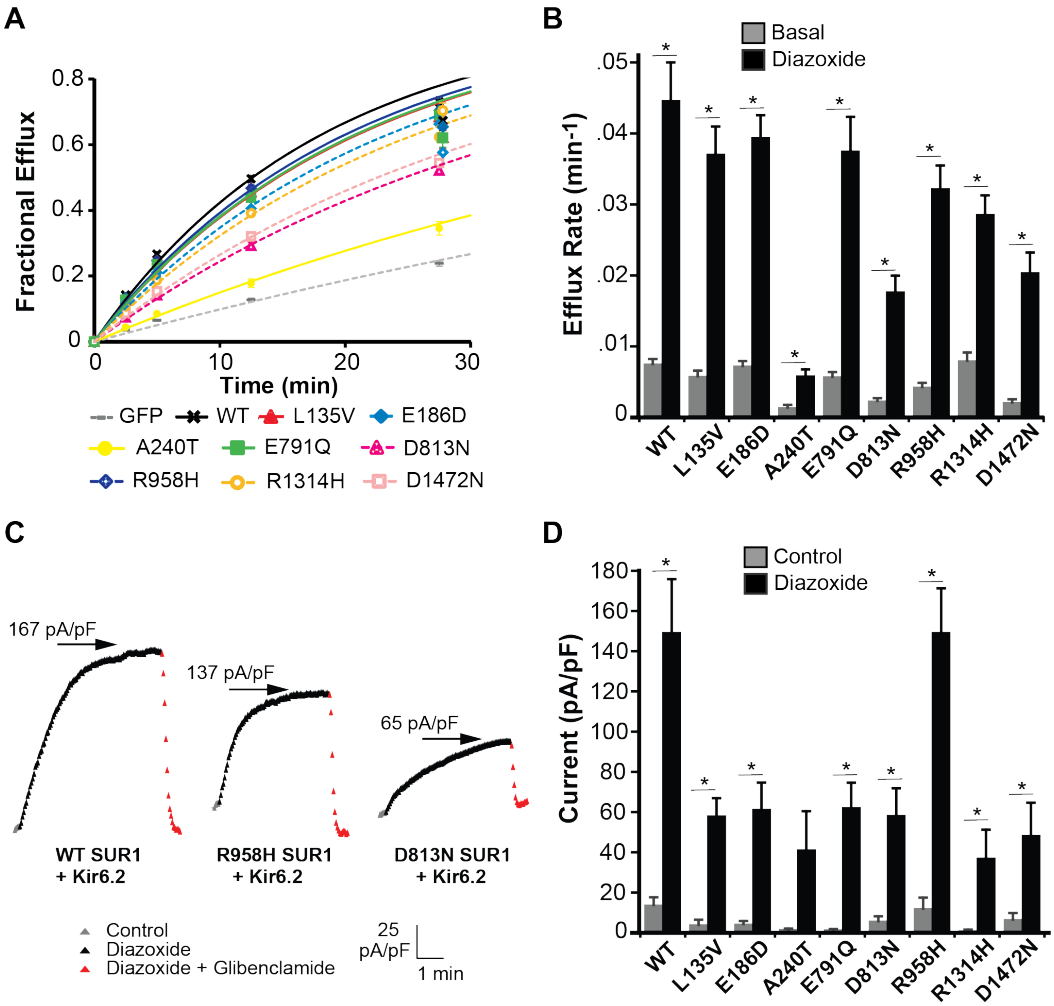

Figure 2.7. Pharmacological recovery of mutant K_{ATP} channels. Diazoxide restores function of K_{ATP} channels (SUR1/Kir6.2) containing mutant SUR1. Panel A shows rubidium efflux in the presence of diazoxide 100μM for wildtype (WT) SUR1 (black curve), mutant SUR1-containing K_{ATP} channels (colored curves), and GFP-alone (gray curve). Panel B shows average efflux rates for wildtype and mutant K_{ATP} channels in basal (gray) versus diazoxide 100μM (black) conditions. For each condition, 7 to 10 cell populations were studied. Panel C depicts whole-cell drug time courses of wildtype and selected mutant K_{ATP} channel currents before drug application (gray, control), during diazoxide 100μM application (black), and during co-application of glibenclamide 10μM with diazoxide 100μM (red). The vertical scale is 25 pA/pF, and the horizontal scale is 1 minute. Arrows indicate the maximal steady-state current-density (pA/pF) achieved during diazoxide 100μM application. Panel D summarizes current density (pA/pF at -40mV) for wildtype and each mutant SUR1-containing K_{ATP} channel, in control (gray) and diazoxide 100μM (black) conditions; 6 to 30 cells were studied per condition. Data are shown as means; T bars indicate standard errors. Asterisks denote $P<0.05$ for the comparison of basal and diazoxide (Panel B), or control and diazoxide (Panel D), calculated by the paired Student's *t*-test.

DISCUSSION

Using exome sequencing, we identified *de novo* and inherited heterozygous mutations in a novel candidate gene, *ABCC8*, potentially associated with familial and idiopathic pulmonary arterial hypertension, in eight independent families, with six of the probands diagnosed as children in the CU-PAH study. We identified an additional four rare or novel predicted damaging missense and splice variants in *ABCC8* in a second cohort (UK-PAH) of adult group I pulmonary arterial hypertension patients with idiopathic, familial or appetite drug-associated disease. Functional analyses demonstrated reduced ATP-sensitive potassium (K_{ATP}) channel activity in all SUR1 mutants tested and pharmacological rescue of K_{ATP} activity by diazoxide. Our results suggest a role for *ABCC8* in the pathogenesis of pulmonary arterial hypertension, and as a potential therapeutic target.

ABCC8 encodes the sulfonylurea receptor 1 (SUR1) protein, a K_{ATP} channel subunit. The eleven identified missense *ABCC8* variants are all rare, located at residues highly conserved across species, and reside in intracellular and transmembrane domains of SUR1, including nucleotide binding fold regions (Figure 2.1). *ABCC8* is highly expressed in the human brain and endocrine pancreas, and moderately expressed in human lungs[196] (Figure 2.2). In pancreatic β-cells, high intracellular ATP concentrations (eg. during post-prandial glucose metabolism) close the channel, causing cell depolarization, activation of voltage-gated calcium channels, leading to insulin secretion.[193]

K_{ATP} channel activity contributes to cell excitability in multiple other tissues,[144] including cardiac atrium.[194] It has been reported that SUR2B is the predominant SUR isoform expressed in cultured pulmonary artery smooth muscle cells,[126] but the details of subunit composition of K_{ATP} channels

in native pulmonary artery smooth muscle and endothelial cells in different conditions remains unclear. There is evidence for K_{ATP} channels in pulmonary artery smooth muscle and endothelial cells and SUR1 expression in pulmonary arteries,[126,197] while K_{ATP} channel activity is upregulated by elevated shear stress in pulmonary vascular endothelial cells.[197] More recently, SUR1 upregulation by hypoxia was reported in cerebral microvascular endothelial cells.[198,199] *KCNK3*, established as the first potassium channelopathy in pulmonary arterial hypertension,[55,75] is also regulated by hypoxia in pulmonary artery smooth muscle cells, and may contribute to hypoxic pulmonary vasoconstriction.[73]

SUR1-dependent K_{ATP} channel loss of function alongside KCNK3 channel loss of function therefore represent possible pathogenic mechanisms in pulmonary arterial hypertension, and pharmacologic recovery of channel function a therapeutic avenue.[55,75] Complementary and redundant potassium channel activity could contribute to the lung-specific phenotype observed clinically in patients with heterozygous *ABCC8* or *KCNK3* mutation.[1,89]

All *ABCC8* variants that we identified and functionally assessed represent loss of function mutations. The disease consequences may vary, as there is clearly incomplete penetrance within our families with several asymptomatic transmitting parents. Dominant and recessively inherited mutations in *ABCC8* cause neonatal/adult-onset diabetes or congenital hyperinsulinism, due to gain or loss of *ABCC8* function, respectively.[191,200] Dominantly inherited *ABCC8* mutations affecting glucose homeostasis display incomplete penetrance, and patients with only one *ABCC8* mutation often have milder or no disease.

Despite loss of *ABCC8* function underlying many cases of congenital hyperinsulinism, the patients in our study have no evidence of hyperinsulinemic hypoglycemia or transient/permanent neonatal diabetes mellitus. This raises the question: why do SUR1-dependent pulmonary arterial hypertension patients not have hyperinsulinism, and *vice versa*, why do hyperinsulinism patients not have evidence of pulmonary arterial hypertension? The L135V and D1472N *ABCC8* variants we identified have been reported as recessive alleles in congenital hyperinsulinism,[186,192,201-203] while D813N and D1472N have been reported as variants in autosomal dominant or recessive congenital hyperinsulinism inherited from unaffected fathers,[187,188] with loss of heterozygosity observed for D1472N.[204]

Imprinting at the 11p15 chromosomal region near the *ABCC8* gene locus can lead to pancreatic endocrine cell proliferation in focal hyperinsulinemic patients possessing loss of function *ABCC8* mutations.[205] Tissue-specific consequences of imprinting near the *ABCC8* gene locus and/or somatic loss of *ABCC8* in the pulmonary vasculature could predispose to lung specific disease in the setting of germline *ABCC8* loss of function mutations. A combination of genetic, developmental, and environmental factors may determine which patients with *ABCC8* mutations develop pulmonary arterial hypertension.

The mechanism of SUR1 loss of function likely varies based on mutation location with the channel subunit. For instance, G111R and D1472N have been previously shown to decrease SUR1 trafficking to the plasma membrane,[187,192,202] while nucleotide binding fold mutations, D813N and R958H, may impair magnesium-nucleotide activation. SUR1 mutation severity impacts viability for pharmacological rescue, as previously demonstrated for KCNK3 mutant channels associated with pulmonary arterial hypertension,[55] and for SUR1 mutants associated with congenital

hyperinsulinism.[206] We observed variable functional recovery by diazoxide of each SUR1 mutant tested. Diazoxide is a SUR1 activator clinically employed as an anti-hypertensive and anti-hyperinsulinism agent. Case reports have already described the successful use of diazoxide to reverse pulmonary hypertension,[207,208] underscoring SUR1-dependent K_{ATP} activation as an intriguing potential basis for pulmonary hypertension therapy.[209]

As mainstay treatment in congenital hyperinsulinism, diazoxide administration overcomes disease-causing *ABCC8* loss-of-function mutations. Rarely, diazoxide administration to hypoglycemic neonates has been associated with pulmonary arterial hypertension;[210] however, this may be secondary to inadequate diuresis with diazoxide treatment, leading to volume overload following systemic blood volume expansion. Ultimately, K_{ATP} channel activators with less pulmonary toxicity may prove more useful for pulmonary hypertension treatment.[211]

In conclusion, we have identified mutations in the *ABCC8* gene as a second potassium channelopathy in pulmonary arterial hypertension, and as a potential therapeutic target.

CONCLUSIONS

Pulmonary arterial hypertension (PAH) is a devastating illness with significant morbidity and high mortality rates. Newer medical treatments have improved clinical outcomes, yet patient prognosis remains poor. Research into disease pathogenesis aims to uncover pathological processes in pulmonary arterioles that may offer novel treatment targets. My thesis work focuses on potassium channel dysfunction as a cause of PAH, and recovery of potassium channel currents as a potential therapeutic avenue.

Our research group had identified loss-of-function *KCNK3* mutations as a cause of pulmonary arterial hypertension in patients heterozygous at the *KCNK3* gene locus. Furthermore, a KCNK3-activator (ONO-RS-082) was shown to recover function of some mutant KCNK3 channels. In the research presented here, we have expanded upon the original characterization of mutant channel dysfunction, to uncover mechanisms of KCNK3 dysfunction and characterize channel function and recovery in more physiological relevant heterozygous conditions.

KCNK3 is an acid-sensitive, two-pore domain potassium channel. We determined that the V221L KCNK3 mutation confers a pH-dependent mechanism of loss-of-function, while the G203D mutation confers a more severe loss-of-function phenotype. Mature KCNK3 channels function as dimers, composed of two KCNK3 subunits that co-assemble. We engineered tandem-linked heterodimeric mutant KCNK3 channels containing one mutant and one non-mutant KCNK3 subunit in order to study the impact of heterozygosity on channel function, and observed intermediate function of mutant WT-V221L KCNK3 heterodimeric compared to WT and V221L homodimeric channels. Thus, the engineered heterodimers reported function of a substantial,

discrete proportion of formed channels in heterozygous conditions. Moreover, we observed pharmacological activation of the mutant heterodimers by ONO-RS-082. When examining V221L KCNK3 channel function in cultured pulmonary artery smooth muscle cells expressing the mutant channels, we observed pharmacological recovery of mutant KCNK3 function as measured by membrane hyperpolarization. Together, we concluded that mutant KCNK3 channels can be pharmacologically targeted for activation in heterozygous KCNK3 conditions.

To understand why heterozygous mutations in *KCNK3* leads to PAH, but no other medical illness, despite widespread tissue expression of *KCNK3*, we turned to experiments with the closely related KCNK9 channel. We observed that *KCNK3* is expressed in healthy and PAH patient lungs, while *KCNK9* is not appreciably expressed. KCNK3 and KCNK9 channels have been shown to be co-expressed in other tissues, such as in the central nervous system, and were shown to co-assemble to form KCNK9-KCNK3 heterodimeric channels. With this in mind, we tested the hypothesis that KCNK9, an acid-sensitive channel that is more maximally activated at physiological pH 7.4, could recover function of mutant KCNK3, which may provide protection against KCNK3 dysfunction in tissues where both *KCNK3* and *KCNK9* are co-expressed. Indeed, we observed that KCNK9 heterodimerizes with KCNK3 to produce robust currents at physiological pH 7.4, and the assembly of KCNK9 with the severe mutant G203D KCNK3 channel recovers some channel function. Therefore, KCNK9-KCNK3 heterodimerization outside of the lung may contribute to the lung-specific phenotype seen in patients with heterozygous *KCNK3* mutation.

In chapter 2, we have reported that loss of function mutations in *ABCC8* are associated with pulmonary arterial hypertension in pediatric and adult patients. The genetic association of *ABCC8* in PAH was independently replicated in a second, separate patient cohort.

ABCC8 encodes the sulfonylurea receptor 1 (SUR1) protein, a beta subunit of the ATP-sensitive potassium (K_{ATP}) channel. Using whole-cell voltage clamp electrophysiology and rubidium flux assays, we tested function of SUR1 mutants assembled with the pore- forming $K_{ir}6.2$ alpha subunit of the K_{ATP} channel. Functional assessment revealed loss of function of all SUR1 mutants studied, in at least one functional assay, and recovery of function of all mutant SUR1-containing K_{ATP} channels upon application of the K_{ATP} channel opener (and SUR1 activator), diazoxide. Therefore, SUR1 dysfunction represents a potential pathogenic mechanism in PAH and therapeutic target.

Thus, we have characterized two potassium channelopathies, in the *KCNK3* and *ABCC8* genes, associated with pulmonary arterial hypertension. In future studies, employing animal models of PAH may prove fruitful in order to investigate the pathophysiological consequences of potassium channel dysfunction. To model heterozygous *KCNK3* and *ABCC8* mutation and the consequences for pulmonary arteries, CRISPR knock-in technology may also be employed to study select mutations (eg. V221L KCNK3) in heterozygous conditions.[212] Evidence of pulmonary dysfunction at the pulmonary arterial level, combined with therapeutic relief of pulmonary arterial pressure by potassium channel opening drugs, may bring the scientific field closer to translating our genetic and experimental discoveries into improved patient care.

BIBLIOGRAPHY

1. Foster MN, Coetzee WA. KATP Channels in the Cardiovascular System. Physiol Rev 2016;96:177-252.
2. Humbert M, Sitbon O, Simonneau G. Treatment of pulmonary arterial hypertension. N Engl J Med 2004;351:1425-36.
3. Ma L, Roman-Campos D, Austin ED, et al. A novel channelopathy in pulmonary arterial hypertension. N Engl J Med 2013;369:351-61.
4. Bohnen MS, Peng G, Robey SH, et al. Molecular Pathophysiology of Congenital Long QT Syndrome. Physiol Rev 2017;97:89-134.
5. Galie N, Humbert M, Vachiery JL, et al. 2015 ESC/ERS Guidelines for the diagnosis and treatment of pulmonary hypertension: The Joint Task Force for the Diagnosis and Treatment of Pulmonary Hypertension of the European Society of Cardiology (ESC) and the European Respiratory Society (ERS): Endorsed by: Association for European Paediatric and Congenital Cardiology (AEPC), International Society for Heart and Lung Transplantation (ISHLT). Eur Heart J 2016;37:67-119.
6. Humbert M, Sitbon O, Chaouat A, et al. Pulmonary arterial hypertension in France: results from a national registry. Am J Respir Crit Care Med 2006;173:1023-30.
7. Peacock AJ, Murphy NF, McMurray JJ, Caballero L, Stewart S. An epidemiological study of pulmonary arterial hypertension. Eur Respir J 2007;30:104-9.
8. McGoon MD, Benza RL, Escribano-Subias P, et al. Pulmonary arterial hypertension: epidemiology and registries. J Am Coll Cardiol 2013;62:D51-9.
9. Morse JH, Jones AC, Barst RJ, Hodge SE, Wilhelmsen KC, Nygaard TG. Mapping of familial primary pulmonary hypertension locus (PPH1) to chromosome 2q31-q32. Circulation 1997;95:2603-6.
10. Nichols WC, Koller DL, Slovis B, et al. Localization of the gene for familial primary pulmonary hypertension to chromosome 2q31-32. Nat Genet 1997;15:277-80.
11. Deng Z, Morse JH, Slager SL, et al. Familial primary pulmonary hypertension (gene PPH1) is caused by mutations in the bone morphogenetic protein receptor-II gene. Am J Hum Genet 2000;67:737-44.
12. International PPHC, Lane KB, Machado RD, et al. Heterozygous germline mutations in BMPR2, encoding a TGF-beta receptor, cause familial primary pulmonary hypertension. Nat Genet 2000;26:81-4.
13. Aldred MA, Vijayakrishnan J, James V, et al. BMPR2 gene rearrangements account for a significant proportion of mutations in familial and idiopathic pulmonary arterial hypertension. Hum Mutat 2006;27:212-3.
14. Cogan JD, Pauciulo MW, Batchman AP, et al. High frequency of BMPR2 exonic deletions/duplications in familial pulmonary arterial hypertension. Am J Respir Crit Care Med 2006;174:590-8.
15. Thomson JR, Machado RD, Pauciulo MW, et al. Sporadic primary pulmonary hypertension is associated with germline mutations of the gene encoding BMPR-II, a receptor member of the TGF-beta family. J Med Genet 2000;37:741-5.
16. Sztrymf B, Yaici A, Girerd B, Humbert M. Genes and pulmonary arterial hypertension. Respiration 2007;74:123-32.
17. Soubrier F, Chung WK, Machado R, et al. Genetics and genomics of pulmonary arterial hypertension. J Am Coll Cardiol 2013;62:D13-21.

18. Archer SL, Weir EK, Wilkins MR. Basic science of pulmonary arterial hypertension for clinicians: new concepts and experimental therapies. Circulation 2010;121:2045-66.
19. Loyd JE, Butler MG, Foroud TM, Conneally PM, Phillips JA, 3rd, Newman JH. Genetic anticipation and abnormal gender ratio at birth in familial primary pulmonary hypertension. Am J Respir Crit Care Med 1995;152:93-7.
20. Trembath RC, Thomson JR, Machado RD, et al. Clinical and molecular genetic features of pulmonary hypertension in patients with hereditary hemorrhagic telangiectasia. N Engl J Med 2001;345:325-34.
21. Chaouat A, Coulet F, Favre C, et al. Endoglin germline mutation in a patient with hereditary haemorrhagic telangiectasia and dexfenfluramine associated pulmonary arterial hypertension. Thorax 2004;59:446-8.
22. Rabinovitch M. Molecular pathogenesis of pulmonary arterial hypertension. J Clin Invest 2012;122:4306-13.
23. Xu W, Koeck T, Lara AR, et al. Alterations of cellular bioenergetics in pulmonary artery endothelial cells. Proc Natl Acad Sci U S A 2007;104:1342-7.
24. Dewachter L, Adnot S, Fadel E, et al. Angiopoietin/Tie2 pathway influences smooth muscle hyperplasia in idiopathic pulmonary hypertension. Am J Respir Crit Care Med 2006;174:1025-33.
25. Thompson K, Rabinovitch M. Exogenous leukocyte and endogenous elastases can mediate mitogenic activity in pulmonary artery smooth muscle cells by release of extracellular-matrix bound basic fibroblast growth factor. J Cell Physiol 1996;166:495-505.
26. Alastalo TP, Li M, Perez Vde J, et al. Disruption of PPARgamma/beta-catenin-mediated regulation of apelin impairs BMP-induced mouse and human pulmonary arterial EC survival. J Clin Invest 2011;121:3735-46.
27. Masri FA, Xu W, Comhair SA, et al. Hyperproliferative apoptosis-resistant endothelial cells in idiopathic pulmonary arterial hypertension. Am J Physiol Lung Cell Mol Physiol 2007;293:L548-54.
28. Hayabuchi Y. The Action of Smooth Muscle Cell Potassium Channels in the Pathology of Pulmonary Arterial Hypertension. Pediatr Cardiol 2016.
29. Landsberg JW, Yuan JX. Calcium and TRP channels in pulmonary vascular smooth muscle cell proliferation. News Physiol Sci 2004;19:44-50.
30. Yu Y, Sweeney M, Zhang S, et al. PDGF stimulates pulmonary vascular smooth muscle cell proliferation by upregulating TRPC6 expression. Am J Physiol Cell Physiol 2003;284:C316-30.
31. Burg ED, Remillard CV, Yuan JX. Potassium channels in the regulation of pulmonary artery smooth muscle cell proliferation and apoptosis: pharmacotherapeutic implications. Br J Pharmacol 2008;153 Suppl 1:S99-S111.
32. Manoury B, Etheridge SL, Reid J, Gurney AM. Organ culture mimics the effects of hypoxia on membrane potential, K(+) channels and vessel tone in pulmonary artery. Br J Pharmacol 2009;158:848-61.
33. Remillard CV, Yuan JX. Activation of K+ channels: an essential pathway in programmed cell death. Am J Physiol Lung Cell Mol Physiol 2004;286:L49-67.
34. Jones PL, Cowan KN, Rabinovitch M. Tenascin-C, proliferation and subendothelial fibronectin in progressive pulmonary vascular disease. Am J Pathol 1997;150:1349-60.

35. Liptay MJ, Parks WC, Mecham RP, et al. Neointimal macrophages colocalize with extracellular matrix gene expression in human atherosclerotic pulmonary arteries. J Clin Invest 1993;91:588-94.
36. Greenway S, van Suylen RJ, Du Marchie Sarvaas G, et al. S100A4/Mts1 produces murine pulmonary artery changes resembling plexogenic arteriopathy and is increased in human plexogenic arteriopathy. Am J Pathol 2004;164:253-62.
37. Balabanian K, Foussat A, Dorfmuller P, et al. CX(3)C chemokine fractalkine in pulmonary arterial hypertension. Am J Respir Crit Care Med 2002;165:1419-25.
38. Archer SL, Marsboom G, Kim GH, et al. Epigenetic attenuation of mitochondrial superoxide dismutase 2 in pulmonary arterial hypertension: a basis for excessive cell proliferation and a new therapeutic target. Circulation 2010;121:2661-71.
39. Chen X, Talati M, Fessel JP, et al. Estrogen Metabolite 16alpha-Hydroxyestrone Exacerbates Bone Morphogenetic Protein Receptor Type II-Associated Pulmonary Arterial Hypertension Through MicroRNA-29-Mediated Modulation of Cellular Metabolism. Circulation 2016;133:82-97.
40. Scorza R, Caronni M, Bazzi S, et al. Post-menopause is the main risk factor for developing isolated pulmonary hypertension in systemic sclerosis. Ann N Y Acad Sci 2002;966:238-46.
41. Zamanian RT, Hansmann G, Snook S, et al. Insulin resistance in pulmonary arterial hypertension. Eur Respir J 2009;33:318-24.
42. Galie N, Corris PA, Frost A, et al. Updated treatment algorithm of pulmonary arterial hypertension. J Am Coll Cardiol 2013;62:D60-72.
43. Elliott CG, Glissmeyer EW, Havlena GT, et al. Relationship of BMPR2 mutations to vasoreactivity in pulmonary arterial hypertension. Circulation 2006;113:2509-15.
44. Rosenzweig EB, Morse JH, Knowles JA, et al. Clinical implications of determining BMPR2 mutation status in a large cohort of children and adults with pulmonary arterial hypertension. J Heart Lung Transplant 2008;27:668-74.
45. van Loon RL, Roofthooft MT, Hillege HL, et al. Pediatric pulmonary hypertension in the Netherlands: epidemiology and characterization during the period 1991 to 2005. Circulation 2011;124:1755-64.
46. Moledina S, Hislop AA, Foster H, Schulze-Neick I, Haworth SG. Childhood idiopathic pulmonary arterial hypertension: a national cohort study. Heart 2010;96:1401-6.
47. Berger RM, Beghetti M, Humpl T, et al. Clinical features of paediatric pulmonary hypertension: a registry study. Lancet 2012;379:537-46.
48. Hansmann G, Hoeper MM. Registries for paediatric pulmonary hypertension. Eur Respir J 2013;42:580-3.
49. Ivy DD, Abman SH, Barst RJ, et al. Pediatric pulmonary hypertension. J Am Coll Cardiol 2013;62:D117-26.
50. Barst RJ, McGoon MD, Elliott CG, Foreman AJ, Miller DP, Ivy DD. Survival in childhood pulmonary arterial hypertension: insights from the registry to evaluate early and long-term pulmonary arterial hypertension disease management. Circulation 2012;125:113-22.
51. Ma L, Chung WK. The genetic basis of pulmonary arterial hypertension. Hum Genet 2014;133:471-9.
52. Vida VL, Padalino MA, Boccuzzo G, et al. Scimitar syndrome: a European Congenital Heart Surgeons Association (ECHSA) multicentric study. Circulation 2010;122:1159-66.

53. Kobayashi D, Cook AL, Williams DA. Pulmonary hypertension secondary to partial pulmonary venous obstruction in a child with Cantu syndrome. Pediatr Pulmonol 2010;45:727-9.
54. Schulze-Neick I, Beghetti M. Issues related to the management and therapy of paediatric pulmonary hypertension. Eur Respir Rev 2010;19:331-9.
55. Adatia I, Haworth SG, Wegner M, et al. Clinical trials in neonates and children: Report of the pulmonary hypertension academic research consortium pediatric advisory committee. Pulm Circ 2013;3:252-66.
56. Gouaux E, Mackinnon R. Principles of selective ion transport in channels and pumps. Science 2005;310:1461-5.
57. Kuhr FK, Smith KA, Song MY, Levitan I, Yuan JX. New mechanisms of pulmonary arterial hypertension: role of Ca(2)(+) signaling. Am J Physiol Heart Circ Physiol 2012;302:H1546-62.
58. Casteels R, Kitamura K, Kuriyama H, Suzuki H. The membrane properties of the smooth muscle cells of the rabbit main pulmonary artery. J Physiol 1977;271:41-61.
59. Gurney AM, Osipenko ON, MacMillan D, Kempsill FE. Potassium channels underlying the resting potential of pulmonary artery smooth muscle cells. Clin Exp Pharmacol Physiol 2002;29:330-3.
60. Platoshyn O, Remillard CV, Fantozzi I, et al. Diversity of voltage-dependent K+ channels in human pulmonary artery smooth muscle cells. Am J Physiol Lung Cell Mol Physiol 2004;287:L226-38.
61. Firth AL, Remillard CV, Platoshyn O, Fantozzi I, Ko EA, Yuan JX. Functional ion channels in human pulmonary artery smooth muscle cells: Voltage-dependent cation channels. Pulm Circ 2011;1:48-71.
62. Patel AJ, Lazdunski M, Honore E. Kv2.1/Kv9.3, a novel ATP-dependent delayed-rectifier K+ channel in oxygen-sensitive pulmonary artery myocytes. EMBO J 1997;16:6615-25.
63. Hulme JT, Coppock EA, Felipe A, Martens JR, Tamkun MM. Oxygen sensitivity of cloned voltage-gated K(+) channels expressed in the pulmonary vasculature. Circ Res 1999;85:489-97.
64. Osipenko ON, Tate RJ, Gurney AM. Potential role for kv3.1b channels as oxygen sensors. Circ Res 2000;86:534-40.
65. Coetzee WA, Amarillo Y, Chiu J, et al. Molecular diversity of K+ channels. Ann N Y Acad Sci 1999;868:233-85.
66. Platoshyn O, Golovina VA, Bailey CL, et al. Sustained membrane depolarization and pulmonary artery smooth muscle cell proliferation. Am J Physiol Cell Physiol 2000;279:C1540-9.
67. Yuan XJ, Goldman WF, Tod ML, Rubin LJ, Blaustein MP. Hypoxia reduces potassium currents in cultured rat pulmonary but not mesenteric arterial myocytes. Am J Physiol 1993;264:L116-23.
68. Yu Y, Platoshyn O, Zhang J, et al. c-Jun decreases voltage-gated K(+) channel activity in pulmonary artery smooth muscle cells. Circulation 2001;104:1557-63.
69. Post JM, Hume JR, Archer SL, Weir EK. Direct role for potassium channel inhibition in hypoxic pulmonary vasoconstriction. Am J Physiol 1992;262:C882-90.
70. Tennant BP, Cui Y, Tinker A, Clapp LH. Functional expression of inward rectifier potassium channels in cultured human pulmonary smooth muscle cells: evidence for a major role of Kir2.4 subunits. J Membr Biol 2006;213:19-29.

71. Evans AM, Osipenko ON, Gurney AM. Properties of a novel K+ current that is active at resting potential in rabbit pulmonary artery smooth muscle cells. J Physiol 1996;496 (Pt 2):407-20.
72. Osipenko ON, Alexander D, MacLean MR, Gurney AM. Influence of chronic hypoxia on the contributions of non-inactivating and delayed rectifier K currents to the resting potential and tone of rat pulmonary artery smooth muscle. Br J Pharmacol 1998;124:1335-7.
73. Olschewski A, Li Y, Tang B, et al. Impact of TASK-1 in human pulmonary artery smooth muscle cells. Circ Res 2006;98:1072-80.
74. Gurney AM, Osipenko ON, MacMillan D, McFarlane KM, Tate RJ, Kempsill FE. Two-pore domain K channel, TASK-1, in pulmonary artery smooth muscle cells. Circ Res 2003;93:957-64.
75. Antigny F, Hautefort A, Meloche J, et al. Potassium Channel Subfamily K Member 3 (KCNK3) Contributes to the Development of Pulmonary Arterial Hypertension. Circulation 2016;133:1371-85.
76. Moudgil R, Michelakis ED, Archer SL. The role of k+ channels in determining pulmonary vascular tone, oxygen sensing, cell proliferation, and apoptosis: implications in hypoxic pulmonary vasoconstriction and pulmonary arterial hypertension. Microcirculation 2006;13:615-32.
77. Platoshyn O, Yu Y, Golovina VA, et al. Chronic hypoxia decreases K(V) channel expression and function in pulmonary artery myocytes. Am J Physiol Lung Cell Mol Physiol 2001;280:L801-12.
78. Archer SL, London B, Hampl V, et al. Impairment of hypoxic pulmonary vasoconstriction in mice lacking the voltage-gated potassium channel Kv1.5. FASEB J 2001;15:1801-3.
79. Smirnov SV, Robertson TP, Ward JP, Aaronson PI. Chronic hypoxia is associated with reduced delayed rectifier K+ current in rat pulmonary artery muscle cells. Am J Physiol 1994;266:H365-70.
80. Yuan JX, Aldinger AM, Juhaszova M, et al. Dysfunctional voltage-gated K+ channels in pulmonary artery smooth muscle cells of patients with primary pulmonary hypertension. Circulation 1998;98:1400-6.
81. Remillard CV, Tigno DD, Platoshyn O, et al. Function of Kv1.5 channels and genetic variations of KCNA5 in patients with idiopathic pulmonary arterial hypertension. Am J Physiol Cell Physiol 2007;292:C1837-53.
82. Wang J, Juhaszova M, Rubin LJ, Yuan XJ. Hypoxia inhibits gene expression of voltage-gated K+ channel alpha subunits in pulmonary artery smooth muscle cells. J Clin Invest 1997;100:2347-53.
83. Platoshyn O, Brevnova EE, Burg ED, Yu Y, Remillard CV, Yuan JX. Acute hypoxia selectively inhibits KCNA5 channels in pulmonary artery smooth muscle cells. Am J Physiol Cell Physiol 2006;290:C907-16.
84. Archer SL, Wu XC, Thebaud B, et al. Preferential expression and function of voltage-gated, O2-sensitive K+ channels in resistance pulmonary arteries explains regional heterogeneity in hypoxic pulmonary vasoconstriction: ionic diversity in smooth muscle cells. Circ Res 2004;95:308-18.
85. Brevnova EE, Platoshyn O, Zhang S, Yuan JX. Overexpression of human KCNA5 increases IK V and enhances apoptosis. Am J Physiol Cell Physiol 2004;287:C715-22.

86. Pozeg ZI, Michelakis ED, McMurtry MS, et al. In vivo gene transfer of the O2-sensitive potassium channel Kv1.5 reduces pulmonary hypertension and restores hypoxic pulmonary vasoconstriction in chronically hypoxic rats. Circulation 2003;107:2037-44.
87. Manoury B, Lamalle C, Oliveira R, Reid J, Gurney AM. Contractile and electrophysiological properties of pulmonary artery smooth muscle are not altered in TASK-1 knockout mice. J Physiol 2011;589:3231-46.
88. Gardener MJ, Johnson IT, Burnham MP, Edwards G, Heagerty AM, Weston AH. Functional evidence of a role for two-pore domain potassium channels in rat mesenteric and pulmonary arteries. Br J Pharmacol 2004;142:192-202.
89. Enyedi P, Czirjak G. Molecular background of leak K+ currents: two-pore domain potassium channels. Physiol Rev 2010;90:559-605.
90. Hodgkin AL, Huxley AF. Potassium leakage from an active nerve fibre. J Physiol 1947;106:341-67.
91. Hodgkin AL, Huxley AF. A quantitative description of membrane current and its application to conduction and excitation in nerve. J Physiol 1952;117:500-44.
92. Hodgkin AL, Katz B. The effect of sodium ions on the electrical activity of giant axon of the squid. J Physiol 1949;108:37-77.
93. Atkinson NS, Robertson GA, Ganetzky B. A component of calcium-activated potassium channels encoded by the Drosophila slo locus. Science 1991;253:551-5.
94. Frech GC, VanDongen AM, Schuster G, Brown AM, Joho RH. A novel potassium channel with delayed rectifier properties isolated from rat brain by expression cloning. Nature 1989;340:642-5.
95. Kubo Y, Baldwin TJ, Jan YN, Jan LY. Primary structure and functional expression of a mouse inward rectifier potassium channel. Nature 1993;362:127-33.
96. Lesage F, Guillemare E, Fink M, et al. TWIK-1, a ubiquitous human weakly inward rectifying K+ channel with a novel structure. EMBO J 1996;15:1004-11.
97. Duprat F, Lesage F, Fink M, Reyes R, Heurteaux C, Lazdunski M. TASK, a human background K+ channel to sense external pH variations near physiological pH. EMBO J 1997;16:5464-71.
98. Kollewe A, Lau AY, Sullivan A, Roux B, Goldstein SA. A structural model for K2P potassium channels based on 23 pairs of interacting sites and continuum electrostatics. J Gen Physiol 2009;134:53-68.
99. Morton MJ, O'Connell AD, Sivaprasadarao A, Hunter M. Determinants of pH sensing in the two-pore domain K(+) channels TASK-1 and -2. Pflugers Arch 2003;445:577-83.
100. Kim Y, Bang H, Kim D. TASK-3, a new member of the tandem pore K(+) channel family. J Biol Chem 2000;275:9340-7.
101. Chapman CG, Meadows HJ, Godden RJ, et al. Cloning, localisation and functional expression of a novel human, cerebellum specific, two pore domain potassium channel. Brain Res Mol Brain Res 2000;82:74-83.
102. Rajan S, Wischmeyer E, Xin Liu G, et al. TASK-3, a novel tandem pore domain acid-sensitive K+ channel. An extracellular histiding as pH sensor. J Biol Chem 2000;275:16650-7.
103. Czirjak G, Enyedi P. Formation of functional heterodimers between the TASK-1 and TASK-3 two-pore domain potassium channel subunits. J Biol Chem 2002;277:5426-32.
104. Clarke CE, Veale EL, Green PJ, Meadows HJ, Mathie A. Selective block of the human 2-P domain potassium channel, TASK-3, and the native leak potassium current, IKSO, by zinc. J Physiol 2004;560:51-62.

105. Czirjak G, Enyedi P. Ruthenium red inhibits TASK-3 potassium channel by interconnecting glutamate 70 of the two subunits. Mol Pharmacol 2003;63:646-52.
106. Kang D, Han J, Talley EM, Bayliss DA, Kim D. Functional expression of TASK-1/TASK-3 heteromers in cerebellar granule cells. J Physiol 2004;554:64-77.
107. Kim D, Cavanaugh EJ, Kim I, Carroll JL. Heteromeric TASK-1/TASK-3 is the major oxygen-sensitive background K+ channel in rat carotid body glomus cells. J Physiol 2009;587:2963-75.
108. Berg AP, Talley EM, Manger JP, Bayliss DA. Motoneurons express heteromeric TWIK-related acid-sensitive K+ (TASK) channels containing TASK-1 (KCNK3) and TASK-3 (KCNK9) subunits. J Neurosci 2004;24:6693-702.
109. Meuth SG, Aller MI, Munsch T, et al. The contribution of TWIK-related acid-sensitive K+-containing channels to the function of dorsal lateral geniculate thalamocortical relay neurons. Mol Pharmacol 2006;69:1468-76.
110. Torborg CL, Berg AP, Jeffries BW, Bayliss DA, McBain CJ. TASK-like conductances are present within hippocampal CA1 stratum oriens interneuron subpopulations. J Neurosci 2006;26:7362-7.
111. Rinne S, Kiper AK, Schlichthorl G, et al. TASK-1 and TASK-3 may form heterodimers in human atrial cardiomyocytes. J Mol Cell Cardiol 2015;81:71-80.
112. Maingret F, Patel AJ, Lazdunski M, Honore E. The endocannabinoid anandamide is a direct and selective blocker of the background K(+) channel TASK-1. EMBO J 2001;20:47-54.
113. Veale EL, Buswell R, Clarke CE, Mathie A. Identification of a region in the TASK3 two pore domain potassium channel that is critical for its blockade by methanandamide. Br J Pharmacol 2007;152:778-86.
114. Zygmunt PM, Petersson J, Andersson DA, et al. Vanilloid receptors on sensory nerves mediate the vasodilator action of anandamide. Nature 1999;400:452-7.
115. Kim HI, Kim TH, Shin YK, Lee CS, Park M, Song JH. Anandamide suppression of Na+ currents in rat dorsal root ganglion neurons. Brain Res 2005;1062:39-47.
116. Chemin J, Monteil A, Perez-Reyes E, Nargeot J, Lory P. Direct inhibition of T-type calcium channels by the endogenous cannabinoid anandamide. EMBO J 2001;20:7033-40.
117. Poling JS, Rogawski MA, Salem N, Jr., Vicini S. Anandamide, an endogenous cannabinoid, inhibits Shaker-related voltage-gated K+ channels. Neuropharmacology 1996;35:983-91.
118. Streit AK, Netter MF, Kempf F, et al. A specific two-pore domain potassium channel blocker defines the structure of the TASK-1 open pore. J Biol Chem 2011;286:13977-84.
119. Patel AJ, Honore E, Lesage F, Fink M, Romey G, Lazdunski M. Inhalational anesthetics activate two-pore-domain background K+ channels. Nat Neurosci 1999;2:422-6.
120. Meadows HJ, Randall AD. Functional characterisation of human TASK-3, an acid-sensitive two-pore domain potassium channel. Neuropharmacology 2001;40:551-9.
121. Li J, Long C, Cui W, Wang H. Iptakalim ameliorates monocrotaline-induced pulmonary arterial hypertension in rats. J Cardiovasc Pharmacol Ther 2013;18:60-9.
122. Jiang L, Zhou T, Liu H. Combined effects of the ATP-sensitive potassium channel opener pinacidil and simvastatin on pulmonary vascular remodeling in rats with monocrotaline-induced pulmonary arterial hypertension. Pharmazie 2012;67:547-52.
123. Zuo X, Zong F, Wang H, Wang Q, Xie W, Wang H. Iptakalim, a novel ATP-sensitive potassium channel opener, inhibits pulmonary arterial smooth muscle cell proliferation by downregulation of PKC-alpha. J Biomed Res 2011;25:392-401.

124. Sahara M, Sata M, Morita T, Hirata Y, Nagai R. Nicorandil attenuates monocrotaline-induced vascular endothelial damage and pulmonary arterial hypertension. PLoS One 2012;7:e33367.
125. Clapp LH, Gurney AM. ATP-sensitive K+ channels regulate resting potential of pulmonary arterial smooth muscle cells. Am J Physiol 1992;262:H916-20.
126. Cui Y, Tran S, Tinker A, Clapp LH. The molecular composition of K(ATP) channels in human pulmonary artery smooth muscle cells and their modulation by growth. Am J Respir Cell Mol Biol 2002;26:135-43.
127. Gopalakrishnan M, Whiteaker KL, Molinari EJ, et al. Characterization of the ATP-sensitive potassium channels (KATP) expressed in guinea pig bladder smooth muscle cells. J Pharmacol Exp Ther 1999;289:551-8.
128. Aguilar-Bryan L, Nichols CG, Wechsler SW, et al. Cloning of the beta cell high-affinity sulfonylurea receptor: a regulator of insulin secretion. Science 1995;268:423-6.
129. Inagaki N, Gonoi T, Clement JP, et al. A family of sulfonylurea receptors determines the pharmacological properties of ATP-sensitive K+ channels. Neuron 1996;16:1011-7.
130. Chutkow WA, Simon MC, Le Beau MM, Burant CF. Cloning, tissue expression, and chromosomal localization of SUR2, the putative drug-binding subunit of cardiac, skeletal muscle, and vascular KATP channels. Diabetes 1996;45:1439-45.
131. Inagaki N, Tsuura Y, Namba N, et al. Cloning and functional characterization of a novel ATP-sensitive potassium channel ubiquitously expressed in rat tissues, including pancreatic islets, pituitary, skeletal muscle, and heart. J Biol Chem 1995;270:5691-4.
132. Inagaki N, Gonoi T, Clement JPt, et al. Reconstitution of IKATP: an inward rectifier subunit plus the sulfonylurea receptor. Science 1995;270:1166-70.
133. Doyle DA, Morais Cabral J, Pfuetzner RA, et al. The structure of the potassium channel: molecular basis of K+ conduction and selectivity. Science 1998;280:69-77.
134. Heginbotham L, Lu Z, Abramson T, MacKinnon R. Mutations in the K+ channel signature sequence. Biophys J 1994;66:1061-7.
135. Inagaki N, Gonoi T, Seino S. Subunit stoichiometry of the pancreatic beta-cell ATP-sensitive K+ channel. FEBS Lett 1997;409:232-6.
136. Clement JPt, Kunjilwar K, Gonzalez G, et al. Association and stoichiometry of K(ATP) channel subunits. Neuron 1997;18:827-38.
137. Shyng S, Nichols CG. Octameric stoichiometry of the KATP channel complex. J Gen Physiol 1997;110:655-64.
138. Noma A. ATP-regulated K+ channels in cardiac muscle. Nature 1983;305:147-8.
139. Kefaloyianni E, Bao L, Rindler MJ, et al. Measuring and evaluating the role of ATP-sensitive K+ channels in cardiac muscle. J Mol Cell Cardiol 2012;52:596-607.
140. Trube G, Hescheler J. Inward-rectifying channels in isolated patches of the heart cell membrane: ATP-dependence and comparison with cell-attached patches. Pflugers Arch 1984;401:178-84.
141. Ashcroft FM, Kakei M. ATP-sensitive K+ channels in rat pancreatic beta-cells: modulation by ATP and Mg2+ ions. J Physiol 1989;416:349-67.
142. Lederer WJ, Nichols CG. Nucleotide modulation of the activity of rat heart ATP-sensitive K+ channels in isolated membrane patches. J Physiol 1989;419:193-211.
143. Dunne MJ, Petersen OH. Intracellular ADP activates K+ channels that are inhibited by ATP in an insulin-secreting cell line. FEBS Lett 1986;208:59-62.

144. Nichols CG. KATP channels as molecular sensors of cellular metabolism. Nature 2006;440:470-6.
145. Cook DL, Hales CN. Intracellular ATP directly blocks K+ channels in pancreatic B-cells. Nature 1984;311:271-3.
146. Kakei M, Noma A, Shibasaki T. Properties of adenosine-triphosphate-regulated potassium channels in guinea-pig ventricular cells. J Physiol 1985;363:441-62.
147. Tucker SJ, Gribble FM, Zhao C, Trapp S, Ashcroft FM. Truncation of Kir6.2 produces ATP-sensitive K+ channels in the absence of the sulphonylurea receptor. Nature 1997;387:179-83.
148. Gribble FM, Tucker SJ, Ashcroft FM. The essential role of the Walker A motifs of SUR1 in K-ATP channel activation by Mg-ADP and diazoxide. EMBO J 1997;16:1145-52.
149. Shyng S, Ferrigni T, Nichols CG. Regulation of KATP channel activity by diazoxide and MgADP. Distinct functions of the two nucleotide binding folds of the sulfonylurea receptor. J Gen Physiol 1997;110:643-54.
150. Gribble FM, Tucker SJ, Haug T, Ashcroft FM. MgATP activates the beta cell KATP channel by interaction with its SUR1 subunit. Proc Natl Acad Sci U S A 1998;95:7185-90.
151. Rubin AA, Roth FE, Taylor RM, Rosenkilde H. Pharmacology of diazoxide, an antihypertensive, nondiuretic benzothiadiazine. J Pharmacol Exp Ther 1962;136:344-52.
152. Wolff F. Diazoxide Hyperglycaemia and Its Continued Relief by Tolbutamide. Lancet 1964;1:309-10.
153. Trube G, Rorsman P, Ohno-Shosaku T. Opposite effects of tolbutamide and diazoxide on the ATP-dependent K+ channel in mouse pancreatic beta-cells. Pflugers Arch 1986;407:493-9.
154. Standen NB, Quayle JM, Davies NW, Brayden JE, Huang Y, Nelson MT. Hyperpolarizing vasodilators activate ATP-sensitive K+ channels in arterial smooth muscle. Science 1989;245:177-80.
155. Galie N, Humbert M, Vachiery JL, et al. 2015 ESC/ERS Guidelines for the diagnosis and treatment of pulmonary hypertension: The Joint Task Force for the Diagnosis and Treatment of Pulmonary Hypertension of the European Society of Cardiology (ESC) and the European Respiratory Society (ERS): Endorsed by: Association for European Paediatric and Congenital Cardiology (AEPC), International Society for Heart and Lung Transplantation (ISHLT). Eur Respir J 2015;46:903-75.
156. Lopes CM, Zilberberg N, Goldstein SA. Block of Kcnk3 by protons. Evidence that 2-P-domain potassium channel subunits function as homodimers. J Biol Chem 2001;276:24449-52.
157. Stearman RS, Cornelius AR, Lu X, et al. Functional prostacyclin synthase promoter polymorphisms. Impact in pulmonary arterial hypertension. Am J Respir Crit Care Med 2014;189:1110-20.
158. Zou B, Flaherty DP, Simpson DS, et al. ML365: Development of Bis-Amides as Selective Inhibitors of the KCNK3/TASK1 Two Pore Potassium Channel. Probe Reports from the NIH Molecular Libraries Program. Bethesda (MD)2010.
159. Skarsfeldt MA, Jepps TA, Bomholtz SH, et al. pH-dependent inhibition of K(2)P3.1 prolongs atrial refractoriness in whole hearts. Pflugers Arch 2016;468:643-54.
160. Yuill KH, Stansfeld PJ, Ashmole I, Sutcliffe MJ, Stanfield PR. The selectivity, voltage-dependence and acid sensitivity of the tandem pore potassium channel TASK-1: contributions of the pore domains. Pflugers Arch 2007;455:333-48.
161. Pei L, Wiser O, Slavin A, et al. Oncogenic potential of TASK3 (Kcnk9) depends on K+ channel function. Proc Natl Acad Sci U S A 2003;100:7803-7.

162. Vandenberg JI, Perry MD, Perrin MJ, Mann SA, Ke Y, Hill AP. hERG K(+) channels: structure, function, and clinical significance. Physiol Rev 2012;92:1393-478.
163. Nerbonne JM, Kass RS. Molecular physiology of cardiac repolarization. Physiol Rev 2005;85:1205-53.
164. Yuill K, Ashmole I, Stanfield PR. The selectivity filter of the tandem pore potassium channel TASK-1 and its pH-sensitivity and ionic selectivity. Pflugers Arch 2004;448:63-9.
165. Archer SL, Souil E, Dinh-Xuan AT, et al. Molecular identification of the role of voltage-gated K+ channels, Kv1.5 and Kv2.1, in hypoxic pulmonary vasoconstriction and control of resting membrane potential in rat pulmonary artery myocytes. J Clin Invest 1998;101:2319-30.
166. Yuan XJ, Wang J, Juhaszova M, Gaine SP, Rubin LJ. Attenuated K+ channel gene transcription in primary pulmonary hypertension. Lancet 1998;351:726-7.
167. Morecroft I, Murray A, Nilsen M, Gurney AM, MacLean MR. Treatment with the Kv7 potassium channel activator flupirtine is beneficial in two independent mouse models of pulmonary hypertension. Br J Pharmacol 2009;157:1241-9.
168. Schiekel J, Lindner M, Hetzel A, et al. The inhibition of the potassium channel TASK-1 in rat cardiac muscle by endothelin-1 is mediated by phospholipase C. Cardiovasc Res 2013;97:97-105.
169. Tang B, Li Y, Nagaraj C, et al. Endothelin-1 inhibits background two-pore domain channel TASK-1 in primary human pulmonary artery smooth muscle cells. Am J Respir Cell Mol Biol 2009;41:476-83.
170. Seyler C, Duthil-Straub E, Zitron E, et al. TASK1 (K(2P)3.1) K(+) channel inhibition by endothelin-1 is mediated through Rho kinase-dependent phosphorylation. Br J Pharmacol 2012;165:1467-75.
171. Wilke BU, Lindner M, Greifenberg L, et al. Diacylglycerol mediates regulation of TASK potassium channels by Gq-coupled receptors. Nat Commun 2014;5:5540.
172. Olschewski A. Targeting TASK-1 channels as a therapeutic approach. Adv Exp Med Biol 2010;661:459-73.
173. Liu C, Cotten JF, Schuyler JA, et al. Protective effects of TASK-3 (KCNK9) and related 2P K channels during cellular stress. Brain Res 2005;1031:164-73.
174. Schmidt C, Wiedmann F, Voigt N, et al. Upregulation of K(2P)3.1 K+ Current Causes Action Potential Shortening in Patients With Chronic Atrial Fibrillation. Circulation 2015;132:82-92.
175. Li H, Durbin R. Fast and accurate short read alignment with Burrows-Wheeler transform. Bioinformatics 2009;25:1754-60.
176. McKenna A, Hanna M, Banks E, et al. The Genome Analysis Toolkit: a MapReduce framework for analyzing next-generation DNA sequencing data. Genome Res 2010;20:1297-303.
177. Genomes Project C, Abecasis GR, Auton A, et al. An integrated map of genetic variation from 1,092 human genomes. Nature 2012;491:56-65.
178. Lek M, Karczewski KJ, Minikel EV, et al. Analysis of protein-coding genetic variation in 60,706 humans. Nature 2016;536:285-91.
179. Kumar P, Henikoff S, Ng PC. Predicting the effects of coding non-synonymous variants on protein function using the SIFT algorithm. Nat Protoc 2009;4:1073-81.
180. Adzhubei IA, Schmidt S, Peshkin L, et al. A method and server for predicting damaging missense mutations. Nat Methods 2010;7:248-9.

181. Dong C, Wei P, Jian X, et al. Comparison and integration of deleteriousness prediction methods for nonsynonymous SNVs in whole exome sequencing studies. Hum Mol Genet 2015;24:2125-37.
182. Kircher M, Witten DM, Jain P, O'Roak BJ, Cooper GM, Shendure J. A general framework for estimating the relative pathogenicity of human genetic variants. Nat Genet 2014;46:310-5.
183. Manichaikul A, Mychaleckyj JC, Rich SS, Daly K, Sale M, Chen WM. Robust relationship inference in genome-wide association studies. Bioinformatics 2010;26:2867-73.
184. Genomes Project C, Auton A, Brooks LD, et al. A global reference for human genetic variation. Nature 2015;526:68-74.
185. Baier LJ, Muller YL, Remedi MS, et al. ABCC8 R1420H Loss-of-Function Variant in a Southwest American Indian Community: Association With Increased Birth Weight and Doubled Risk of Type 2 Diabetes. Diabetes 2015;64:4322-32.
186. Bellanne-Chantelot C, Saint-Martin C, Ribeiro MJ, et al. ABCC8 and KCNJ11 molecular spectrum of 109 patients with diazoxide-unresponsive congenital hyperinsulinism. J Med Genet 2010;47:752-9.
187. Park SE, Flanagan SE, Hussain K, Ellard S, Shin CH, Yang SW. Characterization of ABCC8 and KCNJ11 gene mutations and phenotypes in Korean patients with congenital hyperinsulinism. Eur J Endocrinol 2011;164:919-26.
188. Chandran S, Peng FY, Rajadurai VS, et al. Paternally inherited ABCC8 mutation causing diffuse congenital hyperinsulinism. Endocrinol Diabetes Metab Case Rep 2013;2013:130041.
189. Zhou Q, Garin I, Castano L, et al. Neonatal diabetes caused by mutations in sulfonylurea receptor 1: interplay between expression and Mg-nucleotide gating defects of ATP-sensitive potassium channels. J Clin Endocrinol Metab 2010;95:E473-8.
190. Shi NQ, Ye B, Makielski JC. Function and distribution of the SUR isoforms and splice variants. J Mol Cell Cardiol 2005;39:51-60.
191. Ellard S, Flanagan SE, Girard CA, et al. Permanent neonatal diabetes caused by dominant, recessive, or compound heterozygous SUR1 mutations with opposite functional effects. Am J Hum Genet 2007;81:375-82.
192. Tornovsky S, Crane A, Cosgrove KE, et al. Hyperinsulinism of infancy: novel ABCC8 and KCNJ11 mutations and evidence for additional locus heterogeneity. J Clin Endocrinol Metab 2004;89:6224-34.
193. Ashcroft FM. From molecule to malady. Nature 2006;440:440-7.
194. Flagg TP, Patton B, Masia R, et al. Arrhythmia susceptibility and premature death in transgenic mice overexpressing both SUR1 and Kir6.2[DeltaN30,K185Q] in the heart. Am J Physiol Heart Circ Physiol 2007;293:H836-45.
195. Nessa A, Aziz QH, Thomas AM, Harmer SC, Tinker A, Hussain K. Molecular mechanisms of congenital hyperinsulinism due to autosomal dominant mutations in ABCC8. Hum Mol Genet 2015;24:5142-53.
196. Babenko AP, Polak M, Cave H, et al. Activating mutations in the ABCC8 gene in neonatal diabetes mellitus. N Engl J Med 2006;355:456-66.
197. Chatterjee S, Al-Mehdi AB, Levitan I, Stevens T, Fisher AB. Shear stress increases expression of a KATP channel in rat and bovine pulmonary vascular endothelial cells. Am J Physiol Cell Physiol 2003;285:C959-67.

198. Woo SK, Kwon MS, Geng Z, et al. Sequential activation of hypoxia-inducible factor 1 and specificity protein 1 is required for hypoxia-induced transcriptional stimulation of Abcc8. J Cereb Blood Flow Metab 2012;32:525-36.
199. Simard JM, Tsymbalyuk O, Ivanov A, et al. Endothelial sulfonylurea receptor 1-regulated NC Ca-ATP channels mediate progressive hemorrhagic necrosis following spinal cord injury. J Clin Invest 2007;117:2105-13.
200. Ocal G, Flanagan SE, Hacihamdioglu B, et al. Clinical characteristics of recessive and dominant congenital hyperinsulinism due to mutation(s) in the ABCC8/KCNJ11 genes encoding the ATP-sensitive potasium channel in the pancreatic beta cell. J Pediatr Endocrinol Metab 2011;24:1019-23.
201. Brunetti-Pierri N, Olutoye OO, Heptulla R, Tatevian N. Case report: pathological features of aberrant pancreatic development in congenital hyperinsulinism due to ABCC8 mutations. Ann Clin Lab Sci 2008;38:386-9.
202. Muzyamba M, Farzaneh T, Behe P, et al. Complex ABCC8 DNA variations in congenital hyperinsulinism: lessons from functional studies. Clin Endocrinol (Oxf) 2007;67:115-24.
203. Henwood MJ, Kelly A, Macmullen C, et al. Genotype-phenotype correlations in children with congenital hyperinsulinism due to recessive mutations of the adenosine triphosphate-sensitive potassium channel genes. J Clin Endocrinol Metab 2005;90:789-94.
204. Hardy OT, Hernandez-Pampaloni M, Saffer JR, et al. Diagnosis and localization of focal congenital hyperinsulinism by 18F-fluorodopa PET scan. The Journal of pediatrics 2007;150:140-5.
205. Suchi M, MacMullen CM, Thornton PS, et al. Molecular and immunohistochemical analyses of the focal form of congenital hyperinsulinism. Mod Pathol 2006;19:122-9.
206. Martin GM, Rex EA, Devaraneni P, et al. Pharmacological Correction of Trafficking Defects in ATP-sensitive Potassium Channels Caused by Sulfonylurea Receptor 1 Mutations. J Biol Chem 2016;291:21971-83.
207. Klinke WP, Gilbert JA. Diazoxide in primary pulmonary hypertension. N Engl J Med 1980;302:91-2.
208. Chan NS, McLay J, Kenmure AC. Reversibility of primary pulmonary hypertension during six years of treatment with oral diazoxide. Br Heart J 1987;57:207-9.
209. Adi A, Abbas BB, Hamed MA, Tassan NA, Bakheet D. Screening for Mutations in ABCC8 and KCNJ11 Genes in Saudi Persistent Hyperinsulinemic Hypoglycemia of Infancy (PHHI) Patients. Genes (Basel) 2015;6:206-15.
210. Yildizdas D, Erdem S, Kucukosmanoglu O, Yilmaz M, Yuksel B. Pulmonary hypertension, heart failure and neutropenia due to diazoxide therapy. Adv Ther 2008;25:515-9.
211. Kharade SV, Nichols C, Denton JS. The shifting landscape of KATP channelopathies and the need for 'sharper' therapeutics. Future Med Chem 2016;8:789-802.
212. Paquet D, Kwart D, Chen A, et al. Efficient introduction of specific homozygous and heterozygous mutations using CRISPR/Cas9. Nature 2016;533:125-9.